A NOVEL TRANSFERRED-ARC REACTOR

A

THESIS

BY

PAUL JOSEPH PARISI, B.A.Sc.

Department of Chemical Engineering

McGill University

Under the Supervision of Dr. W.H. Gauvin

Submitted to the Faculty of Graduate Studies and Research of McGill University in partial fulfilment of the requirements for the degree of Master of Engineering

McGill University
MONTREAL, Quebec

August 1984

A NOVEL TRANSFERRED-ARC REACTOR

by

PAUL JOSEPH PARISI, B.A. Sc.

ABSTRACT

A novel type of transferred-arc reactor, in which an annular sleeve surrounds the arc over the major portion of its length was designed. An experimental prototype was tested, using steel powders as feed material, to assess the effects of the major design parameters and operating characteristics on the efficiency of energy utilization.

The measured electrical characteristics indicated that the total arc voltage depended strongly on the arc length and much less on current and plasmagen volumetric flow rate. Gas injected tangentially along the inner surface of the sleeve tended to stabilize the arc and reduced the arc voltage by 5 to 7 volts. The addition of a tangentially-injected particulate feed increased the arc voltage by 25 to 30 volts for an argon arc and 20 volts for a nitrogen arc. The particulate size (75 to 88 microns, and 149 to 177 microns) did not have an effect on the voltage. For a given arc length and current the total arc voltage and hence power of a nitrogen arc is double that of an argon arc.

The total power transferred by the arc to the sleeve, anode and particulate feed (and thus potentially usable) exceeded 80%. The energy utilized to melt a steel particulate feed was 0.91 kWh/kg despite the fact that 70% of the arc's power was lost to the cooled interior surfaces of the reactor. The fraction of the arc's power lost to the exhaust gas stream was less than 3%.

UN NOUVEAU TYPE DE RÉACTEUR À ARC TRANSFÉRÉ

par

PAUL JOSEPH PARISI, B.A. Sc.

RÉSUMÉ

Un nouveau type de réacteur à arc-transféré a été conçu, dans lequel une manche annulaire entoure l'arc sur la plus grande partie de sa longueur. Un prototype expérimental a été construit, dans lequel des poudres d'acier de différentes grosseurs ont été injectées pour déterminer l'influence des divers paramètres et caractéristiques d'opération sur l'efficacité d'utilisation de l'énergie électrique.

Les mesures obtenues indiquent que la tension totale de l'arc dépend fortement de sa longueur, et beaucoup moins du courant et de l'écoulement volumétrique du gaz plasmagène. L'injection tangentielle de gaz le long de la surface interne de la manche tend à stabiliser l'arc et réduit la tension par 5 à 7 volts.

L'alimentation tangentielle de particles augmente la tension par 25 à 30 volts pour un arc d'argon et par 20 volts pour un arc d'azote. Deux fractions de poudres d'acier ont été utilisées (une de 75 à 88 microns, l'autre de 149 à 172 microns) mais ces dimensions différentes n'ont pas eu d'effet sur la tension. Pour une longueur

d'arc et pour un courant donnés, la tension et par conséquent la puissance d'un arc d'azote sont double de celles d'un arc d'argon.

La puissance totale transférée par l'arc à la manche, à l'anode et à la poudre injectée dans le réacteur excéde 80%, et représente l'énergie utilisable dans un réacteur industriel. L'énergie utilisée pour fondre les poudres d'acier est de 0.91 kWh/kg malgré le fait que 70% de la puissance de l'arc est absorbée par le refroidissement du réacteur. Seulement 3% de cette puissance est perdue dans les gaz d'échappement. Dans chaque essai, moins de 0.1% des poudres d'alimentation ont été perdus dans ceux-ci. Ce fait est d'une importance considérable, puisqu'il démontre l'habilité de ce type de réacteur à traiter une alimentation de poudres très fines.

ACKNOWLEDGEMENTS

The author wishes to express his gratitude to all those who contributed to the work presented in this thesis.

To the members of the Plasma Technology Group, in particular Professor R.J. Munz, Dr. H.K. Choi, Mr. H. Tarki, Mr. P. Stuart and Mr. E. Chin.

To. Mr. R. Belanger and the staff of the IREQ workshop for their prompt and high quality construction of essential items of equipment.

To Mr. J.B. Dumont of the Chemical Engineering Stores at McGill University.

To Mr. G. Ouellette of IREQ for his technical advice on electric circuits.

To IREQ and in particular to Dr. M.G. Drouet and Dr. W.P. Schimmel for supporting this project and for providing laboratory space and equipment.

To Mrs. H. Avedesian for her excellent typing of this thesis, and to Mr. C. Desy for the preparation of the drawings.

Finally, to the author's family for their understanding, patience and encouragement, and to his friends for making his stay in Montreal a pleasant one.

TABLE OF CONENTS

EXPERIMENTAL SECTION

APPENDICES

LIST OF FIGURES

LIST OF TABLES

7

GENERAL INTRODUCTION

GENERAL INTRODUCTION

Arc plasmas are receiving increasing attention, not only as an intriguing research field, but as an industrial technique for the heating and chemical treatment of a variety of materials. A number of arc plasma reactors or furnaces have been proposed over the past twenty years to take advantage of the unique properties of arc plasmas and also to overcome some of the problems involved in their use.

For the past five years, the McGill University Plasma Laboratory has been investigating the electrical and heat transfer characteristics of transferred-arcs. Based on this information and on the design of some earlier plasma reactors, the Noranda Research Centre developed a new reactor that appears to be particularly well suited for high-temperature chemical or metallurgical reactions, while allowing a high degree of energy utilization.

The purpose of this study was to construct a prototype model of this new reactor and to determine its operating characteristics, including the transferred-arc's electrical characteristics and the various modes of heat transfer from the plasma column to various parts of the reactor components, under a variety of operating conditions. Initial tests were carried out

using axially-injected plasmagen gas only. A second phase of the project involved the injection of a tangential carrier gas while finally the injection of particulate feed with the carrier gas was undertaken to simulate an actual industrial process.

In accordance with the practice in the Plasma Laboratory, this thesis is presented as a number of individual sections, which are complete in themselves. The two main sections are:

(i) A review of the pertinent literature of transferred-arc theory, the design of commercial and laboratory plasma reactors and the current applications of plasma to metallurgical processing.

(ii) An experimental section with a detailed description of the experimental system design and operating procedures, the characterization of an argon plasma in the reactor and the determination of the energy distribution in the reactor system under a variety of operating conditions.

From this experimental evidence, conclusions are presented and recommendations for further work are offered.

LITERATURE REVIEW

LITERATURE REVIEW

INTRODUCTION

A review of the fundamentals of plasma physics and of plasma technology in general, including applications and generating devices, can be found in several books and review articles. For the purpose of this thesis, the books by Baddour and Timmins (1967), Hoyaux (1968) and Howatson (1976) are the most pertinent. Of the review articles, those of Waldie (1972 a,b) Rykalin (1976), Fauchais (1980, 1982), Bhat (1981), Kassabji and Fauchais (1981), Fauchais et al. (1981, 1983) and Sheer et al. (1982) are the most relevant, from a general point of view.

Because the present research project is aimed at a better understanding of the fundamental operating characteristics of a transferred-arc plasma reactor for metallurgical processing, only those references which are particularly pertinent to this area of plasma technology will be reviewed here.

DEFINITION OF A PLASMA

The term "plasma" is used to designate gaseous mixtures consisting of dissociated molecules, atoms, ions and free electrons.

In a more practical sense, the term plasma is applied to the gaseous state of substances from the moment the gas acquires a noticeable electrical conductivity, and is thus influenced by electrical and magnetic fields.

Plasmas are subdivided into non-thermal or cold plasmas and thermal plasmas, depending upon the pressure of the environment. At low pressures, the average kinetic energy of the electrons (or electron temperature) is significantly higher than that of the heavier ions, atoms and molecules. At higher pressures, the difference between the electron and heavier particle temperature is less marked. Figure 1 illustrates how electron and ion temperatures for an arc plasma vary with pressure. At pressures approaching atmospheric conditions these temperatures are essentially the same and the plasma is said to be in local thermodynamic equilibrium. They are referred to as thermal plasmas. In this review we are mainly concerned with thermal plasmas, as they are the most relevant to high-temperature chemical and metallurgical processing. The temperature of a thermal plasma is an important property which can be used to predict other thermodynamic and transport properties of the plasma. For example, it is possible to calculate the enthalpy of the plasma as a function of its temperature, as shown in Figure 2. The steep increases in enthalpy result from the dissociation and ionization of the gas that occur as the temperature is increased.

FIGURE 1

LOW-PRESSURE VERSUS HIGH-PRESSURE ARCS

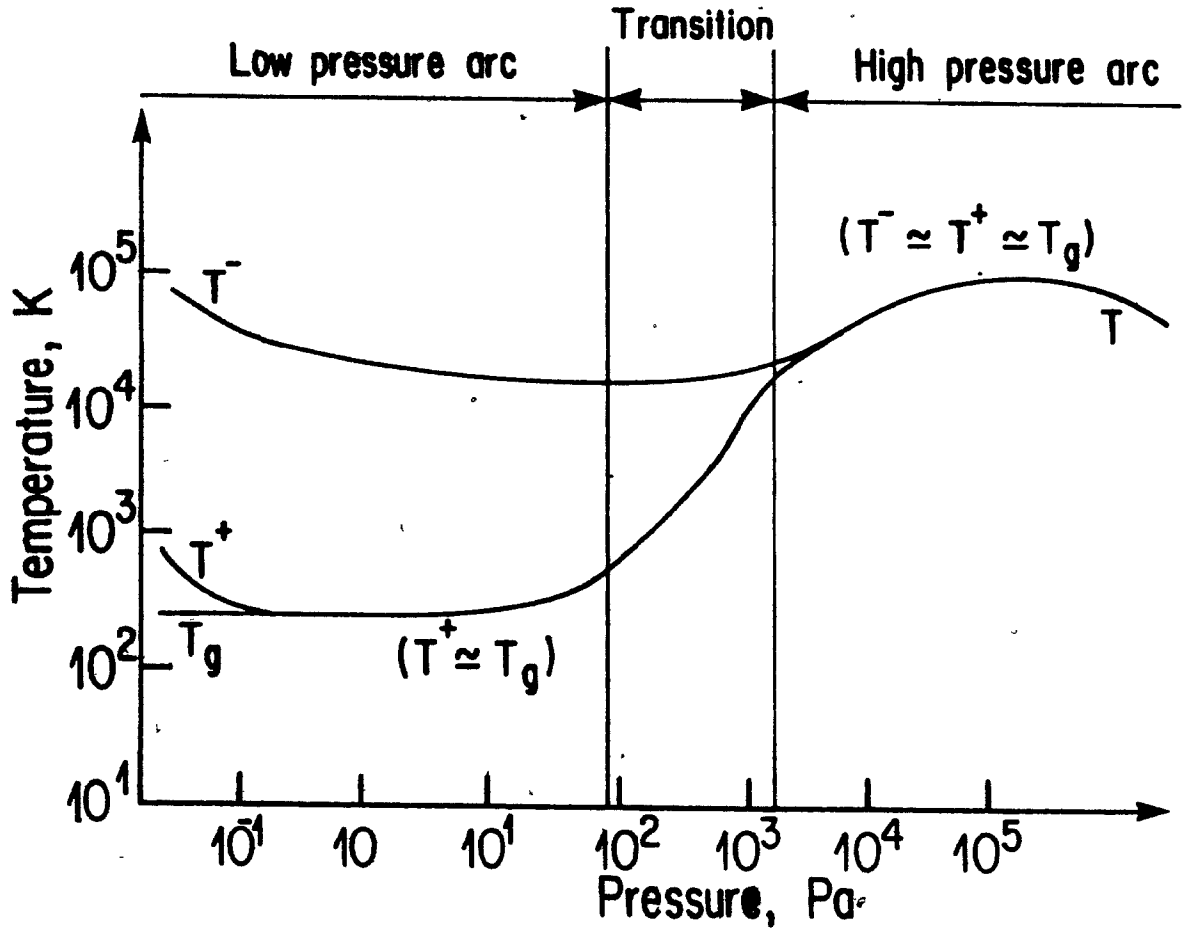
Transition
Low pressure arc
High pressure arc
$(T^- \simeq T^+ \simeq T_g)$
T^-
T
T^+
T_g
$(T^+ \simeq T_g)$
Temperature, K
10^5
10^4
10^3
10^2
10^1
10^{-1}
10
10^1
10^2
10^3
10^4
10^5
Pressure, Pa

FIGURE 2

ENTHALPIES AS A FUNCTION OF TEMPERATURE

AT ATMOSPHERIC PRESSURE

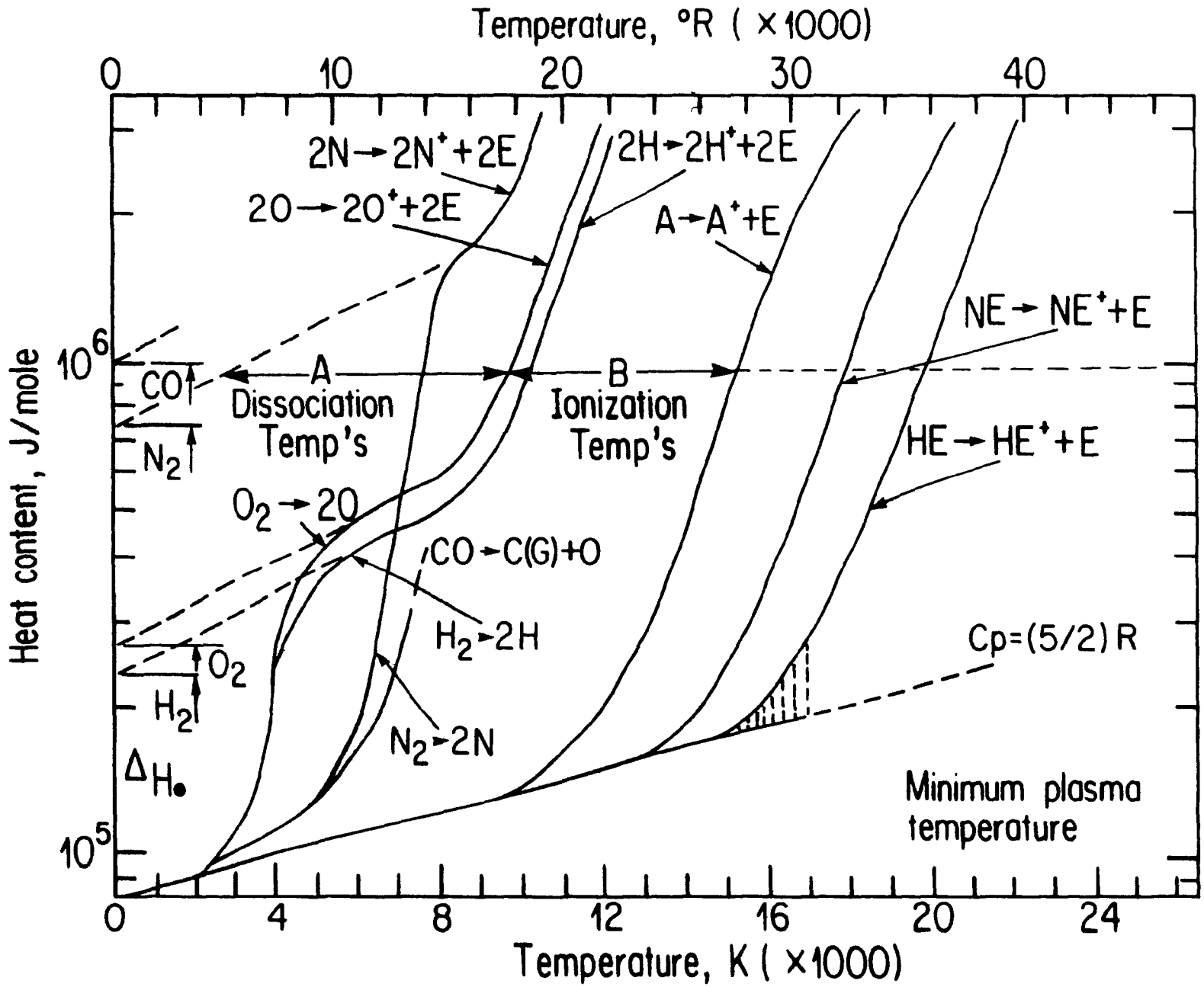
Temperature, °R (×1000)
0
10
20
30
40
2N → 2N⁺ + 2E
2H → 2H⁺ + 2E
2O → 2O⁺ + 2E
A → A⁺ + E
NE → NE⁺ + E
HE → HE⁺ + E
A
Dissociation Temp's
B
Ionization Temp's
CO
N2
O2 → 2O
CO → C(G) + O
H2 → 2H
O2
H2
N2 → 2N
ΔH°
Cp = (5/2) R
Minimum plasma temperature
Heat content, J/mole
10^6
10^5
0
4
8
12
16
20
24
Temperature, K (×1000)

PLASMA DEVICES

Plasmas can be generated between electrodes that carry the current to the plasma region. These types of plasmas are known as arc plasmas. A plasma can also be generated without electrodes in high-frequency inductance or capacitance-coupled generators. High-frequency plasma generators are used primarily in the laboratory when high levels of purity (absence of contamination from electrode erosion) are required and/or corrosive gases are utilized as the plasmagen gas. The high cost and low efficiency of these plasma generators is such that they have limited industrial applications. High frequency plasma generators and their applications have been well described by Galthier et al. (1973), by Eckert (1974) and Boulos et al. (1980).

Arc plasmas are formed by striking an arc between two or more electrodes. Arc plasma generators are classified into two categories: the jet plasma torch and the transferred-arc reactor.

In a jet plasma torch, the arc is struck between a pair of electrodes. The plasma-forming gases (or plasmagen gases) are introduced into the arc where they are heated. The hot plasma gases are then ejected at high velocity out of an exit nozzle. The various types of jet plasma torches in existence, their design, operating characteristics and the methods used to stabilize the arc are well

described by Kassabji and Fauchais (1981). The objectives of the jet plasma torch are to produce a hot gas which can then be used for heating, chemical synthesis or drying. The applications and uses of jet plasma torches have been reviewed by Fauchais et al. (1981, 1983). A description of some of the commercially available systems is given by Camacho (1982), Hartman (1982) and Fey et al. (1982).

In a transferred-arc reactor, the material to be treated acts as one of the electrodes, generally the anode. The efficiency of this device is generally higher than the non-transferred plasma torch because the heat transferred to the anode contributes to the process and is not lost as in non-transferred devices.

A review of transferred-arc theory, reactors and applications will now be conducted since a transferred-arc plasma reactor is the focus of attention of this thesis.

TRANSFERRED-ARC PLASMAS

A transferred-arc can be divided into three regions. The anode region, adjacent to the anode surface, the cathode region, adjacent to the cathode and the arc column generated between the two. The voltage gradients near both the anode and cathode surfaces are very steep (particularly near the anode) while that of the arc

column is in general less steep and constant with arc length. This is shown in Figure 3. The nature of the arc voltage characteristics in all three regions is a function of the anode and cathode materials, plasmagen gas, gas velocity arc current and arc stabilization. Each of these three regions will now be discussed separately.

ARC COLUMN

The arc column forms the bulk of the plasma volume in a transferred-arc reactor. The electrical characteristics and methods of arc stabilization are important considerations in the design of this type of reactor. The arc column is also a major source of radiant energy which must be used effectively in order to have efficient energy utilization. A knowledge of the gas composition within the arc column is critical when attempting to measure arc properties and also when attempting to perform dissociation reactions in the reactor.

i. Electrical Characteristics

The electrical characteristics of the arc column depend on the plasmagen gas, and on the gas velocity, method of arc stabilization and total arc power. It also depends on the anode and cathode fall voltages which are in turn functions of all the above factors in addition to electrode materials and geometry.

FIGURE 3

THE THREE REGIONS OF A TRANSFERRED-ARC

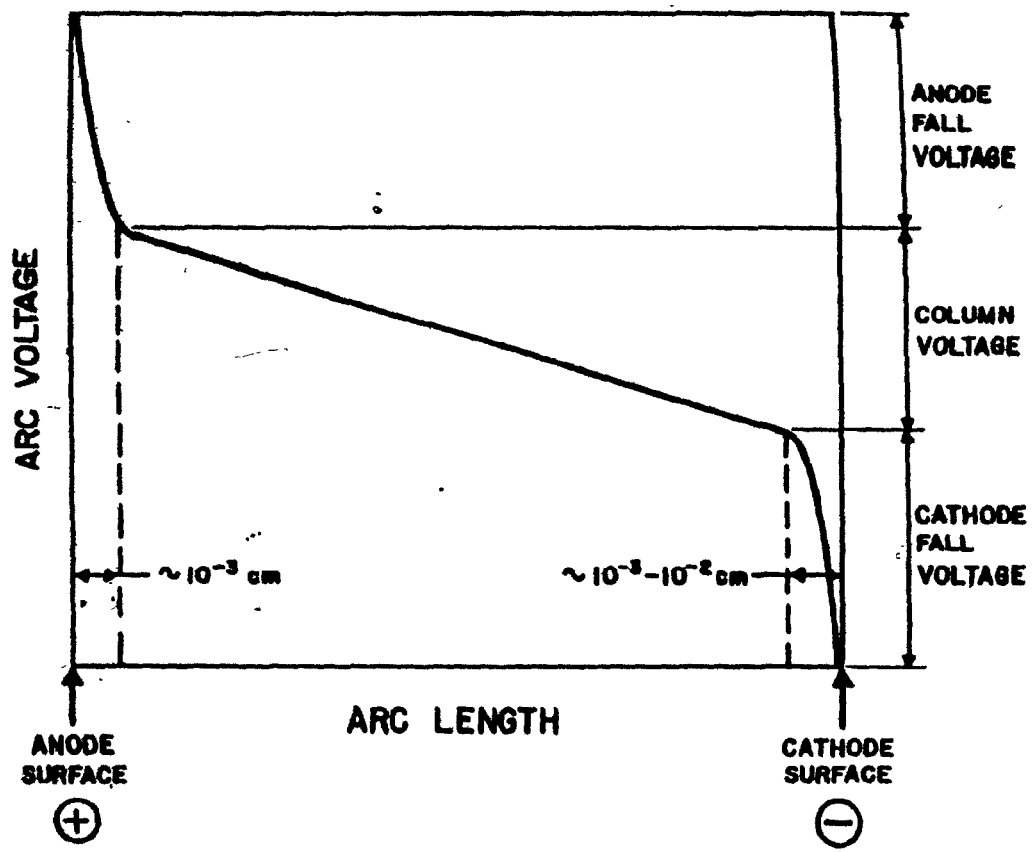
ANODE
FALL
VOLTAGE
COLUMN
VOLTAGE
CATHODE
FALL
VOLTAGE
ARC VOLTAGE
~10⁻³ cm
~10⁻³-10⁻² cm
ARC LENGTH
ANODE
SURFACE
CATHODE
SURFACE
⊕
⊖

The electrical characteristics of an argon transferred-arc plasma has been studied in detail by Choi and Gauvin (1982). They measured the current voltage characteristics of the plasma arc as a function of arc length, cathode nozzle diameter and arc current using a solid water-cooled copper anode. Some of their results are presented in Figure 4. Using a molten copper anode, slightly lower arc voltages were observed at higher currents. As is evident from Figure 4, the arc voltage is strongly dependent on arc length and inlet gas velocity (at the cathode), but much less on the current. Similar measurements were performed by Olsen (1959).

Mehmetoglu and Gauvin (1983), while investigating voltage, temperature and velocity characteristics of an argon transferred-arc discovered that the plasmagen gas velocity and not its flow rate had a major effect on arc voltage. Thus reducing the nozzle diameter at the cathode to increase the gas velocity, with the flow rate unchanged, increased the arc voltage noticeably.

Tsantrizos and Gauvin (1982) repeated this work using nitrogen as the plasmagen gas. The general behaviour was nearly the same as in the case of argon with the important difference that the total arc voltage was in all cases nearly double that of an argon plasma. Their results are shown in Figure 5.

FIGURE 4

ARGON ARC VOLTAGE VARIATION WITH ARC LENGTH

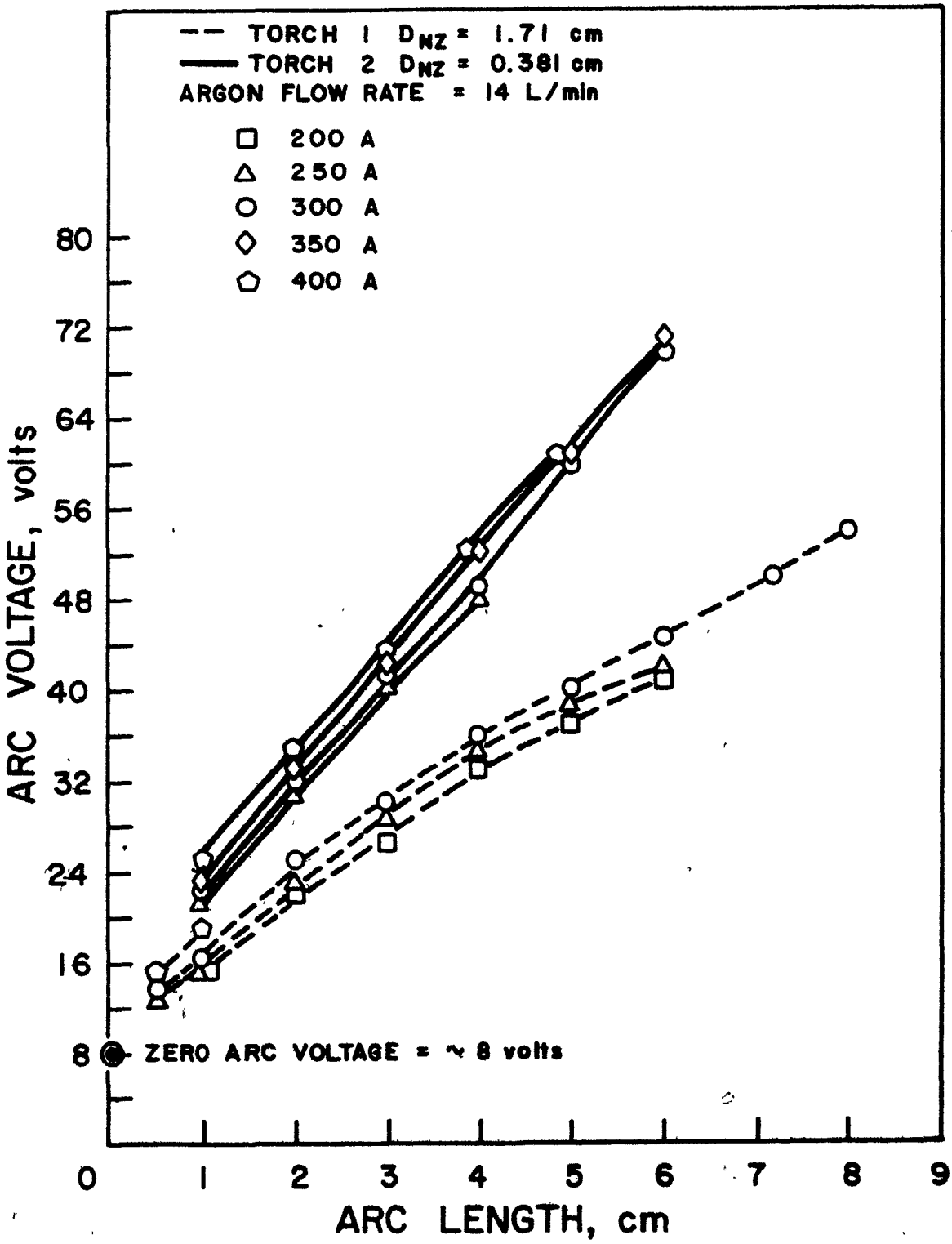
-- TORCH 1 D_{NZ} = 1.71 cm
—— TORCH 2 D_{NZ} = 0.381 cm
ARGON FLOW RATE = 14 L/min
200 A
250 A
300 A
350 A
400 A
ARC VOLTAGE, volts
80
72
64
56
48
40
32
24
16
8
ZERO ARC VOLTAGE = ~ 8 volts
0
1
2
3
4
5
6
7
8
9
ARC LENGTH, cm

FIGURE 5

NITROGEN ARC VOLTAGE VARIATION WITH ARC LENGTH

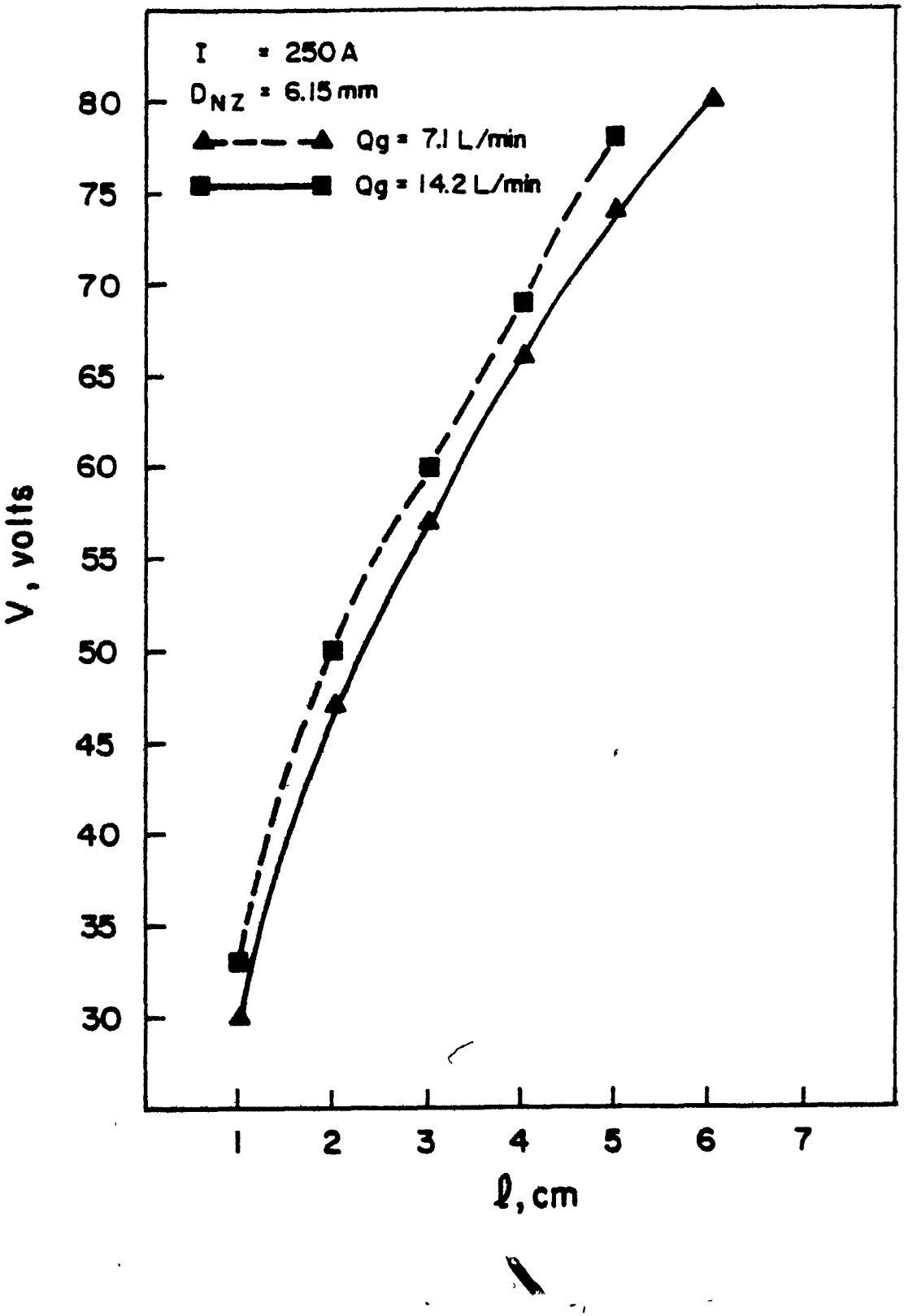
I = 250 A
D_{NZ} = 6.15 mm
Qg = 7.1 L/min
Qg = 14.2 L/min
V, volts
80
75
70
65
60
55
50
45
40
35
30
1
2
3
4
5
6
7
ℓ, cm

ii. Arc Column Energy Balance

The energy balance for a radiative high-pressure thermal arc can be written by subtracting the radiative power density P_r from the power density released by heating in the Elenbass-Heller Equation (Hoyaux 1968):

$$\sigma E^2 - P_r = -\frac{1}{r}\frac{d}{dr}(r\,k\,dT/dr) \qquad (1)$$

where σ = the electrical conductivity

k = the thermal conductivity

E = the electric field (assumed to be uniform)

The solution to this equation can only be solved numerically since both σ and k vary with temperature.

Mehmetoglu and Gauvin (1983) have shown that the amount of radiation emitted by an arc column is primarily a function of the gas used, the arc length and the applied current.

iii. Arc Stabilization

Electric arcs by their nature tend to be unstable. For example, for the arc column shown in Figure 6, if a force F_1 were to be applied to displace the plasma arc column off its axis, a force F_2 would be created by the displacement of the column from

FIGURE 6

ARC ELECTROMAGNETIC INSTABILITIES

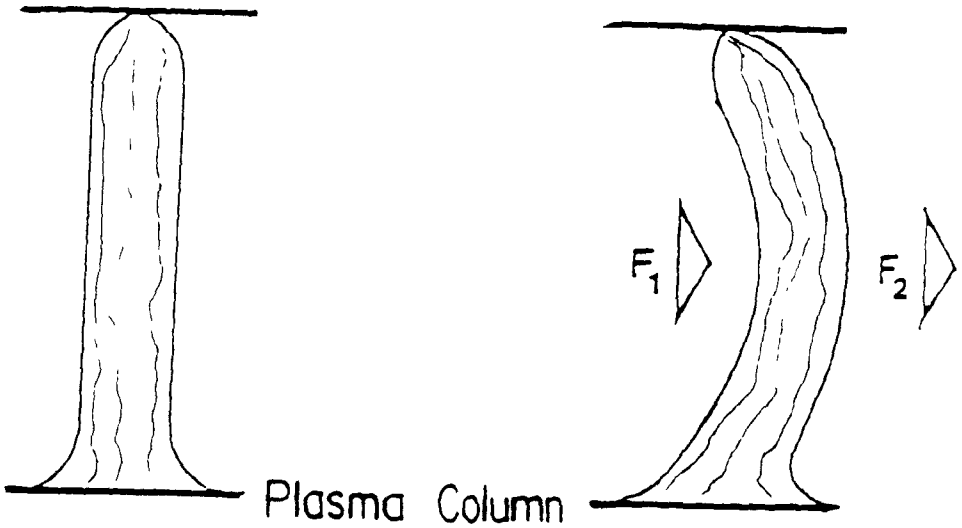
F1
F2
Plasma Column

its neutral axis and the direction of the force would be such as to magnify the displacement. Thus the displacement will be emphasized and made larger until the column is extinguished.

The self-induced magnetic lines of force $\vec{B}$ are concentrated inside the bend and are dispersed outside the bend of the displaced arc column. The effect of concentrating the magnetic lines of force results in a Lorentz force ($\vec{F} = \vec{J} \times \vec{B}$) interaction between the plasma arc column and the self-generated magnetic field. The direction of the Lorentz force is such as to magnify the initial bending of the plasma column. This effect is the cause for lightning discharges and other arcs in nature being jagged and short-lived.

In order to have a continuous stable arc it is necessary to utilize a method of arc stabilization. Numerous methods have been identified. The simplest form of arc stabilization is wall stabilization. In this situation, the arc column is surrounded by a cold cylindrical wall. Any deviation of the arc column towards the wall will result in an increase in heat losses to the wall. This will reduce the column temperature and hence its electrical conductivity The arc is thus encouraged to return to its original axis.

The arc can be stabilized by transpiration when a cold sheath of gas is injected into the annular region between the arc and a cylindrical wall surrounding the arc. This gas also serves to cool the cylindrical wall. The arc is stabilized in much the same manner as in a wall-stabilized arc.

The third method of stabilization is vortex stabilization. In this case either a liquid or a gas is injected in a tangential manner along the inner surface of the cylindrical wall confining the arc. In the case of a gas, the swirling gas motion establishes a pressure gradient which is everywhere centrally-directed and forces the column to remain on the cylinder axis, as shown in Figure 7 The tangentially-injected gas also serves to cool the cylindrical wall. When a liquid is injected tangentially along the inner surface of the cylindrical wall, its tangential motion ensures that it flows along the wall surface because of the centrifugal forces. The liquid serves to cool the wall. Also, as the liquid evaporates, a region of relatively cool gas is formed between the arc and the walls. The arc is thus prevented from wandering from its axis in much the same manner as transpiration stabilization. This method of stabilization was first investigated by Maecker (1951).

The arc can be stabilized by an external magnetic coil. The magnetic field generated by the coil interacts with the plasma in a direction normal to the direction of the magnetic field. The magnetic lines of force can be made to point to the center axis of the arc, stabilizing and constricting the latter.

Sheer et al. (1973) while investigating the use of plasma arcs for the simulation of reentry vehicles designed a "fluid convection cathode". The cathode assembly shown in Figure 8 is comprised of a conical cathode tip surrounded by a concentric

FIGURE 7

RADIAL PRESSURE VARIATIONS OF VORTEX-STABILIZED ARC DUE TO GAS SWIRL

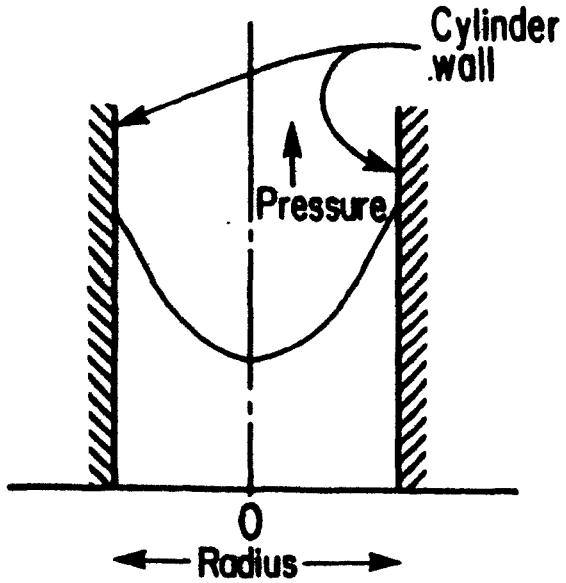
Cylinder
wall
Pressure
0
Radius

FIGURE 8

FLUID CONVECTION CATHODE

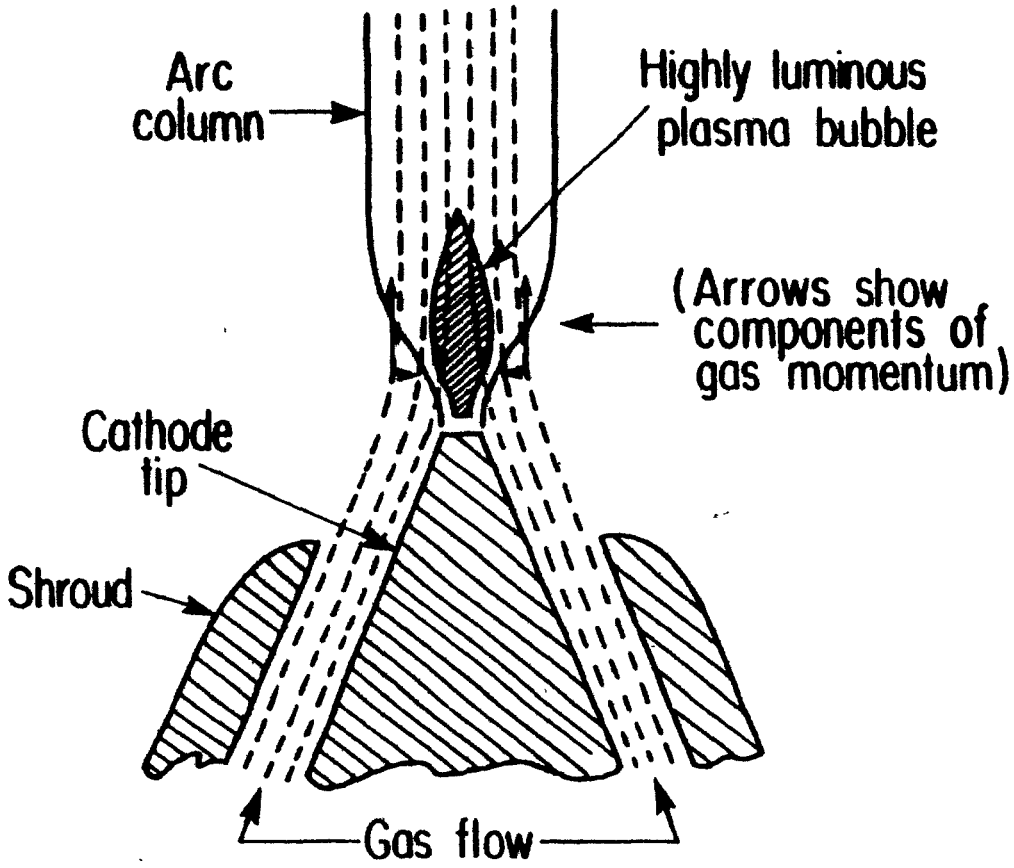
Arc column
Highly luminous plasma bubble
(Arrows show components of gas momentum)
Cathode tip
Shroud
Gas flow

sheath nozzle. The gas is injected across the column in the region of the contraction zone near the tip of the cathode. This is the region of the arc column where a natural inwardly-directed pressure gradient exists as a result of the MHD body force due to the non-uniform self-magnetic field of the contraction zone. This technique of injection has a favorable influence on the column properties. The convergent flow has a component parallel to the axis, which is azimuthally invariant and which exerts a strong stabilizing effect on the column. The flow also has a centrally-directed radial component of momentum, which exerts a fluid mechanical constriction on the column. This causes an increase in column temperature and voltage gradient.

Sheer et al. (1982) and Kassabji and Fauchais (1981) have extensively reviewed the various methods of arc stabilization.

iv. Arc Gas Composition

Since LTE (local thermodynamic equilibrium) exists in thermal arc, at least away from surfaces or the arc edges, the degree of ionization can be calculated thermodynamically from the ionization potential, using the Saha Equation. In logarithmic form: (from Howatson 1976)

$$\log_{10}\left[x^2/(1-x^2)\right]P = -5040\,V_i/T + (5/2)\log_{10} T - 6.5 \qquad (2)$$

where P = pressure (atm)

T = temperature (K)

x = degree of ionization (fraction)

V_i = ionization potential (volts)

Olsen (1959) calculated the plasma composition at various temperatures using the Saha Equation and using the assumption of the perfect gas law, LTE and quasi-neutrality. From this, Chang and Szekely (1982) show the fraction of gases ionized versus temperature at one atmosphere (Figure 9).

CATHODE REGION

The cathode fall region is an electrically connecting zone between the cathode and the arc column, characterized by a marked potential drop. Choi (1980), in his thesis, gives an extensive review of the pertinent theory and relevant literature dealing with this region of the arc.

i. Cathode Fall Voltage

Few accurate measurements of the cathode fall voltage have been made in thermal arcs, owing to the harsh environment and small

FIGURE 9

DEGREE OF IONIZATION OF SEVERAL GASES VERSUS TEMPERATURE

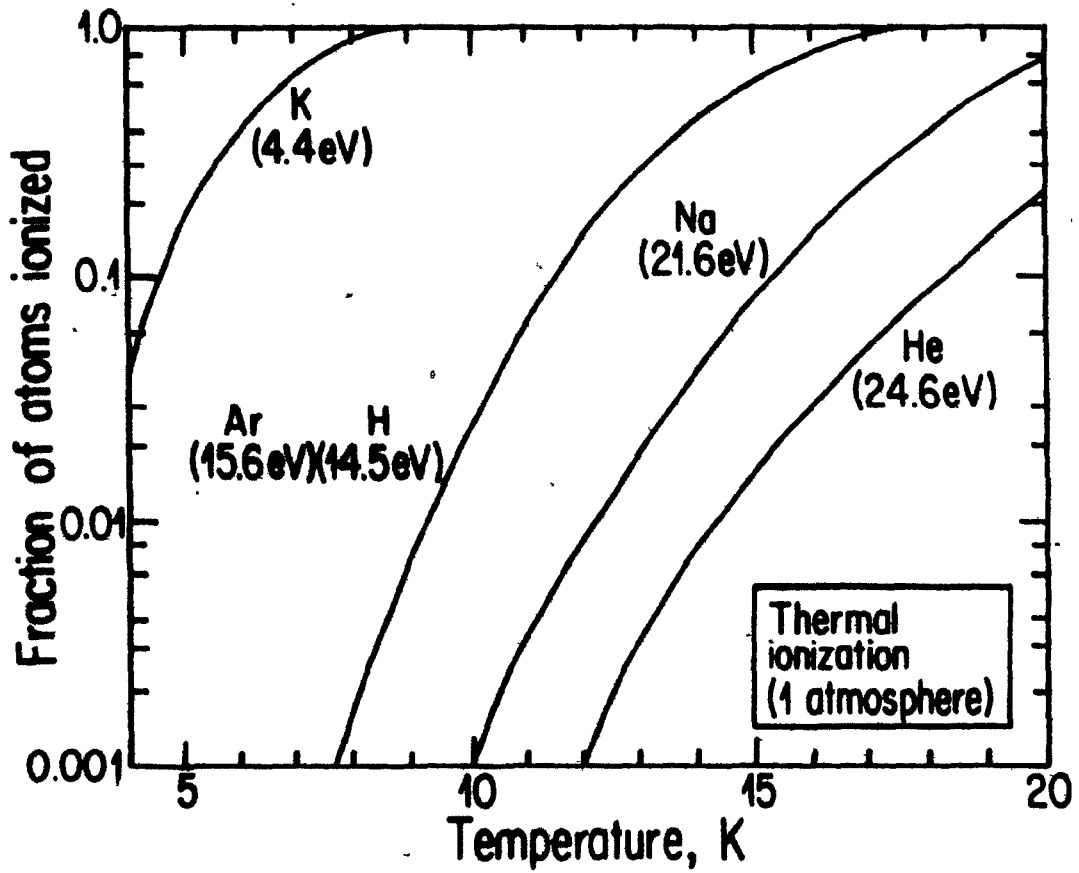
1.0
0.1
0.01
0.001
Fraction of atoms ionized
K
(4.4eV)
Na
(21.6eV)
He
(24.6eV)
Ar
(15.6eV)
H
(14.5eV)
Thermal
ionization
(1 atmosphere)
5
10
15
20
Temperature, K

distances over which the fall voltage occurs. The thickness of the cathode fall as well as the anode fall region is in the order of one mean free path length of the electrons. For atmospheric-pressure, high-intensity arc, this thickness is in the range of 10^{-3} to 10^{-2} mm. The transition region would have a thickness of the order of one millimeter.

ii. Cathode Materials

Cathode can be classified as being either hot or cold. Hot cathodes depend on thermionic emission for the ejection of electrons into the arc. It is possible to calculate the current density due to thermionic emission with the Richardson-Dushman Equation:

$$J_s = A\, T^2 \exp(-e V_\phi / KT) \qquad (3)$$

where J_s = saturation current density

A = 60 A/cm^2K^2

e = 1.6×10^{-19} (electron elementary charge)

K = Boltzmann's constant

V_ϕ = work functions

Guile (1971) has measured the work function for a number of materials in an argon atmosphere. His data are reproduced in Figure 10.

FIGURE 10

THERMIONIC WORK FUNCTIONS VERSUS

BOILING TEMPERATURE OF VARIOUS METALS

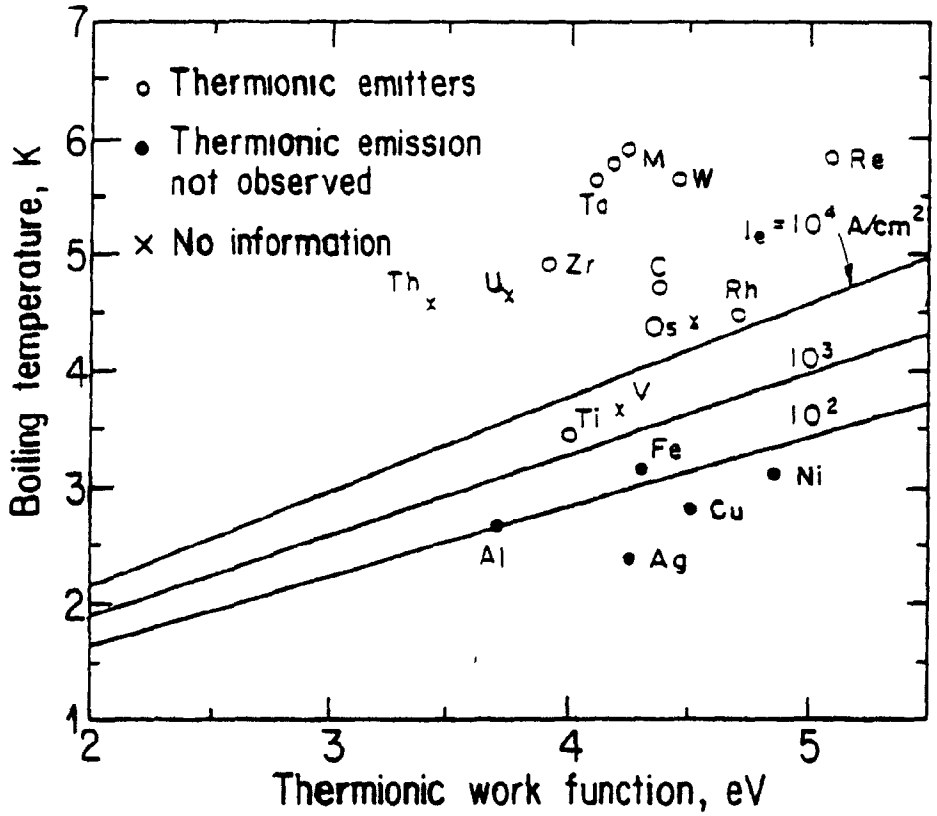
Boiling temperature, K
Thermionic work function, eV
o Thermionic emitters
• Thermionic emission not observed
× No information
$I_e = 10^4$ A/cm^2
10^3
10^2
Th
U
Zr
C
Rh
Os
Ti
V
Fe
Ni
Cu
Al
Ag
Ta
M
W
Re

The most commonly-used hot cathode material is thoriated tungsten shaped to a point (for less than 1000 A) or as a button (up to 5000 A) Tungsten cannot be used with aggressive oxidizing gases. Depending on the plasmagen gas and current density, a life time ranging from 200 hours to 1000 hours can be expected

Cathodes for which the electron emissions are ascribed to field emissions are referred to as non-thermionic or cold cathodes, because the overall temperatures of the cathode are substantially below that required for thermionic emissions These cathodes are most often made of copper and can operate in oxidizing gases such as air with lifetimes of up to 1000 hours. Factors affecting electrode erosion and measurements of electrode erosion rates have been reported by Wilson (1955), Fey and McDonald (1979) and Guile (1981) Holm (1949) calculated by means of an energy balance on the cathode spot the erosion rates of tungsten, copper and carbon cathodes for various currents Below 1000 A, tungsten had the lowest erosion rate. Above 1000 A, a carbon cathode would have the lowest erosion rate and copper the highest.

ANODE REGION

The anode fall region, like the cathode fall region, is an electrically connecting zone between the anode and the arc column, and is characterized by a marked potential drop Choi (1981)

in his thesis has extensively reviewed the pertinent theory and literature dealing with this region of the arc

1. Anode Fall Voltage

The anode fall voltage is difficult to measure or estimate with good accuracy Direct (based on probe measurements) and indirect (based on anode energy balance) measurements of anode falls have been reported The errors involved in these measurements are usually large, sometimes exceeding 100 percent

Busz-Peuckert and Finkelburg (1955, 1956) using a tungsten cathode and a water-cooled copper anode found that the anode fall voltage for an argon plasma varied with both arc length and current and concluded that it was related to the temperature of the plasma immediately adjacent to the anode. For an argon arc, they measured anode fall voltages from as low as 1 volt to a maximum of 12 volts at high arc-lengths and low arc-currents.

Cobine and Burger (1955) used the ionization potential of copper (7 68 eu) as the probable upper limit of the anode fall voltage and zero as the minimum limit, while investigating the energy transfer to the anode and anodic erosion rates

Choi and Gauvin (1982) measured total anode and cathode fall voltages for an argon transferred-arc with a tungsten cathode and copper anode at between 6 5 and 8.5 volts Tsantrizos and

Gauvin (1982) using a similar arrangement to that used by Choi measured the combined anode and cathode fall voltages of nitrogen at between 15 and 20 volts.

Dinulescu and Pfender (1982) have demonstrated that the anode fall voltage could become negative in the presence of a diffuse arc. This was confirmed by Choi and Gauvin (1982) by means of an anode energy balance.

ii. Anode Energy Balance

An energy balance on an anode must take into account all the modes of energy transfer to and from the anode.

A simple anode heat transfer model for a cold (solid) anode was proposed by Schoeck (1963) According to his model, the energy entering the anode surface consisted of heat transfer by convection (Q_{conv}) from the plasma jet through the boundary layer, radiative heat transfer from the arc to the anode (Q_{ra}), energy supplied by kinetic energy of the electrons comprising the arc current and penetrating the anode surface (Q_{jw}) and the heat of condensation of the electrons (work function) penetrating the anode surface (Q_{ϕ}). The energy leaving the anode surface consisted of the heat conducted away into the anode (Q_c) and, the heat radiated by the anode surface (Q_{re}). Thus the following expression for the

energy based on unit area could be written.

$$Q = Q_c + Q_{re} = Q_{conv} + Q_{ra} + Q_{jw} + Q_{\phi} \tag{4}$$

For a molten anode, such as that in a plasma melting furnace, a slightly different energy balance must be used. The energy transferred to the anode would consist of the following terms. the kinetic energy caused by the acceleration of the electrons through the anode fall (Q_a), the thermal energy transferred to the electrons from the hot gas in the arc column (Q_k) (Thompson effect), the energy equal to the work function of the material (Q_{ϕ}), the energy transferred by convection from the hot gases (Q_{conv}), by conduction from the hot gases (Q_{cd}), by radiation from the hot gases (Q_{ra}) and by chemical reaction and joule heating (Q_{chj}). Energy losses would consist of energy lost by conduction (Q_c), evaporation of the metal (Q_{evap}), radiation from the metal surface (Q_{re}), and energy lost by sputtering (Q_{sp}) and the energy conducted away by the surrounding gases (Q_{cs}). Thus the overall energy balance equation can be expressed as follows:

$$Q = Q_c + Q_{evap} + Q_{re} + Q_{sp} + Q_{cs} = \tag{5}$$

$$Q_{conv} + Q_{cd} + Q_{ra} + Q_{chj} + Q_a + Q_k + Q_{\phi}$$

The last three terms of Equation (5) can be expressed in the following manner.

$$Q_a = I \cdot V_a \tag{6}$$

$$Q_\phi = I \cdot V_\phi \tag{7}$$

$$Q_k = I \cdot V_k = I \, (5/2 \, (k \, (T_e - T_w) \, / e)) \tag{8}$$

where V_a is the anode fall voltage, V_ϕ is the work function, k is the Boltzmann constant, T_e is the electron temperature, T_w is the wall temperature, and e is the electronic charge.

Cobine and Burger (1955) while studying anode energy transfer with a high-current short-duration arc (1/120 s) found that the power losses by radiation and heat conduction within the electrode are very much smaller than the power lost by the evaporation of the metal vapour. By simplifying Equation (5) they were able to estimate the heat lost by metal evaporation and thus the anode erosion rate and anode spot temperature for a number of metals.

Choi (1982) measured heat transfer to the anode using a water-cooled flat copper anode. He utilized a simplified form of Equation (4):

$$Q = Q_c = Q_{ra} + Q_{conv} + Q_a + Q_k + Q_\phi \tag{9}$$

He measured the heat transfer to the anode by convection and radiation. He was able to estimate the heat transfer due to the work function (Q_ϕ) and the Thompson effect (Q_k). He also measured the energy transfer out of the anode by the cooling water. Rewriting Equation (8) he was able to estimate the anode fall voltage.

$$Q = Q_c = Q_{ra} + Q_{conv} + I\ (V_\phi + V_k + V_a) \qquad (10)$$

The fall voltage thus measured a varied range from -2.7 to 1.3 volts for an argon arc. The amount of energy transfer accounted for by the three electrical terms $[I\ (V_\phi + V_k + V_a)]$ was 55 to 75 percent of the total energy transferred to the anode. The energy transfer by convection was small for long arcs, but was significant for shorter arcs (less than 2 cm). The energy transfer by radiation from the anode was small in all cases studied.

PLASMA FURNACE DESIGN

There is little doubt that the perception of plasma technology as a promising tool for industrial chemical and metallurgical processing has improved sharply during recent years. This is due in part to the availability of commercial plasma generating systems capable of reliable performance at powers of 10 MW and higher, and also to the realization that the use of electricity as the major source of energy

does not necessarily affect adversely the economic viability of a process. In many applications, the quality of the heat energy supplied by a thermal plasma due to both its very high temperature level (or its thermodynamic "availability", in other words) combined with the fact that the heat can be transferred by mixing directly to the system (that is, without the necessity of a heat transfer surface) is so high that it frequently outweighs the apparent price advantage of fossil fuels. In addition, the plasmagen gas may frequently be used as a reactant for such reactions as oxidation, reduction, chlorination, etc.

The economic feasibility of a process depends, of course, on many more factors than the cost of electricity, and the unique characteristics of a plasma system must be thoroughly understood before a reliable techno-economic analysis can be undertaken.

So far, the attention of the workers in the field has been largely directed at the behaviour of the various torches which have been developed and at the characteristics of the plasma flames or transferred-arcs they generate. A great deal of effort has also been devoted to studies of the kinetics of reactions performed in a plasma environment and to develop new systems in which the reactions are either impossible or at least very difficult to achieve at lower temperatures. To the author's knowledge, however, very little attention has been given to the design of the reactors in which these reactions are to be performed.

Before describing the latest designs of plasma furnace, which are likely to dominate the field of plasma technology applications, at least in the near future, it is interesting to review very briefly the evolution in design which has occurred in the recent past. Most of these designs have never progressed beyond the laboratory stage but each, in its own way, has contributed to a better understanding of the advantages and disadvantages of using thermal plasmas in chemical and metallurgical processing. Some of these earlier types of furnace have been reviewed by Hamblyn (1977). They include the so-called Expanded Plasma Furnaces, in which an attempt was made to increase the contact time between a particulate feed and a plasma flame by expanding the plasma flame. Whyman (1967) used a rotating water-cooled copper cylinder to achieve this purpose, using the viscous drag-forces at the wall, rotating at up to 1000 RPM, to expand a stationary D.C. transferred-arc at the centerline. Bryant et al. (1970) used this type of reactor to evaporate alumina particles, but plugging and other operational difficulties limited his work to a batch operation.

ROTATING PLASMA FURNACE

Somewhat more promising appeared to be the design of a new generation of rotating furnaces, which can be classified into horizontal, sloping and vertical drum furnaces.

i. Horizontal-Drum Furnaces

Horizontal drums have been studied by Grosse et al. (1963), Foex et al. (1972), and Sayce and Selton (1972). They consist of a drum lined with the material to be treated and they are rotated along their horizontal axis at speeds varying between 500 and 1500 RPM. A plasma jet directed along the horizontal axis at one end of the drum is used to heat the reactor. Material leaving the reactor is quenched and collected at the opposite end. The furnaces have been used sporadically to melt and evaporate refractory oxides on a small scale. Difficulty in feeding the material and withdrawing the product prevented further development.

ii. Sloping-Drum Furnaces

To facilitate withdrawal of the molten products, Yeroushalmi et al. (1971, 1979) inclined the drum at a fixed angle with the horizontal. They used this type of furnace to reduce tricalcium phosphate with silica and coke to produce phosphorus in a continuous mode. Again, difficulties in achieving gas-tight feeding and severe restriction in the level of power that can be used have limited further development.

iii. Vertical-Drum Furnaces

In this type of furnace, the feed material, introduced at the top, is flung by centrifugal forces to the rotating wall where

they form a layer of molten material with a parabolic shape. The plasma flame is directed downward along the axis of the furnace. This type has been used for the study of the melting of alumina and of silica by Howie and Sayce (1974) and for the fuming of low-grade tin slags by Barret et al. (1975). Bonet (1976) and Sheer et al. (1973) have proposed a variation of the vertical-drum furnace design that would combine the advantages of extended contact times of the rotating drum furnaces and the ability to handle fine particulate of the expanded plasma furnaces. In spite of their conceptual originality, it is difficult to visualize industrial applications based on this design except for very small scales of operation.

RECENT FURNACE DESIGN

Considerable work has been devoted in the past - and is still being devoted - in attempts in contacting a finely-divided feed material directly with a plasma flame. Owing to the high viscosity of a very hot gaseous stream, it is very difficult to inject small solid particles into such a medium. However it was observed by Maecker (1953) that a zone of low pressure existed around the cathode tip into which gas and solid particles could be injected.

Sheer et al. (1973) developed the "fluid convection cathode reactor" to take advantage of this phenomenon. In their most advanced design, the plasma was established between a single cathode and three

transpiration anodes. This enabled them to vaporize silica with an energy expenditure of only 1100 kW per ton. The National Physics Laboratories in the U.K. have developed a more powerful version of this design by replacing the transpiration anodes with plasma jets (Hamblyn 1977).

The difficulty with this design is the impossibility of injecting the feed material into the plasma with 100% efficiency. At best, 80 to 85% of the powder can penetrate. This problem makes it impossible to effect industrial operations where complete conversion is required, such as in the thermal decomposition of MoS_2 to yield molybdenum metal with a sulphur content of less than 0.15%, which corresponds to a 99.9% elimination of sulphur (Kubanek et al. 1977).

MOLTEN-POOL PLASMA FURNACE

This type of furnace was originally developed as an improved version of the conventional electric arc furnace in which the carbon electrodes were replaced by plasma transferred-arc generators. With the use of a transferred-arc, the molten pool serves as anode, thus releasing the heat from electron-recombination directly into the anode pool.

Molten-pool plasma furnaces can be further classified as either closed-hearth or ingot-withdrawing furnaces.

i. Closed-Hearth Furnaces

Two of the earliest reports on plasma remelting furnaces where the anode consisted of the molten metal product were those of McCullough (1962) and of Magnolo (1964). They utilized a 60-kW Linde Plasmarc furnace to melt 150-kg batches of AISI 4340 steel. The chemical and physical properties of the steels melted in this furnace were claimed to be equal to those of high-quality vacuum-melted steels.

Commercial utilization of this type of plasma furnace commenced in 1973 with the commissioning of a 10-ton plasma furnace by UEB Edelstahlwerke at Freital, East Germany. (Lachner et al. 1973, Esser et al. 1973, 1974.) The furnace was fired with three d.c. 3-MW plasma torches utilizing either argon or a mixture of argon and nitrogen as plasmagen gas. The quality of the produced steel was comparable to that obtained in an electric furnace. (Fielder et al. 1975.) In 1977, a 30-ton furnace was started at the same plant. Features of the 30-ton unit were similar to those of the 10-ton furnace except that a fourth torch had been added. Lugscheider (1981) reports specific power consumption of 450-500 kWh/ton in the 30-ton furnace. In the U.S.S.R., a plasma furnace of 100-ton capacity is now operating using six 3.5-MW plasma torches. (Bhat, 1981.)

Curr et al. (1983) of Mintek in South Africa have recently described an experimental 100-kVA furnace shown in Figure 11, with a

FIGURE 11

MINTEK REACTOR

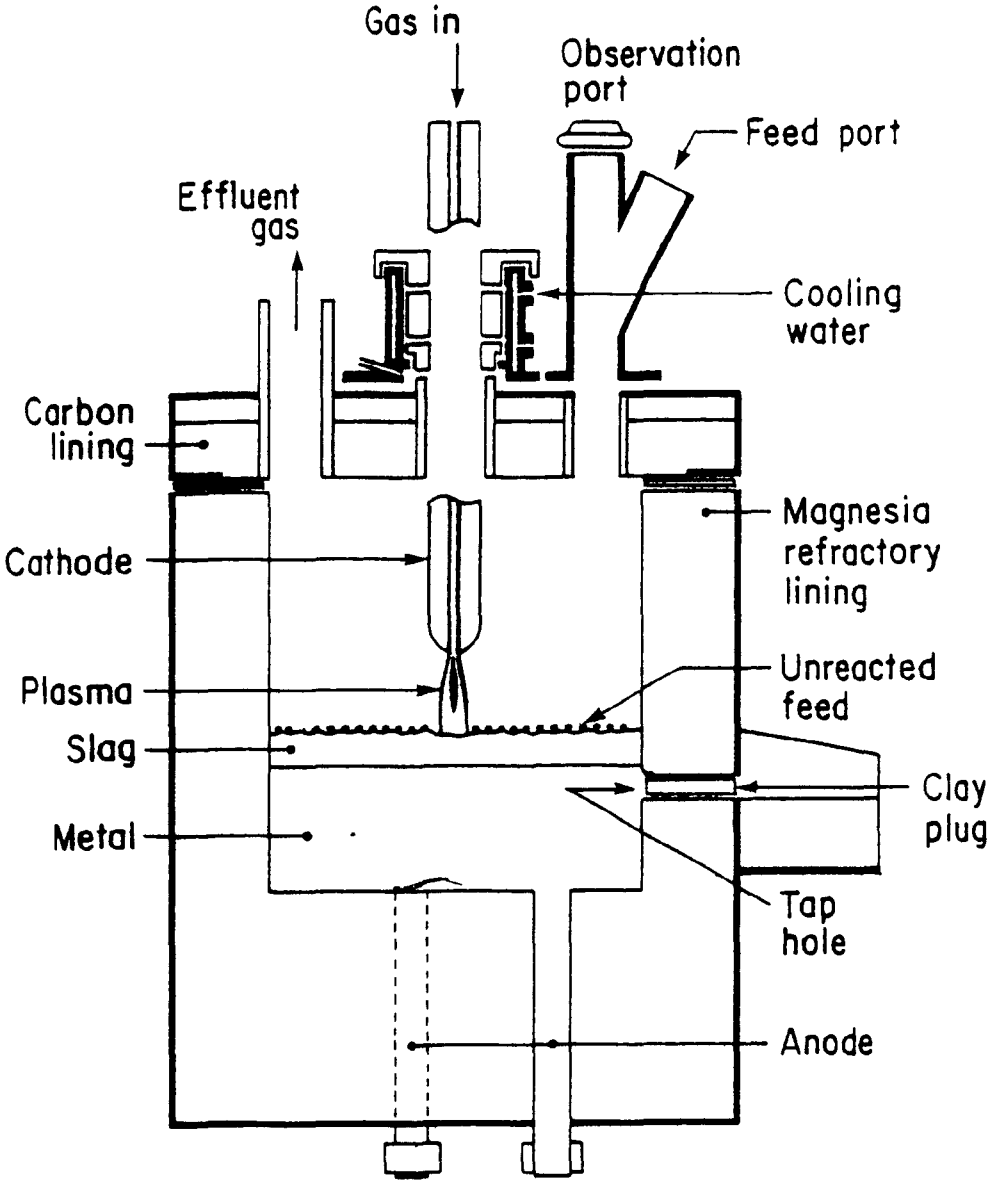
Gas in
Observation port
Feed port
Effluent gas
Cooling water
Carbon lining
Magnesia refractory lining
Cathode
Plasma
Unreacted feed
Slag
Clay plug
Metal
Tap hole
Anode

hollow graphite cathode, through which a mixture of argon and nitrogen was passed as the plasmagen gas Based on this work Middleburg Steel and Alloys have recently ordered a 20-MW plasma furnace from ASEA, Sweden, to be commissioned in October 1984

Pickles et al (1977) described a 3-phase AC reactor developed at the University of Toronto, shown in Figure 12 with the arc struck between three hollow graphite electrodes, through which the plasmagen gas is injected The feed falls by gravity through the chimney where it is pre-treated in counter current contact with the effluent gases before passing through the arc and into the crucible This appears to be a promising design providing the feed material is not too fine and contamination with carbon from the electrodes can be tolerated

A combined induction-plasma furnace shown in Figure 13 has been developed in Japan by Daido Steel Co (Asada and Adachi, 1971). Bhat (1981) has described a 2-ton furnace of this design and its use by Daido Steel Co for producing high-quality resistance steels and super alloys Tezuka et al (1974) have described its use for the melting of nickel base alloys

ii Ingot-Withdrawal Furnaces

A semi-continuous furnace consisting of 3 to 6 plasma torches located radially in order to melt an axially-fed ingot was

FIGURE 12

UNIVERSITY OF TORONTO REACTOR

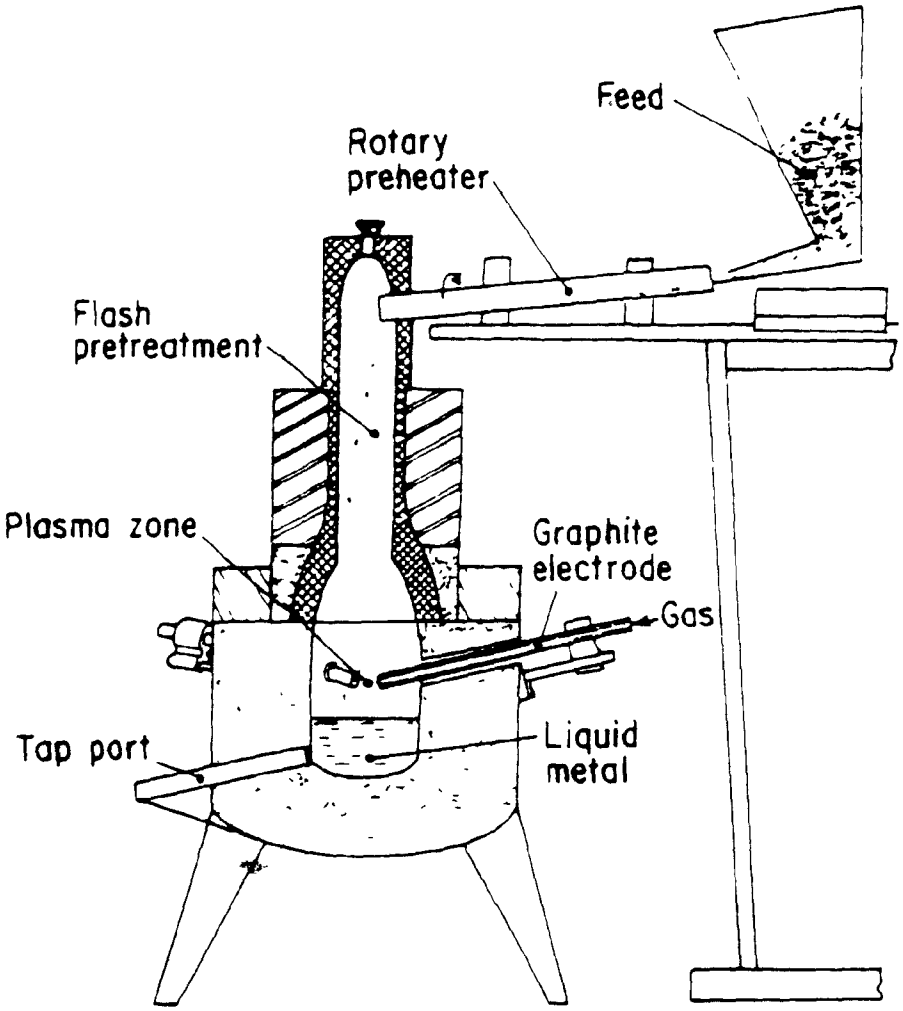
Feed
Rotary
preheater
Flash
pretreatment
Plasma zone
Graphite
electrode
Gas
Tap port
Liquid
metal

FIGURE 13

DAIDO STEEL CO.

COMBINED INDUCTION AND PLASMA FURNACE

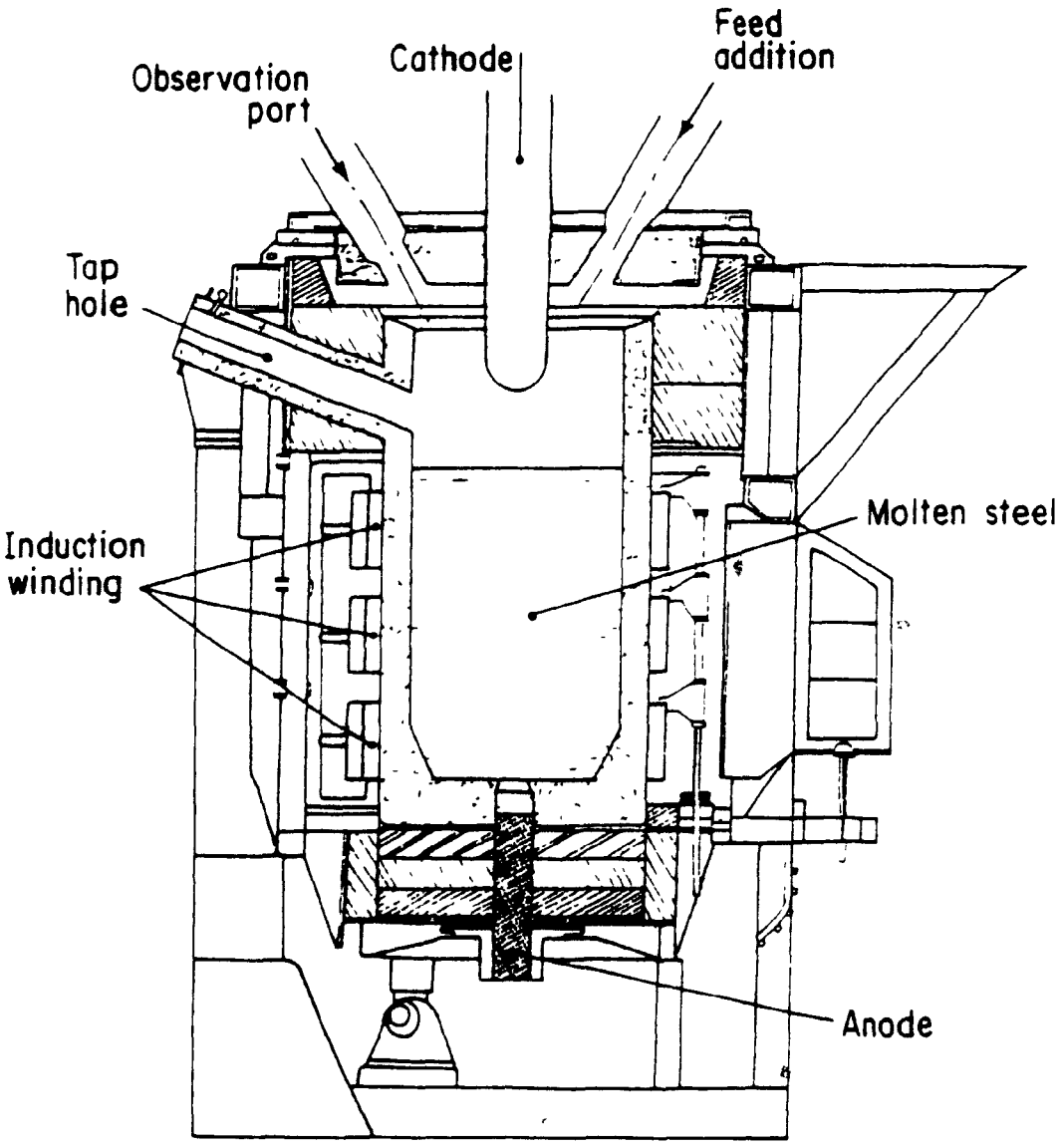
Observation port
Cathode
Feed addition
Tap hole
Induction winding
Molten steel
Anode

developed at the Paton Welding Institute in the U.S.S.R. (Rykalin, 1976). Rykalin (1976) also described high and low-pressure furnaces with an axial plasma torch for melting of horizontal rods as well as a furnace with radial plasma torches for the melting of bulk charges into ingots, that have been developed at the Baikov Institute of Metallurgy.

A low-pressure plasma beam furnace in which a direct-current argon plasma is transferred from a hollow tungsten cathode to the workpiece (Takei and Ishigami, 1971) was developed by Ulvac in Japan. Bhat (1981) has described a 2.4 MW plasma beam furnace installed by Ulvac and used to melt and cast titanium alloys and sponge.

Roman (1983) has described a plasma furnace used by United Technologies U.S.A. for the recovery of highly alloyed scrap in which the scrap is melted into an ingot that is continuously withdrawn.

ROTATING CATHODE FURNACES

In a class by itself is this type of furnace shown in Figure 14 originally conceived by Tylko when employed by Tetronics Limited in the U.K. (1974). Wrongly called an "expanded precessive plasma", the plasma is struck between an orbiting inclined cathode and an anode ring or an anodic pod of molten metal. Feed material is "rained" into the conical high temperature zone thus created. Rotation speeds of up to 2000 RPM were used.

FIGURE 14

TETRONICS FURNACE

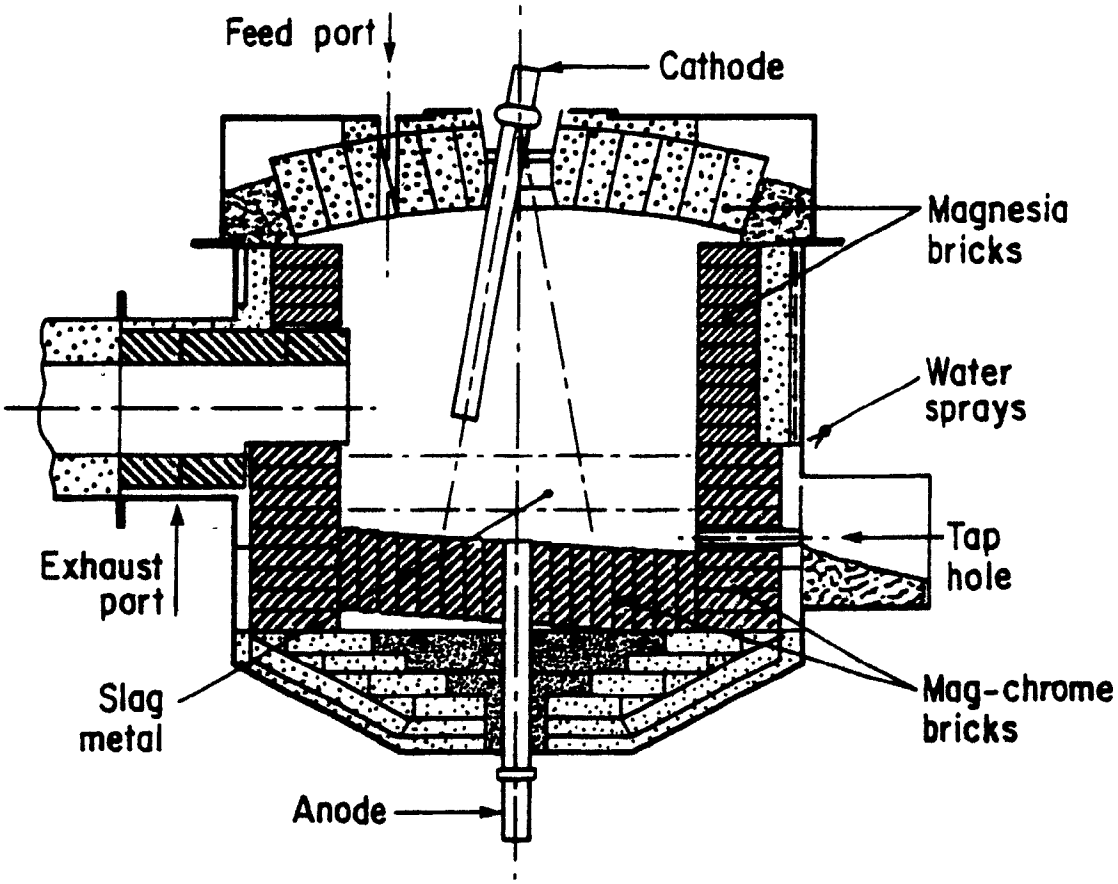
Feed port
Cathode
Magnesia bricks
Water sprays
Tap hole
Exhaust port
Slag metal
Mag-chrome bricks
Anode

After Tylko's departure, Tetronics proceeded with the development of this furnace. A 1400 kW furnace has been constructed in association with Foster Wheeler Limited (1979) and has been used to determine the feasibility of producing a variety of ferroalloys (Monk 1981). On his part, Tylko is continuing his work with K. Reid, at the Mineral Research Centre of Minnesota (Reid et al., 1981).

FALLING-FILM PLASMA FURNACES

Two types of falling-film plasma furnaces, cyclonic and tubular have been developed.

i. Cyclonic Falling-Film Furnaces

Blank and Ward (1967) described the development of a cyclone furnace for the removal of zinc from lead blast furnace slags. Plasma cyclone furnaces permit the processing of highly endothermic reductions or vaporizations, and provide good contact times without the loss of particles in the high velocity gas stream. A 200-kW plasma-fired cyclone furnace for the reduction of silica to silicon monoxide has been patented (Hamblyn et al., 1976).

ii. Tubular Falling-Film Furnaces

Chase and Skriven (1974) patented a laboratory falling-film plasma furnace utilizing a d.c. plasma jet torch. The furnace

was used to reduce ilmenite and tricalcium phosphate. The ore particles were fed tangentially into the reactor where they were forced to the reactor wall by centrifugal forces. There they melted and formed a falling-film of molten ore with which the gaseous phase could react.

MacRae et al. (1979) of the Bethlehem Steel Co. developed a more sophisticated version shown in Figure 15 in which they reduced hematite with mixtures of hydrogen and methane, and vanadium trioxide with coke fines, at powers up to 1 MW. In this reactor, powders were injected tangentially and centrifuged onto the reactor inner wall which functioned as the anode, to form a falling film. The film provided a reaction site for the reactants so that good residence times and contact were achieved. The film also thermally insulated and protected the water-cooled anode.

Kassabji et al. (1978, 1981) have built a similar design, the difference being that the sleeve was constructed of segmented graphite rings in order to allow the stretching of the arc, following its initiation. The reactor has been operated at powers up to 700 kW for the reduction of iron ore with hydrogen. In both furnaces the molten bath in the bottom crucible is heated only by convection in contact with the fairly cool spent gases.

The most recent falling-film furnace is the Noranda - Hydro-Québec furnace designed by Gauvin and Kubanek (1981) and

FIGURE 15

BETHLEHEM STEEL CO. REACTOR

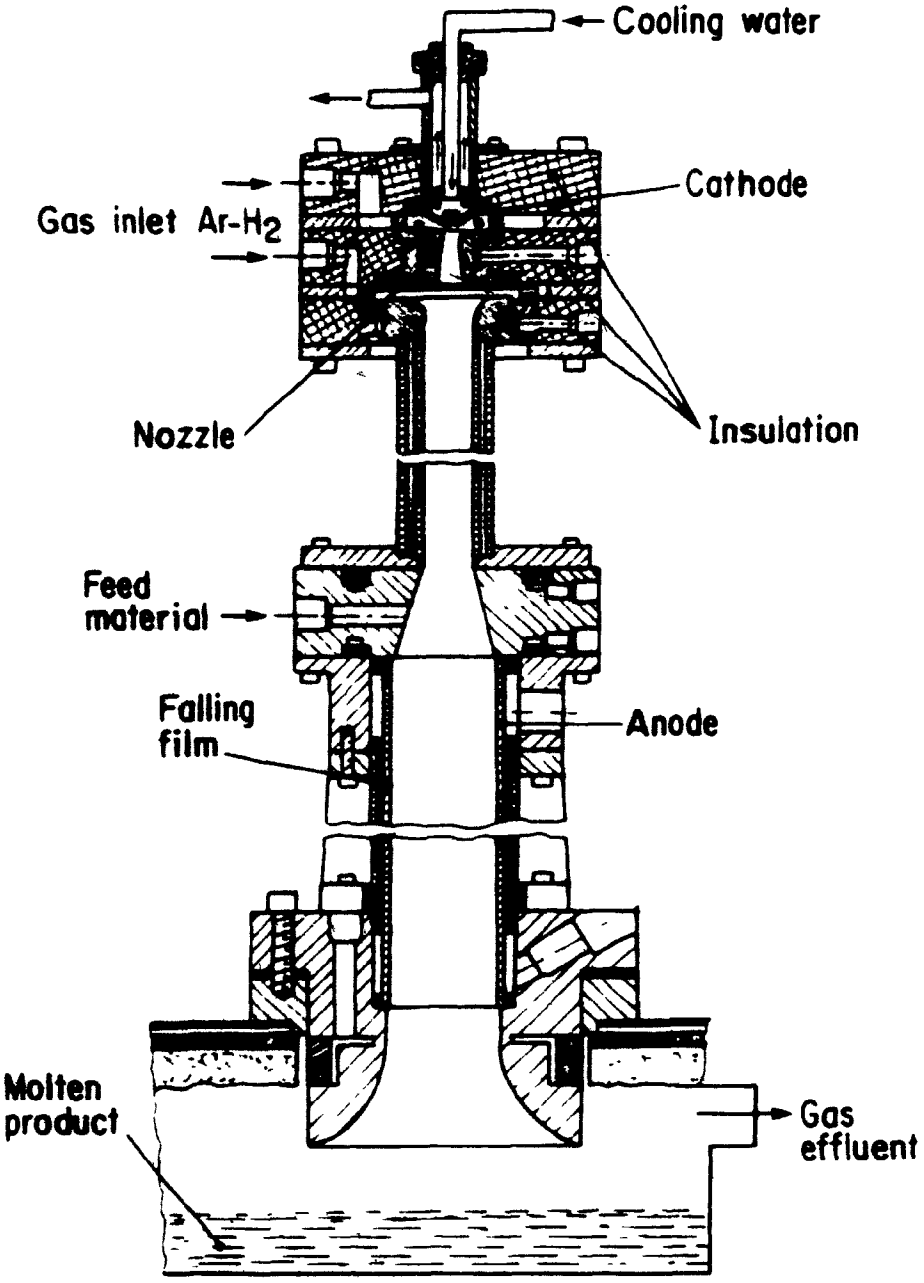
Cooling water
Cathode
Gas inlet Ar-H2
Nozzle
Insulation
Feed material
Falling film
Anode
Molten product
Gas effluent

shown in Figure 16. This furnace differs from the preceding ones in that the molten bath in the bottom crucible serves as the anode. The plasma arc column extends over the entire length of the reactor. The charge in the bottom crucible can be melted much in the same manner as in the molten-pool furnaces when the furnace is charged and ignited. Once started, feed particles are fed tangentially at the top of the sleeve and form a falling film along its inner surface, where the desired high-temperature reaction begins to occur, maintained by the intense radiation from the arc. This type of reactor is very efficient as the falling film absorbs all of the radiant heat generated by the plasma arc. The other major region of heat transfer from the arc is at the anode, which serves to heat the molten pool in the bottom crucible, thus enabling it to be also used as a reaction site. The feed carrier gas which is optically thin serves to stabilize the arc by its centrifugal motion, pick up little radiant heat from the plasma and helps maintain the walls and roof of the furnace cool. As no cooling is required at the sleeve and at the anode this reactor is very efficient. Also as both the sleeve and crucible (anode) can serve as reaction sites, residence times for reactions can be adjusted to meet the needs of the reaction taking place.

This reactor will be described in greater detail in the Experimental Section, as the study of its operating characteristics forms the major objective of this thesis.

FIGURE 16

NORANDA - HYDRO-QUÉBEC REACTOR

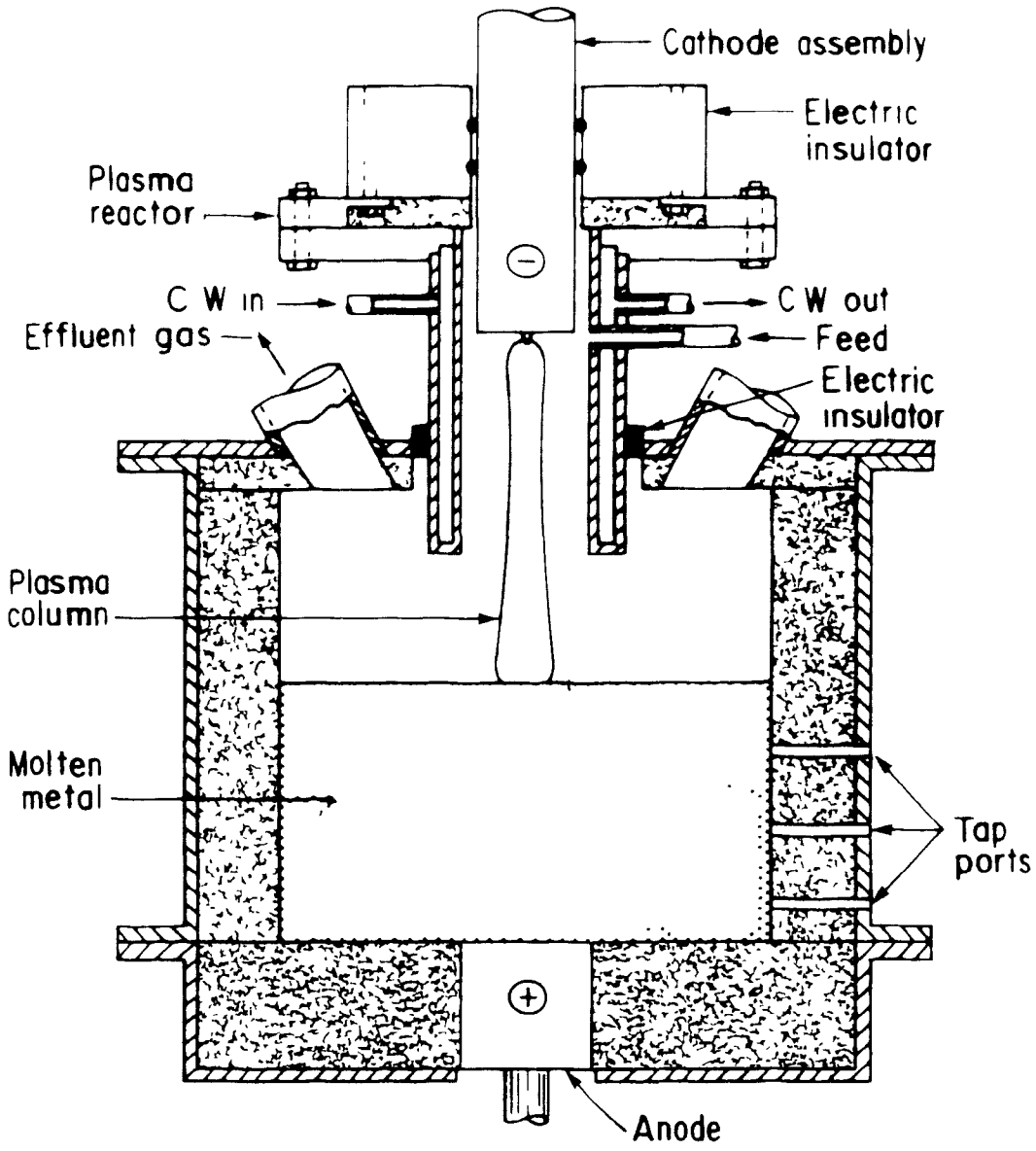
Cathode assembly
Electric insulator
Plasma reactor
C W in
C W out
Effluent gas
Feed
Electric insulator
Plasma column
Molten metal
Tap ports
Anode

The latest developments in the design and operation of plasma devices and reactors has been described in a series of review articles by Fauchais (1982), Rykalin (1976, 1980), Gauvin et al. (1980), Aubreton and Fauchais (1978), Hamblyn (1977), Bhat (1972, 1981), and Savce (1971).

THE APPLICATIONS OF PLASMAS TO EXTRACTIVE METALLURGY

Plasma metallurgical processes are beginning to make an appearance on a commercial scale. The commercialization of plasma processes stems in large part from the development of advanced highly efficient plasma generating devices. The development of plasma reactors has not, however, progressed nearly as fast. The oil crisis of the 1970's which caused oil and fossil fuels in general to increase in price much more rapidly than electrical energy also helped spur the development of commercial plasma processes. Finally, the reluctance of operators to switch from conventional fuels to electricity is slowly disappearing. The widespread use of electric furnaces in steelmaking based on scrap, in the production of highly-alloyed steels and of ferroalloys is ample proof that electrical energy can be used industrially on an economic basis in many applications.

The advantages of plasma furnaces compared to conventional electric furnaces have been well documented and are based on actual

operating data Bhat 1981, Lugscheider 1981 and Gauvin and Choi 1983 They include

1. Higher melting efficiency compared to similar sizes of conventional electric arc furnaces

2. Ability to produce alloys with low carbon content

3. Superior recovery of the alloy metals contained in the scrap and of those added to the melt.

4. Ability to inject and alloy the melt with nitrogen through the gas phase instead of through the use of expensive nitrogen containing alloys

5. Higher quality product compared to that from conventional electric arc or induction melting furnaces.

6. Achieving low oxygen and hydrogen residuals in the melt.

7. Reduction of iron losses to below two percent.

8. Suppression of noise to a level below 60 dB.

9. Elimination of discontinuous shock loading of the electric power transmission mains (flicker).

10. Thirty percent lower capital investment compared to a modern Ultra High Power (UHP) electric arc furnace system.

Compared to conventional pyrometallurgical reduction and smelting techniques based on fossil fuels, plasma processes would have the following additional advantages

1. Flexibility in reductant selection.

2. Ability to concentrate energy with resultant smaller reactor size and pollution abatement systems

3. Ability to operate independently of oxygen potential

4. Ability to transfer heat energy to the gas phase with high efficiency and without the contamination of combustion products.

5. Much lower capital investment requirements resulting from smaller reactor size and the ability to handle finely-divided feed material, without expensive feed preparation.

6. Reduced manpower needs resulting from continuous operation and ease of automation for plasma processes.

7. Less restrictions in choice of plant location; ability to locate near ore supply as electricity can be transported to the site cheaply and efficiently.

Plasma metallurgical processes that have been developed and demonstrated on either a commercial or laboratory scale include:

1. Plasma melting and remelting

2 Reduction of iron oxides

3 Ferroalloy production

4 Refractory metal production

1. Plasma Melting and Remelting

The largest commercial development of plasma melting and remelting applications has been in the U.S.S.R , East Germany and Japan (Bhat 1981)

At Freital, East Germany, VEB Edelstahlwerke has been operating a 9-MW plasma melting furnace since 1973 and a 30-ton - 20-MW (four torches) furnace since 1977. In the U.S S.R., plasma furnaces of 100-ton capacity are now operating using six 3.5-MW plasma torches. Reportedly these furnaces are being used for smelting ferroalloys and hot metals preparations using a combined charge of steel scrap and direct reduced iron (Bhat 1981) Specific power consumption is 600-650 kWh/ton in the 10-ton furnace and 450-500 kWh/ton in the 30-ton furnace.

Daido Steel Company of Nagoya, Japan has pioneered the use of combined transferred-arc plasma with induction melting furnaces (Asada and Adachi, 1971). These furnaces have been used for the melting and refining of iron and nickel-base alloys (Tezuka et al. 1974). Between 1968 and 1981, Daido Steel designed, built and sold to customers in Japan 28 plasma induction furnaces (Bhat 1981).

They range in capacity up to two tons, depending upon the type of metal or alloy processed. In addition to the many advantages already listed, Daido Steel Company also claim the following:

1. Vacuum-tight enclosure is not required.
2. Repeated charging of scrap or charge can be done easily.
3. Melt rate and therefore productivity are higher than those in conventional induction or electric arc furnaces.
4. Superior removal of impurities through the use of slags, deoxidants and reactive gases.
5. Quality of product similar to that produced in vacuum induction furnaces, but at a lower cost.

Daido Steel Company (Hiratake 1981) have developed a plasma arc melting unit for the processing of nuclear waste. The furnace is capable of melting 1700 200-liter drums per year. It is interesting to note that Thomas Barton, is currently testing at the Royal Military College in Kingston, Ontario, a small experimental unit for the destruction of chemical wastes such as PCB (Barton 1982) indicating a growing interest in waste disposal by thermal means, which appears to be cheaper than more conventional methods. Ulvac has developed a

process using a plasma beam melting furnace for the melting of reactive metals. Furnaces up to 2-4 MW comprised of six 400-kW plasma guns and capable of casting 3-ton slab ingot of titanium and titanium alloys have been put in operation (Bhat 1981) in Japan, China and India. The plasma beam torch is comprised of a hollow cathode transferring an arc to a molten bath which is contained in a continuous-casting mould. The operation is carried out in a vacuum and very small amounts of high-purity argon are fed down the bore of the hollow cathode to create the plasma beam. The plasma beam furnace process eliminates two or three steps when compared to conventional titanium alloy manufacturing. In addition the titanium can be cast into any shape desired.

Plasma arc remelting furnaces up to 3.6 MW in size are being used for the manufacture of high-purity specialty metals and alloys in the Soviet Union (Bhat 1981). The main advantages of the process are (Paton 1966):

1. Remelting in atmospheres of inert or reactive gas.
2. Remelting using thin slag cover.
3. Remelting with simultaneous deoxidation of the metal with hydrogen.
4. Alloying steels with nitrogen.
5. Large surface for gas-metal interactions.
6. Negligible loss of volatile elements.

ii. Reduction of Iron Oxides

Gilles and Clump (1970) investigated the hydrogen reduction of iron oxide in a 25-kW direct-current plasma jet reactor. This work demonstrated the feasibility of this type of reduction, but the energy requirements were approximately 100 times greater than those required theoretically, owing largely to the small scale of the experiments.

Don MacRae of the Bethlehem Steel Company (Gold et al. 1975) was the first to demonstrate the technical viability of the plasma reduction of iron ores, using first a 100 kW and later a 1 MW d.c. falling-film plasma furnace. The lowest energy consumption was 2400 kWh/ton of iron.

At the Cockerill steel plant in Belgium (Fey et al. 1981), a tuyere in a blast furnace producing 1.8 million tons of metal per year was retrofitted in 1978 for operation with plasma superheated gas. The use of the plasma heaters has resulted in a reduction of the coke consumption rate by 60% in that single tuyere.

SKF of Sweden (1983) have developed a number of processes using plasma heaters. The Plasmared Process utilizes plasma heaters to preheat and upgrade reducing gases for the direct reduction of iron ore. A 50,000 t/year plant started operation in 1981. The Plasmasmelt, Plasmadust and Plasmazinc processes utilize plasma heaters to preheat reducing gas at the tuyere of the blast furnace.

A preliminary economic analysis indicates that the Plasmasmelt process might be competitive with conventional blast furnace iron production. A 70,000-ton/year Plasmadust plant for the reduction of steel mill waste oxides in order to recover their metal content (mainly zinc) is scheduled to start up in 1984.

iii. Ferroalloy Production

The feasibility of ferrochrome production has been investigated by Tetronics Ltd. in conjunction with Mintek Ltd. of South Africa in an expanded precessive plasma furnace (Barcza et al. 1981). Further tests were performed by Mintek (Curr et al. 1983) using a hollow graphite cathode transferred-arc reactor. A 20-MW furnace to be built by ASEA, Sweden is scheduled to start up in October 1984 for the production of ferrochrome.

MacRae et al. (1976) have demonstrated the feasibility of the continuous production of ferrovanadium at 500 kW in the Bethlehem Steel falling-film plasma furnace using carbon and vanadium trioxide. Energy requirements were 3240 kWh/ton of alloy. Gauvin and Choi (1983) have reported having little difficulty in treating vanadium pentoxide in the Noranda reactor with iron and carbon to produce a ferrovanadium alloy meeting steel industry specifications.

Plasma production of ferroalloys of tantalum and niobium is still in the laboratory stage (Gauvin and Choi, 1983).

iv. Refractory Metal Production

The refractory metals belonging to Groups IV B, V B and VI B of the Periodic Table generally exhibit high strengths and good corrosion resistance. Because of their high melting points and their free-energy of formation characteristics they require elevated process temperatures. The high temperatures and gas enthalpies that can be achieved with plasma reactors are ideally suited for refractory metal production.

The production of molybdenum by the plasma decomposition of molybdenum disulfide has been investigated using high-frequency plasma generators by Huska and Clump (1967) and in a transferred-arc reactor at the National Physical Laboratory in the U.K. (Sayce 1971). These attempts showed the difficulty in driving the sulphur content of the product down to the level of 0.15% S, required by industry. Following the experimental study by Munz and Gauvin (1975), the technical and economic feasability of producing commercial grade molybdenum by the decomposition of molybdenum disulfide using a transferred-arc reactor was finally demonstrated by Gauvin et al. (1981). They obtained a product containing 0.085% sulphur which is below the maximum sulphur content of 0.15% demanded by the steel industry.

Gauvin and Choi (1983) have investigated the production of zirconium and titanium via the dissociation of their respective

chlorides in a transferred-arc plasma reactor In the proposed process the metal chloride would also be produced from its oxide in a plasma reactor. The technical feasibility of this step has been demonstrated by Biceroglu and Gauvin (1980).

The reduction of tungsten trioxide with hydrogen in a helium plasma jet has been carried out (Ettingler et al. 1979). Yields as high as 95% were reported. Ettingler et al. (1979) also report on a number of approaches used for the production of tungsten metal, tungsten carbide and tantalum carbide. Methane was introduced with the metal or oxide powder in a helium plasma jet to carbonize and reduce the metal.

CONCLUSIONS

As is evidenced by the limited commercial utilization of plasmas in metallurgical processing, much work remains to be done in the areas of plasma reactor design and in adapting or modifying metallurgical processes to best take advantage of thermal plasmas many unique characteristics.

REFERENCES

REFERENCES

Asada, C. and Adachi, T., "On Plasma Induction Melting," 3rd Int. Symp. on Electroslag and Other Special Melting Technologies, Ed. Bhat, G.K. and Simkovich, A., p. 165 (June 1971)

Aubreton, J. and Fauchais, P., "Les fours à plasma," Rev. Gén Therm., Fr. 200-201 (Août-Septembre 1978)

Baddour, R.F. and Timmins, R.S. ed. "The Application of Plasma to Chemical Processing," M.I.T. Press (1967)

Barcza, N.A., Curr, T.R., Winship, W.D. and Heanly, C.P., "The Production of Ferrochromium in a Transferred-Arc Plasma Furnace," 39th Electric Furnace Conference, p. 243-260 (December 1981)

Barrett, M.F. et al., "Oxide Fuming in Tin Slags by Use of Electrical Heating," Trans. Instn. Min. Metall. 84 (829), p. C231-C238 (December 1975)

Barton, T., "Plasma Technology and the Environment," Symp. on Ind. Opportunities for Plasma Technology, Toronto (October 1982)

Bhat, G.K., "Plasma Technology and Its Industrial Applications," A survey report prepared for EPRI, Pittsburgh, Pa. (December 1981)

Biceroglu, O. and Gauvin, W.H., "Chlorination Kinetics of Zirconium in an R.F. Plasma Flame," AIChE Journal 26 (5) p. 734-743 (September 1980)

Blank, R.F. and Ward, D.H., "Development of a Cyclone Furnace Process for Slag Fuming," Advances in Extractive Metallurgy, London Inst. of Mining and Metall., p. 224-244 (1967)

Bonet, C., "Thermal Plasma Processing," Chem. Eng. Prog., 72 p. 63-69 (December 1976)

Boulos, M.I., Gagné, R. and Barnes, R.N., "Effect of Swirl and Confinement on the Flow and Temperature Field in an Inductively Coupled R.F. Plasma," C.J.Ch.Eng., 58 (June 1980)

Bryant, J.W. et al., "A Cathode Assembly for Feeding Powders into the Plasma of Expanded d.c. Arcs," J. of Sci. Instr., J. of Phys. E. 2, p. 779-781 (1969)

Busz-Peuckert, G. and Finkelburg, W., Z. Phys. 140, p 540 (1955)

Busz-Peuckert, G. and Finkelburg, W , Z. Phys. 144, p. 244 (1956)

Camacho, S.L., "Tasc Plasma Arc Torch Technology," Symp. on Ind. Opportunities for Plasma Technology, Toronto (October 1982)

Chang, C.W. and Szekely, J., "Plasma Applications in Metal. Processing," J. of Metals; 34, (2) p. 152, (February 1982)

Chase, J.D. and Skriven, J.F., "Process for the Beneficiation of Titaniferous Ores Utilizing a Hot Wall Continuous Plasma Reactor," U.S. Patent 3856918 (1974)

Choi, H.K., "Operating Characteristics and Energy Distribution in Transferred-Arc Plasma Systems," Ph.D. Thesis, McGill University (August 1980)

Choi, H.K. and Gauvin, W.H., "Operating Characteristics and Energy Distribution in Transferred-Arc Systems," Plasma Chemistry and Plasma Processing 2, (4) p. 361-386 (December 1982)

Cobine, J.D. and Burger, E.F., "Analysis of Electrode Phenomena in the High-Current Arc," J. of Applied Physics 26 (7) p. 895-900 (1955)

Curr, T.R. et al., "The Design and Operation of Transferred-Arc Plasma Systems for Pyrometallurgical Applications," Proc. of the 6th Int. Symp. on Plasma Chemistry, Montreal, p. 175-180 (July 1983)

Dinulescu, H.A. and Pfender, E., "The Anode Boundary Layer of High-Intensity Arcs," J. Appl. Phys. 51 (6) p. 3149-3157 (June 1980)

Eckert, H.W., "The Induction Arc: A State of the Art Review," High. T. Science 6 p. 99-134 (1974)

Esser, F. et al., "On the Theory of Remelting Solid Metallic Charges in Plasma Torch Furnaces," 4th Int. Conf. on Vacuum Metallurgy, p. 145-148 (1973)

Esser, F. et al., "Theory of Remelting and Melting-Down of Solid Metallic Charges in the Plasma Furnace - A Contribution to Optimizing the Process of Plasma Primary Melting," New Hutte 19 (10) p. 577-586 (1974)

Ettingler, L.A., "Applications of High-Temperature Plasmas," Mitre Corp. for Electricité de France, Contract No. 14-070 (1979)

Fauchais, P., "Utilisation industrielle actuelle et potentielle des plasmas: synthèse, traitement des poudres, traitements metallurgiques et traitements des surfaces," Revue Phys. Appl. 15 p. 1281-1301 (1980)

Fauchais, P., Bourdin, E. et Coudert, J.E., "Généralités sur les traitements physiques et chimiques en plasma thermique," L'actualité Chimique p. 15-35 (décembre 1981)

Fauchais, P., "Les Réacteurs et Fours à Plasmas," Journal du Four Electrique (7) (septembre 1982), (9) (novembre 1982), (1) (janvier-février 1983)

Fauchais, P., Bourdin, E. and Coudert, J.E., "Generalities on the Physical and Chemical Processes in a Thermal Plasma," Int. Chem. Eng. 23 (2) (April 1983)

Fey, M.G. and Kemeny, G.A., "Method of Direct Ore Reduction Using a Short Gap Arc Heater," U.S. Patent 3765870 (1971)

Fey, M.G. and McDonald, J. "Electrode Erosion in Electric Arc Heaters," AIChE Symp. Series (1979)

Fey, M.G. et al., "Plasma Systems for Ironmaking," 2nd Int. Seminar on Pilot Plants, Am. Vac. Soc. (September 1981)

Fey, M.G., Meyer, T.V. and Philbrook, W.D., "Thermal Plasma System for Industrial Processes," Symp. on Ind. Opportunities for Plasma Technology, Toronto (October 1982)

Fielder, H. et al., "Plasma Melting of Alloy Steels and Obtainable Properties," Industrial Heating (June 1975)

Foex, M. et al., "A Plasma Transferred-Arc Heated Rotary Furnace," Special Ceramics, Popper, P. (ed.) British Ceramic Research Assoc. 5 p. 175-183 (1972)

Foster-Wheeler/Tetronics: News Feature, "Plasma Process is Ready for Metal Recovery," Chem. Eng. 86 (4) (1979)

Galthier, F., Collongues, R. et Reboux, J., "Les Fours à Plasma Haute Fréquence," Les Hautes Temperatures, Chaudron, G. et Trombe, F. ed. 1 Masson et Cie, Paris (1973)

Gauvin, W.H., Kubanek, G.R., and Irons, G.A., "The Plasma Produotion of Ferromolybdenum - Process Development and Economics," Journal of Metals, 33 (1) p. 42-46 (January 1981)

Gauvin, W.H. and Kubanek, G.R., "A Novel Transferred-Arc Plasma Reactor for Chemical and Metallurgical Applications," patent pending (1981)

Gauvin, W.H. and Choi, H.K., "Plasmas in Extractive Metallurgy," Proc. of Symp. on Plasma Processing and Synthesis of Materials, Sponsored by the Materials Research Society, Boston (November 1983)

Gilles, H.L. and Clump, C.W., "Reduction of Iron Ore with Hydrogen in a Direct-Current Plasma Jet," Ind. Eng. Chem. 9 (2) p. 194-207 (1970)

Gold, R.G. et al., "Plasma Reduction of Iron Oxide with Hydrogen and Natural Gas at 100-kW and 1-MW," Metal-Slag-Gas Reactions and Processes, Foroulis, Z.A. and Smeltzer, W.W. ed. Electrochemical Society, p. 969 (1975)

Grosse, A.V. et al., "The Centrifugal Plasma Jet Furnace," Int. Conf. on Materials Philadelphia (February 1964)

Guile, A.E., "Arc Electrode Phenomena," IEE Reviews 118, p. 1131 (1971)

Guile, A.E., "Factors in Erosion of Non-Refractory Cathodes of Electric Arc Heaters," Proceedings of the Fifth Int. Symp. on Plasma Chemistry, Edinburgh (July 1981)

Hamblyn, S.M.L., German Patent 2531481 to Lonza, A.G. (February 1976)

Hamblyn, S.M.L., "Plasma Technology and its Applications to Extractive Metallurgy," Mineral Sci. Engng. 9 (3) (July 1977)

Hartman, J., Foster, T. and George, L., "Accurex Arc Plasma Torch Technology," Symp. on Ind. Opportunities for Plasmas Technology, Toronto (October 1982)

Hiratake, S., "Processing of Nuclear Wastes by Plasma Arc Melting," Int. Conf. on Pilot Plants, Am. Vac. Soc. (September 1981)

Holm, R., "The Vaporization of the Cathode in the Electric Arc," J. Applied Phys. 20 (July 1949)

Howatson, A.M., "An Introduction to Gas Discharges," 2nd Ed., Pergamon Press (1976)

Howie, F.J. and Sayce, I.G., "Plasma Heating for Refractory Metals," Rev. int. hautes temp. et refract. 11 (1974)

Hoyaux, M., "Arc Physics," Springer Verlag, New York (1968)

Kassabji, F. et al., "Technical and Economical Studies for Metal Production by Plasma Steelmaking Operations," 4th Int. Symp. on Plasma Chem., Zurich (August 1979)

Kassabji, F. et al., "Description d'un Four à Plasma de 0,7 MW pour la Réduction des Oxydes de Fer," Revue Int. des Hautes Temp. et Refract. 18, (2) p 123-139 (1981)

Kassabji, F. et Fauchais, P., "Les générateurs à plasma," Revue Phys. Appl. 16 p. 549-577 (1981)

Kubanek, G.R. and Gauvin, W.H., "Recent Developments in Plasma Jet Technology," C.J. Ch. Eng. 45 p. 251-257 (October 1967)

Kubanek, G.R., Munz, R.J. and Gauvin, W.H., "Plasma Decomposition of Molybdenum Disulfide," Proc. 3rd Int. Symp. on Plasma Chem., Limoges (July 1977)

Lachner, W. et al., "Results with Plasma Torch Furnaces for Melting High Quality Steels from High Alloy Scrap," Proc. 4th Int. Conf. on Vacuum Metall. (1973)

Lugscheider, W., "Utilisation du Four à Plasma en Aciérie Electrique," J. du four electrique 10 p. 29-33 (décembre 1981)

MacRae, D.R. et al., "Ferrovanadium Production by Plasma Carbothermic Reduction of Vanadium Oxide," 34th Electrical Furnace Conf., St. Louis (December 1976)

MacRae, D.R., "Plasma Processing in Extractive Metallurgy: The Falling-Film Plasma Reactor," Plasma Chemical Processing, A.I.Ch.E. Symp. Series 186 (75) (1979)

Maecker, H., "A Light Arc for High Power Outputs," Fulschrift Für Physik, 129 p. 108-122 (1951)

Maecker, H., "Electron Density and Temperature in the Column of the High-Current Carbon Arc," Z. Physik 136 p. 119-136 (1953)

Magnolo, G., "The Plasmarc Furnace," Can. Min. Metall. Bul. 57 p. 57-62 (1964)

McCullough, R.J., "Electric Furnace Proceedings," AIME 20 p. 319 (1962)

Mehmetoglu, M.T. and Gauvin, W.H., "Characteristics of a Transferred-Arc Plasma," AIChE Journal 29 (2) p. 207-215 (March 1983)

Monk, J.R., Foster Wheeler Energy Ltd., "Applications of Plasma to Metallurgical Processes," Proc. 5th Int. Symp. on Plasma Chemistry Edinburgh p. 162-167 (1981)

Olsen, H.N., "Thermal and Electrical Properties of an Argon Plasma," The Physics of Fluids 2 (2) p. 614-623 (November-December 1959)

Ono, K. and Moriyama, J., "Fundamentals Study on Carbothermic Reduction of Niobium Oxide in High-Temperature Vacuum Furnace," 4th Int. Conf. on Vacuum Metallurgy (1973)

Paton, B.E. et al., "The Transferred Plasma Arc Jet Remelting of Metals and Alloys," Automatic Welding 19, (8) p. 1-5 (1966)

Pickles, C.A. et al., "Investigation of a New Technique for the Treatment of Steel Plant Waste Oxides in an Extended Arc Flash Reactor," Advances in Extractive Metallurgy, The Inst. of Mining and Metallurgy (1977)

Reed, T.B. and Meyer, R.V., "Thermal Plasmas: Plasma-Flame Temperature Measurement Using Aureole Isotherm," Bull. Am. Phys. Soc. 9 p. 494 (1964)

Reid, K.J., Moore, J.J. and Tylko, J.K., "The Applications of the Sustained Shockwave Plasma Reactor in Process Metallurgy," 2nd World Congress of Chem. Eng., Montreal (October 1981)

Roman, W., United Technologies, U.S.A., "Plasma Processing for Materials," 6th Int. Symp. of Plasma Chemistry Workshop, Sherbrooke (July 1983)

Rykalin, N.N., "Plasma Engineering in Metallurgy and Inorganic Materials Technology," Pure and Appl. Chem. 48 p. 179-194, Pergamon Press (1976)

Rykalin, N.N., "Thermal Plasma in Extractive Metallurgy," Pure and Appl. Chem. 52, p. 1801-1815 (1980)

Sayce, I.G. "Plasma Processing in Extractive Metallurgy," Advances in Extractive Metallurgy and Refining, London Inst. of Min. and Metall. (October 1971)

Sayce, I.G. and Selton, B., "Preparation of Ultrafine Refractory Powders Using the Liquid-Wall Furnace," Special Ceramics, British Ceramics Research Association 5 p. 155-171 (1972)

Schoeck, P.A., "Modern Developments in Heat Transfer," Ibele, W. ed. Academic Press, New York and London (1963)

Sheer, C. et al., "Arc-Vaporization of Refractory Powders," Proc. of the Fine Particles Symp. Electrochem. Soc., Boston (October 1973)

Sheer, C. et al., "Invited Review: Development and Application of High Intensity Convective Electric Arc," Chem. Eng. Commun. 19 p. 1-47 (1982)

SKF Steel Engineering A.B., Information Brochure Hofors, Sweden (1983)

Takei, H. and Ishigami, Y., J. Vac. Sci. Tech. 8 (6) (1971)

Tezuka, By. H. et al., "Refining of Nickel-Base Alloys in a Plasma Induction Furnace," Proc. of 4th Int. Conf. on Vacuum Metall. (1974)

Tsantrizos, P. and Gauvin, W.H., "Operating Characteristics and Energy Distribution in a Nitrogen Arc Plasma," C.J. Ch. Eng., 60 (6) p. 822-830 (1982)

Tylko, J.K., "High Temperature Treatment of Materials," Can. Pat. 957733 Granted to Tectronics Ltd. (1974)

Waldie, B., "Review of Recent Work on the Processing of Powders in High Temperature Plasma: Part I Processing and Economic Studies," The Chem. Eng. 259, p. 92-96 (1972)

Whyman, D., "A Rotating Wall d.c. Arc Plasma Furnace," J. Sci. Instruments 44, p. 525 (1967)

Wilson, W.R., "High-Current Arc Erosion of Electric Contact Materials," A.I.E.E. Trans., 74 (657) (1955)

Yeroushalmi, D., "Development of High Temperature Rotary Furnace Axially Heated by an Arc Plasma," High Temp.-High Press., 3 (3) (1971)

Yeroushalmi, D. et al., Journal du Four Electrique et des Industries Electrochimiques, 4 p. 24 (1979)

EXPERIMENTAL SECTION

EXPERIMENTAL SECTION

INTRODUCTION

There is little doubt that the perception of plasma technology as a promising tool for industrial chemical and metallurgical processing has improved sharply during recent years. This is due in part to the availability of commercial plasma generating systems capable of reliable performance at powers of 10 MW and higher, and also to the realization that the use of electricity as the major source of energy does not necessarily affect adversely the economic viability of a process. In many applications, the quality of the heat energy supplied by a thermal plasma due to both its very high temperature level (or its thermodynamic "availability" in other words) combined with the fact that the heat can be transferred by mixing directly to the system (that is, without the necessity of a heat transfer surface) is so high that it frequently outweighs the apparent price advantage of fossil fuels. In addition the plasmagen gas may frequently be used as a reactant for such reactions as oxidation, reduction, chlorination, etc.

The economic feasibility of a process depends of course on many more factors than the cost of electricity, and the unique

characteristics of a plasma system must be thoroughly understood before a reliable technoeconomic analysis can be undertaken.

To date, the attention of the workers in the field has been largely directed at the behavior of the various torches which have been developed and the behavior of the plasma flame or transferred-arc they generate. A great deal of effort has also been devoted to studies of the kinetics of reactions performed in a plasma environment and to develop new systems in which the reactions are either impossible or at least very difficult to achieve at lower temperatures. To the author's knowledge, very little attention has been given to the design of the reactors in which these reactions are to be performed.

Many of the earlier furnace designs have never progressed beyond the laboratory or pilot stage. These have been described by Hamblyn (1977). These include expanded plasma furnaces and rotating plasma furnaces. A rotating cathode furnace with a plasma arc struck between an orbiting inclined cathode on the roof of the furnace and an annular anode ring or an anodic pool of molten metal was developed by Tylko for Tetronics (1974). A 1400-kW furnace of this type has been constructed in association with Foster Wheeler Limited (1979).

Molten-pool plasma furnaces which are essentially a conventional electric furnace with the electrodes being replaced

by plasma transferred-arc generators have enjoyed the greatest commercial success to date. A 10-ton plasma furnace fired with three d.c. 3-MW plasma torches was commissioned in 1973 by V.E.B. Edelstahlwerke at Freital, East Germany (Lachner et al., 1973). A 30-ton four-torch furnace was started in 1977. Bhat (1981) has reported that a similar 100-ton furnace having six 3.5-MW plasma torches is now operating in the U.S.S.R.

Curr et al. (1983) of Mintek in South Africa have described a 20-MW furnace having a hollow graphite cathode that was recently ordered from ASEA, Sweden and is to be commissioned in October 1984.

A combined induction-plasma furnace has been developed in Japan by Daido Steel Co. (Asada and Adachi, 1971). It has been used for melting high-quality super-alloys. Ulvac Ltd. of Japan has developed a low-pressure plasma beam furnace in which a direct current argon plasma is transferred from a hollow tungsten cathode to the workpiece (Takei and Ishigami, 1971). Furnaces up to 2.4-MW of this type have been used to melt and cast titanium alloys and sponge.

In order to reduce energy losses to the furnace walls and roofs and to utilize as much of the energy generated in the plasma torch as possible, Chase and Skriven (1974) patented a falling-film plasma furnace utilizing a d.c. plasma jet torch.

The ore particles were fed tangentially into the reactor where they were forced to the reactor wall by centrifugal forces. There they melted and formed a falling-film of molten ore with which the gaseous phase could react.

MacRae et al. (1979) of the Bethlehem Steel Co. developed a more sophisticated version shown in Figure 1 in which they reduced hematite with mixtures of hydrogen and methane, and vanadium trioxide with coke fines at powers up to 1 MW. In this reactor, powders were injected tangentially and centrifuged onto the reactor inner wall, which functioned as the anode, to form a falling film. The film provided a reaction site for the reactants so that good residence times and contact were achieved. The film also thermally insulated and protected the water-cooled anode.

The most recent falling-film furnace is the Noranda - Hydro-Québec furnace designed by Gauvin and Kubanek (1981), and shown in Figure 2. This furnace differs from the Bethlehem furnace in that the molten bath in the bottom crucible serves as the anode. The plasma column surrounded by a sleeve over most of its length extends over the entire length of the reactor. The charge in the bottom crucible can be melted much in the same manner as in the molten-pool furnaces. Feed particles are fed tangentially at the top of the sleeve, at the same height as the cathode, and form a falling film along its inner surface, where the desired high-

FIGURE 1

BETHLEHEM STEEL CO.

FALLING FILM-REACTOR

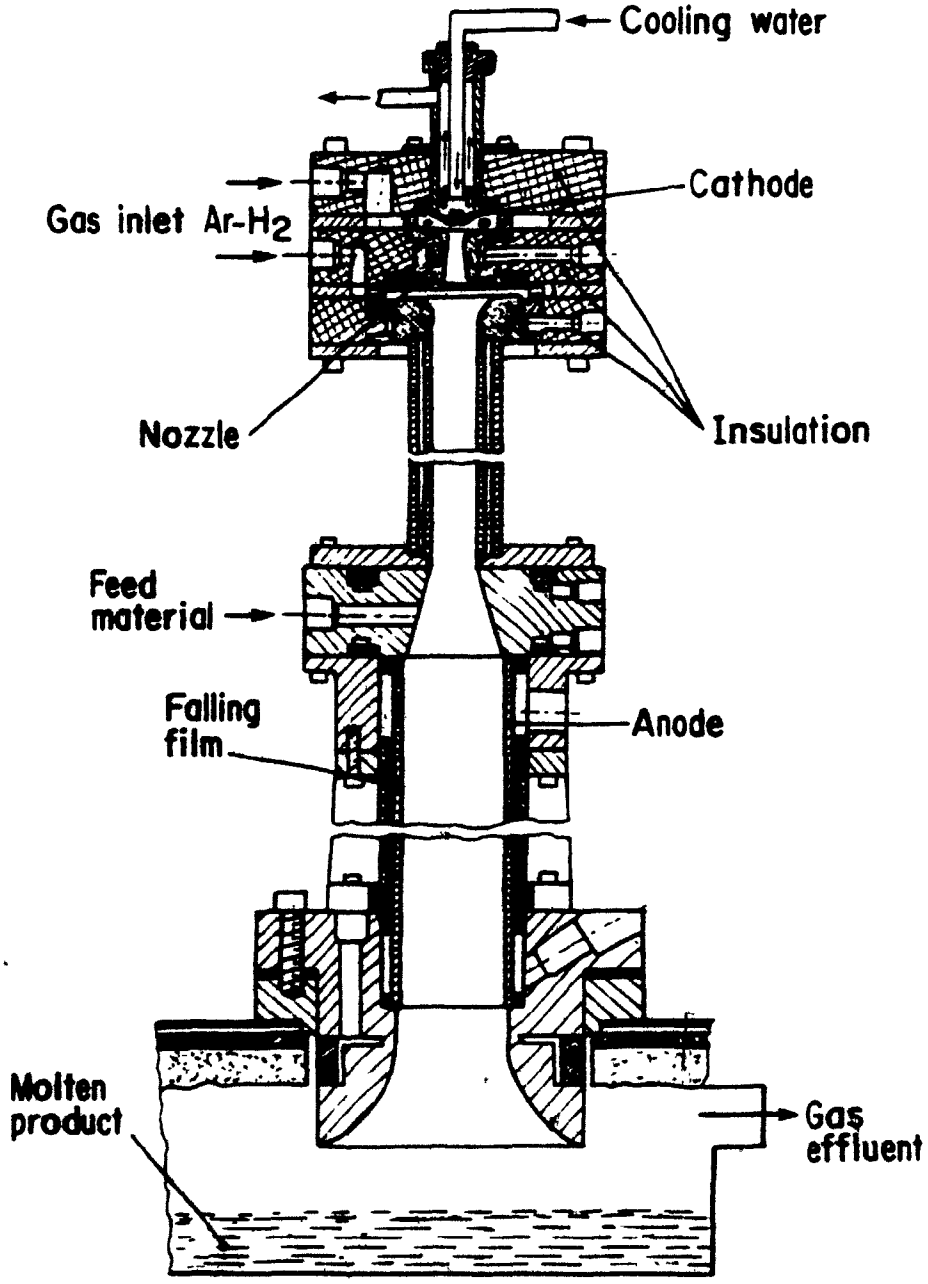
Cooling water
Cathode
Gas inlet Ar-H2
Nozzle
Insulation
Feed material
Falling film
Anode
Molten product
Gas effluent

FIGURE 2"

NORANDA - HYDRO-QUÉBEC REACTOR

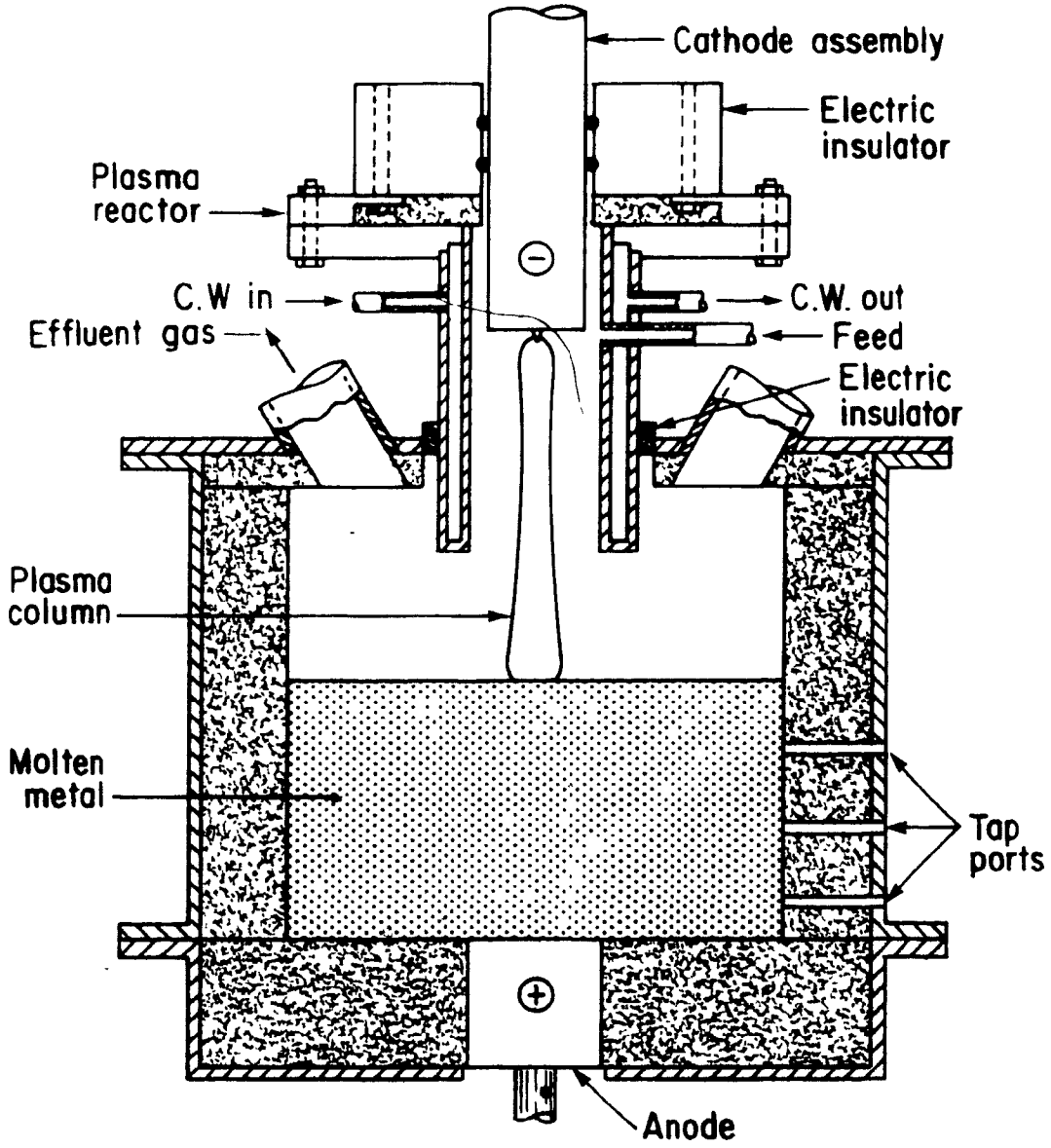
Cathode assembly
Electric insulator
Plasma reactor
C.W in
C.W. out
Effluent gas
Feed
Electric insulator
Plasma column
Molten metal
Tap ports
Anode

temperature reaction begins to occur, maintained by the intense radiation from the arc. This type of reactor is very efficient as the falling film absorbs all of the radiant heat generated by the plasma arc. The other major region of heat transfer from the arc is at the anode, taking advantage of the anode fall. This serves to heat the molten pool in the bottom crucible, thus enabling it to be also used as a reaction site.

The feed carrier gas which is optically thin serves to stabilize the arc by its centrifugal motion, picks up little radiant heat from the plasma and helps maintain the walls and roof of the furnace cool. As no cooling is required at the sleeve and at the anode, this reactor is very efficient. Also as both the sleeve and crucible (anode) can serve as reaction sites, residence times for reactions can be adjusted to meet the needs of the reaction taking place.

The study of the operating characteristics of this reactor forms the major objective of this thesis.

Plasma furnaces are beginning to be used commercially in melting and remelting and in pyrometallurgical applications, though their use is far from being widespread. Apart from suffering from the major disadvantage of using costly electric energy, plasma furnaces offer the operator a number of well-documented advantages (Gauvin and Choi, 1983). It is only by considering all of the

advantages and disadvantages of using plasma furnaces and comparing these to competing technologies that a proper evaluation of the economic viability of using plasma furnaces can be made.

Compared to conventional electric arc furnaces the advantages of plasma furnaces are:

1. Higher melting efficiency compared to similar sizes of conventional electric arc furnaces.

2. Ability to produce alloys with low-carbon contents.

3. Superior recovery of the alloy metals contained in the scrap and of those added to the melt.

4. Ability to inject and alloy the melt with nitrogen through the gas phase instead of through the use of expensive nitrogen containing alloys.

5. Higher quality product compared to that from conventional electric or induction melting furnaces.

6. Achieving low oxygen and hydrogen residuals in the melt.

7. Suppression of noise to a level below 60 dB

8. Elimination of discontinuous shock loading of the electric power transmission mains (flicker).

9. Thirty percent lower capital investment compared to a modern Ultra High Power (UHP) electric arc furnace system.

10. Reduction of iron losses to below two percent.

Compared to conventional pyrometallurgical reduction and smelting techniques based on fossil fuels, plasma processes would have the following additional advantages:

1. Flexibility in reductant selection.

2. Ability to concentrate energy with resultant smaller reactor size and pollution abatement systems.

3. Ability to operate independently of oxygen potential.

4. Ability to transfer heat energy to the gas phase with high efficiency and without the contamination of combustion products.

5. Much lower capital investment requirements resulting from smaller reactor size and the ability to handle finely divided feed material, without expensive feed preparation.

6. Reduced manpower needs resulting from continuous operation and ease of automation for plasma processes.

7. Less restriction in choice of plant location; ability to locate near ore supply as electricity can be transported to the site cheaply and efficiently.

As already mentioned, plasma furnaces have achieved some commercial success in melting and remelting applications. Some commercial success has been achieved using plasma reactors for pyrometallurgical processing. Mintek has recently ordered a 20-MW hollow graphite cathode transferred-arc reactor from ASEA of Sweden

for the production of ferrochrome. Bethlehem Steel has used their falling-film reactor at powers up to 1-MW for the production of steel and ferrovanadium. Gauvin and Choi (1983) have reported little difficulty in treating vanadium pentoxide in a transferred-arc reactor with iron and carbon to produce a ferrovanadium alloy meeting the steel industry standards.

The high melting points and high free-energy of formation characteristics of the refractory metals make them ideally suited for production in plasma reactors.

The commercial feasibility of producing molybdenum by the plasma decomposition of molybdenum disulfide in a transferred-arc reactor has been demonstrated by Gauvin et al. (1981) of the Noranda Research Centre. They obtained a product containing 0.085% sulphur which is below the maximum sulphur of 0.15% demanded by the steel industry.

Gauvin and Choi (1983) have investigated the production of zirconium and titanium via the dissociation of their chlorides in a transferred-arc reactor. Ettingler et al. (1979) have reduced tungsten trioxide with hydrogen in a helium plasma jet with yields as high as 95%.

As is evidenced by the limited commercial utilization of plasmas in metallurgical processing, much work remains to be

done in the areas of plasma reactor design and in adapting or modifying metallurgical processes to best take advantage of thermal plasmas many unique characteristics.

This study in large part is a continuation of the work done by Mehmetoglu and Gauvin (1983), Choi and Gauvin (1982) and Tsantrizos and Gauvin (1982), in their investigation of the electrical and energy transfer characteristics of an argon and nitrogen transferred arc.

The specific objectives of this study are:

- To study the operating characteristics of the Noranda - Hydro-Québec reactor in particular.

- To study the electrical characteristics of a transferred-arc in the presence of a surrounding sleeve with a flow tangential carrier gas containing solid particles surrounding the arc.

- To study the energy transferred from the arc to the various components of the reactor including the sleeve, anode, cathode reactor walls and roof, with and without particulate injections.

- In a preliminary way, to determine the reactors efficiency in transferring energy to the particulate feed.

It is important to note that all parts of the reactor are cooled in order to measure the energy distribution within the reactor. Thus, the melting efficiency or the efficiency with which energy is transferred to the particulate feed is expected to be much smaller than in an uncooled, insulated reactor that would be used in commercial practice. It is planned to determine the true efficiency that would be obtained in an industrial reactor in a further study which is soon to be undertaken in the laboratory on an uncooled reactor which will closely simulate a commercial system.

EXPERIMENTAL

A general description of the system under study can be summarized as follows: an argon or nitrogen plasma was struck between a tungsten cathode tip containing 2% thorium and an anode consisting of molten steel. The arc was surrounded by a cylindrical sleeve over most of its length. Steel powder as a solid feed was injected with a carrier gas tangentially along the inner surface of the sleeve at the same level as the cathode tip. The injected powder was melted under the effect of the intense radiation from the arc and formed a film, along the inner surface of the sleeve. The molten film flowed down the sleeve and then dripped into the molten bath at the bottom of the reactor, which functioned as an anode. A more detailed description of the

operating procedure along with the measurements taken during the experiments will be presented in the Experimental Procedures Section.

APPARATUS

The apparatus used in this study is shown schematically in Figure 3A. A photo of the entire system is shown in Figure 3B. It consisted of the following separate units:

1. Power Supply
2. High-Frequency Starter
3. Gas and Water Flow Instrumentation
4. Cathode Assembly
5. Reactor Vessel
6. Powder Feeder.

1. Power Supply

The power was supplied by a 60-kW rectifier (Miller Welder Model SRS-1500F 7). The input voltage was 3-phase, 60-c.p.s., 575-volt while the output circuit could provide 400 volts in open circuit. The rectifier was equipped with a remote control, which contained a current regulator, ammeter and voltmeter.

FIGURE 3A

SCHEMATIC DIAGRAM OF

THE OVERALL SYSTEM

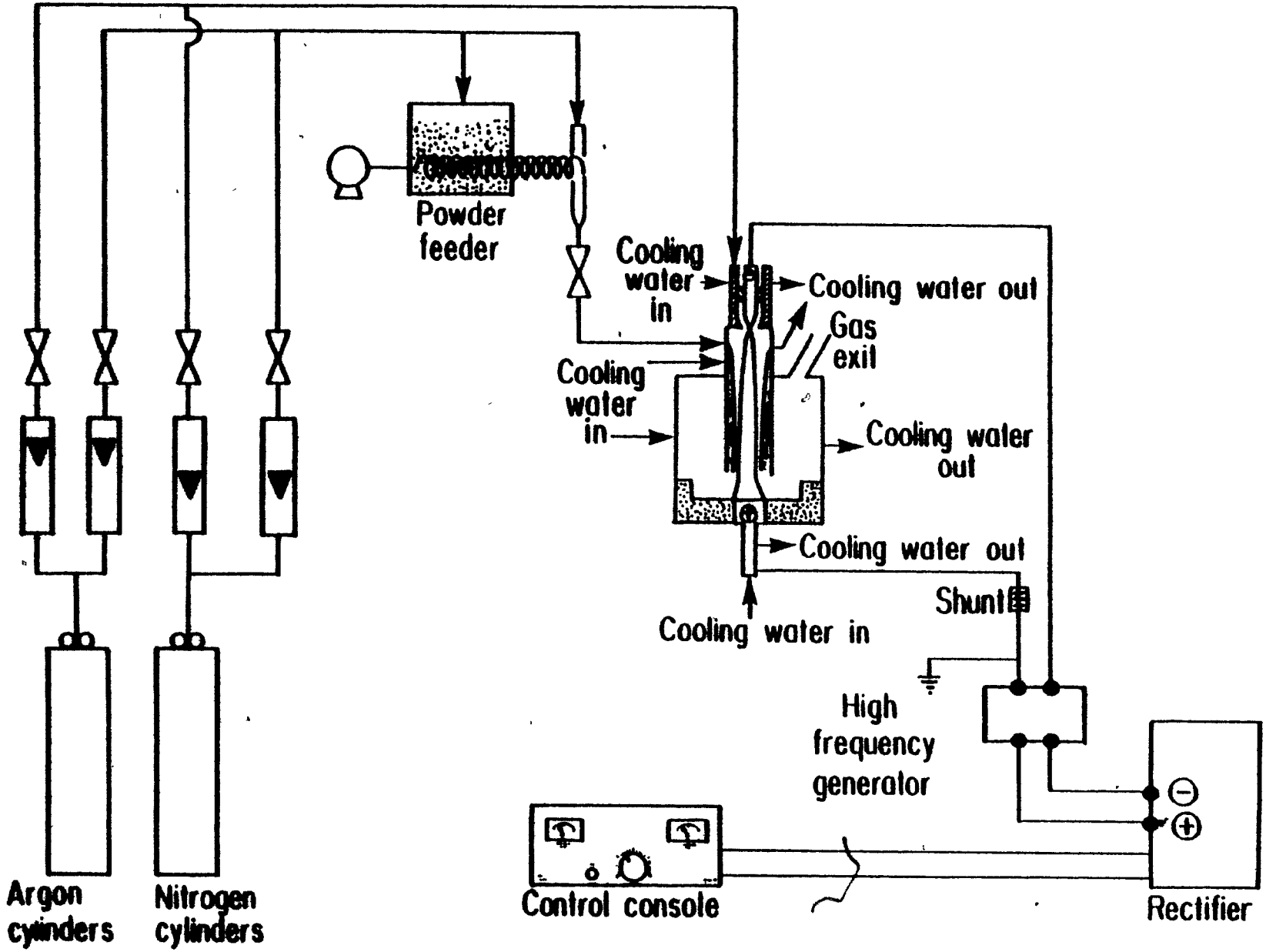
Powder feeder
Cooling water in
Cooling water out
Gas exit
Cooling water in
Cooling water out
Cooling water out
Cooling water in
Shunt
High frequency generator
Argon cylinders
Nitrogen cylinders
Control console
Rectifier

FIGURE 3B

PHOTOGRAPH OF APPARATUS

2. High-Frequency Starter

The High-Frequency Starter used was a Miller Welder HF-15-1. The input voltage was 115 volts and the maximum current throughput was 500 amperes. The unit was connected in series with the direct-current circuit from the rectifier to the reactor. A remote switch was used to activate the unit to ignite the plasma arc.

3. Gas and Water Flow Instrumentation

Argon gas, with a purity of 99.996% and nitrogen gas, with a purity of 99.991% were supplied from gas cylinders and regulated by two-stage pressure regulators. The outlet pressure was maintained at a constant value of 300 kPa. The flow was measured with Wallace and Tierman calibrated rotameters.

Water for cooling the reactor was supplied at 310 kPa and the flow was regulated by four Brooks water rotameters.

4. Cathode Assembly

The cathode assembly design is based on the Sheer et al. (1973) "Fluid Convective Cathode" design. The design is similar to that used by Mehmetoglu (1980), Choi (1981) and Tsantrizos (1981) at McGill University, and by Gauvin et al. (1981) at the Noranda Research Centre.

The cathode assembly, shown in Figure 4, was comprised essentially of a water-cooled conical tungsten 2% thorium cathode tip surrounded by a water-cooled concentric sheath nozzle, through which the plasma gas (argon or nitrogen) was introduced. Two different nozzle orifice diameters of 0.75 and 1.0 cm were used. The cathode tip protruded slightly out of the nozzle to facilitate arc ignition. The cathode assembly was attached to a threaded rod which was connected to a motor. Rotation of the threaded rod permitted accurate positioning of the cathode assembly in its axial position. The motor was operated with a precision speed controller and a forward, stop and reverse switch.

5. Reactor Vessel

A schematic of the complete reactor assembly vessel is shown in Figure 5. The reactor chamber consisted of a water-cooled 18.3-cm I.D. 316 stainless steel hollow shell 9. cm in height. The top consisted of a 0.64-cm thick water-cooled plate from which was suspended a 5.74-cm I.D. 12-cm long water-cooled cylindrical sleeve or jacket. The whole structure rested on a base constructed of 0.64-cm thick copper. A 7.62-cm O.D. copper anode was lead-soldered to the centre of the copper base. The anode was cooled from below by a jet of water impinging on its lower surface. The base, with the exception of the anode surface, was covered with a layer of magnesite (MgO).

FIGURE 4

CATHODE ASSEMBLY

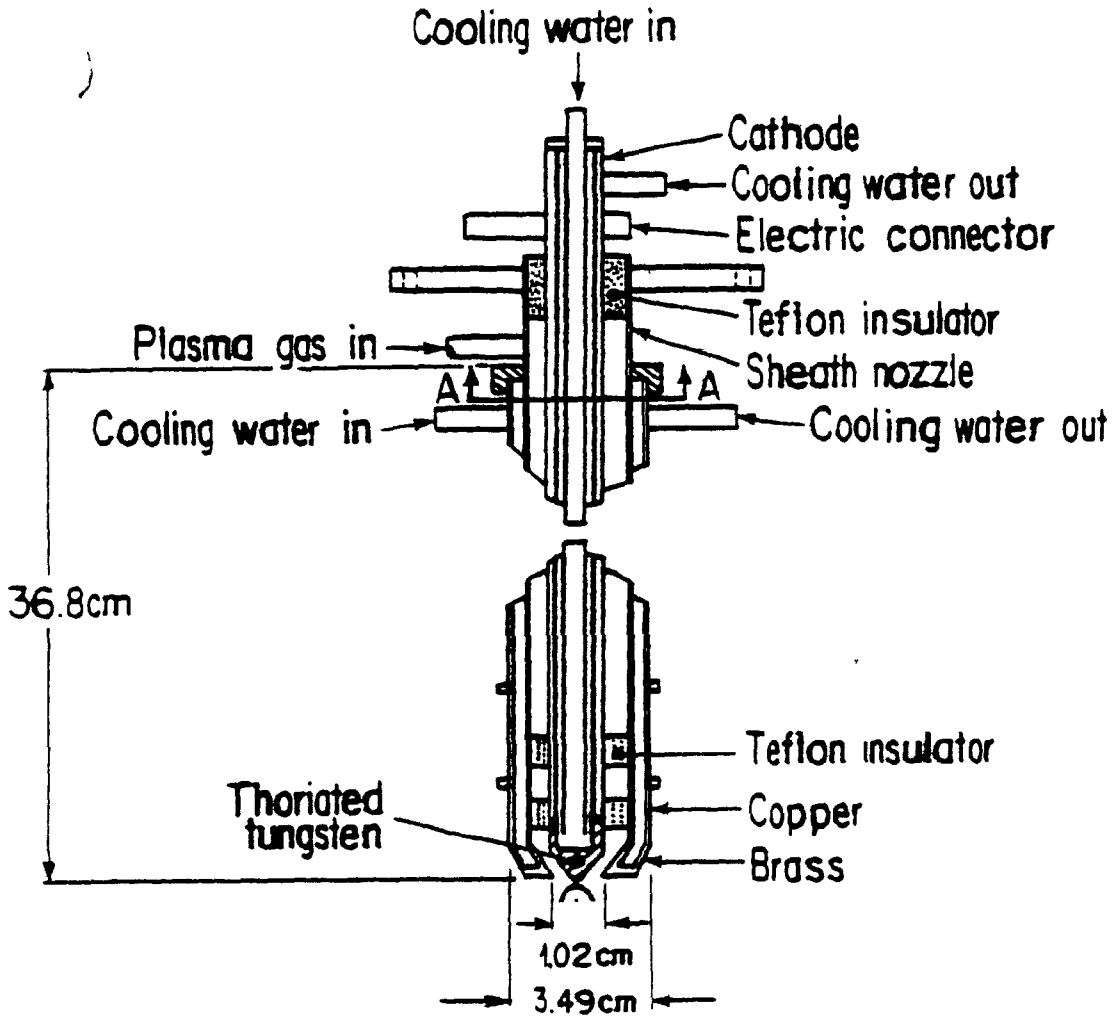
Cooling water in
Cathode
Cooling water out
Electric connector
Teflon insulator
Plasma gas in
Sheath nozzle
A
A
Cooling water in
Cooling water out
36.8cm
Teflon insulator
Thoriated tungsten
Copper
Brass
1.02cm
3.49cm

Section A–A

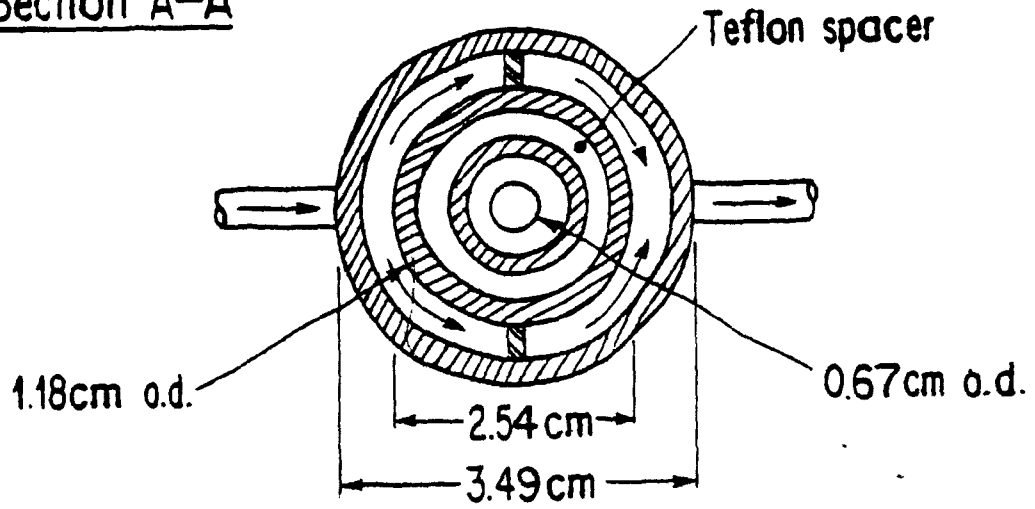
Teflon spacer
1.18cm o.d.
0.67cm o.d.
2.54cm
3.49cm

FIGURE 5

REACTOR VESSEL

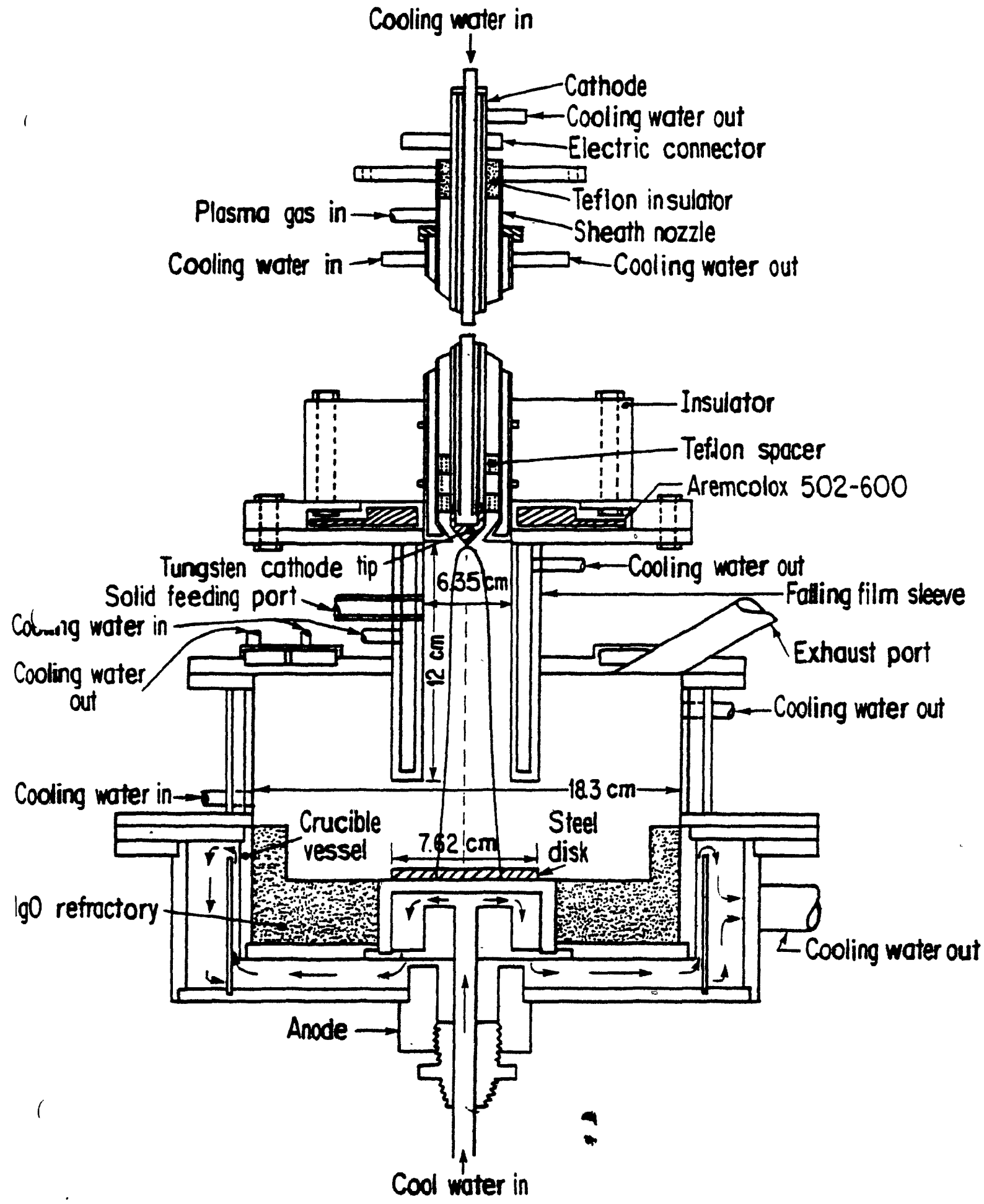
Cooling water in
Cathode
Cooling water out
Electric connector
Teflon insulator
Plasma gas in
Sheath nozzle
Cooling water in
Cooling water out
Insulator
Teflon spacer
Aremcolox 502-600
Tungsten cathode tip
6.35 cm
Cooling water out
Solid feeding port
Falling film sleeve
Cooling water in
Exhaust port
Cooling water out
12 cm
Cooling water out
Cooling water in
18.3 cm
Crucible vessel
7.62 cm
Steel disk
lgO refractory
Cooling water out
Anode
Cool water in

The upper opening of the sleeve was covered by a ceramic disk made of Aremcolox 502-600 machineable ceramic. An opening at the center permitted the entry of the cathode assembly. Above the ceramic, a phenolic ring insulator was used to position the cathode assembly precisely and also to electrically isolate the cathode assembly from the rest of the reactor.

Asbestos-based gasket rings 0.32-cm thick were used as seals, and also served as electrical and thermal insulators at each flange. The top of the reactor was secured to the reactor cylindrical body by means of eight 0.95-cm thick bolts suspended on teflon washers in order to ensure that the bolts were not in electrical contact with the top flange. The reactor shell was secured to the reactor base by means of six clamps, each capable of exerting a force of 2670 N. The use of these clamps permitted easy and quick access to the interior of the reactor.

The gas effluent was exhausted from the reactor by way of three 2.54-cm O.D. 316 stainless steel tubes on the roof of the reactor. The gas-conveyed solid feed material was fed tangentially along the inner surface of the sleeve through a 0.64-cm O.D. x 0.048 cm I.D. 316 stainless steel tube. The tube entered the sleeve 2.5-cm below its upper extremity.

6. Powder Feeder

For low feed rates, below 60 g/min a powder feeder built by Plasma Arcos S.A., in Belgium, was used. In this feeder, the powder was introduced into the carrier gas stream by a rotating disk as shown in Figure 6. The feed rate could be adjusted by varying the disk rotation speed.

For higher feed rates, a screw feeder was used. It consisted of a 14-cm square plexiglass hopper through which passed a 2.5-cm screw. At the end of the screw the particles entered the carrier gas stream which passed over the end of the screw perpendicularly. The screw was powered by a variable-speed motor. The feed rate could be adjusted by changing the screw rotation speed from 25 to 36 kg/h.

MEASUREMENT TECHNIQUES AND INSTRUMENTATION

1. Measurements of Arc Voltage and Arc Geometry

In order to understand the electrical characteristics of the transferred-arc plasma, the total arc voltage was measured as a function of various operating parameters which were in this case the arc current, the arc length, the plasmagen gas flow rate, the nozzle geometry, the tangential feed gas flow rate, the particle feed rate

FIGURE 6

ARCOS POWDER FEEDER

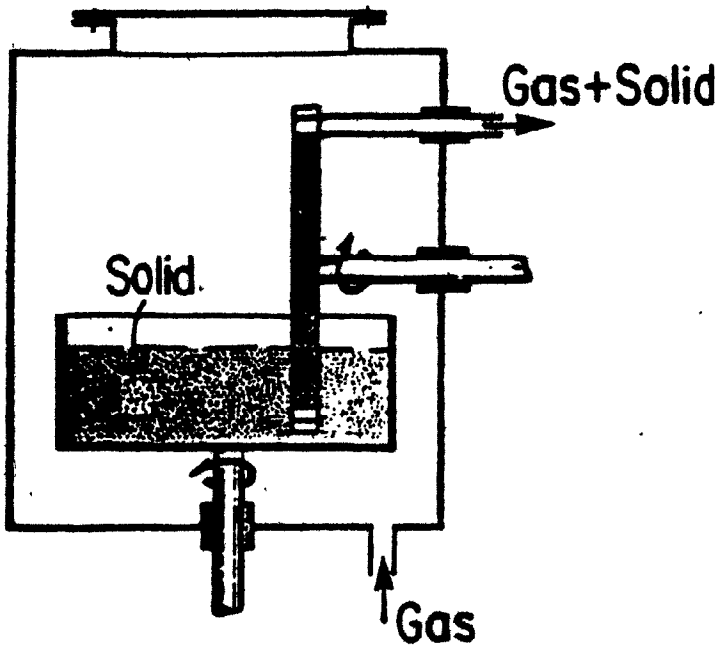
Gas+Solid
Solid
Gas

and the particle size. Accurate voltage measurements were made by connecting the leads to the cathode and those to the shunt, to a precision voltmeter (Fluke Model 8024B Multimeter) and a strip chart recorder (Hewlett Packard 7402A). The positive lead was connected to the shunt in order to ensure that it was at ground potential, to avoid damage to the recorder. A correction had to be applied for the voltage drop between the shunt and the anode. The resistance of the electrical connection between the shunt and the anode was measured to be 7.8×10^{-4} ohms. Therefore at 200 amperes the correction was 0.16 volt and 0.31 volt at 400 amperes. The arc current was measured via the same voltmeter and strip chart recorder connected to a shunt which was connected in series with the arc. The reading accuracy of the arc current and voltage were ±2 A and ±0.5 V, respectively.

To determine the effect of the operating conditions on the luminous plasma profile, still photographs of the plasma were taken using a 35-mm Nikon F-3 camera with a 55-mm Macro lens. A welding type filter was used to reduce the light intensity of the arc. A 400 ASA film was used with an exposure time of 1/250 second at F-22.

2. Calorimetric Measurements

The fraction of the input arc power transferred to the anode, cathode tip, annular cathode nozzle, reactor shell and roof

and falling-film sleeve were determined by measuring coolant flow rates and water temperature rise for each section. Five grounded K-type thermocouples (3.175 mm O.D.) were used for measuring water temperature. An additional thermocouple of the same type was used for measuring gas temperature. The thermocouples were connected to a digital temperature meter (Syscom # 5200 kc) through a 6-point rotary selector. The precision of the temperature meter was ±5°C. Four separately calibrated rotameters were used for obtaining coolant flow rates. Typical flow rates for the cathode tip and nozzle were 1 L/min; for the falling-film sleeve: 6 L/min; for the reactor shell and roof: 2 L/min; and for the anode: 3 L/min. The reading accuracy of the flow rate was 0.025 L/min for the cathode nozzle; 0.1 L/min for the falling-film sleeve; 0.1 L/min for the reactor shell and roof and 0.1 L/min for the anode.

PROCEDURES

In this section, the procedures involved in operating the experimental apparatus and instruments described in the previous sections are explained. Included in this section are start-up, shut-down and operation of the transferred-arc, measurement of overall energy distribution and calibration of the powder feeder.

1. Arc Start-up, Shut-down and Operation

Before the arc was initiated, preparation of the electrodes was performed. The anode surface was polished and cleaned with acetone. The cathode tip was cleaned with a fine abrasive paper and sharpened when necessary with a file. The anode steel disk was cleaned with a fine abrasive paper, weighed and its thickness measured before being placed on the permanent copper anode. The reactor shell and sleeve assembly were then positioned and secured in place by means of the six clamps provided for this purpose. All electrical, water and gas connections were made and checked. All wires connecting the instruments to the reactor were disconnected and the instruments themselves unplugged from the wall electrical outlets in order to prevent any possibility of damage to the instruments by the use of the high-frequency generator. The cooling water supplies to the cathode and nozzle, sleeve, reactor shell and roof and anode were turned on and the desired flow rates were set and recorded. The water temperature was noted. The cathode tip was lowered to a position of about 5 mm from the anode surface by means of the motor controller. The argon flow rate to the cathode was adjusted to 14 L/min. The high-frequency generator was turned on to check electrode alignment and spark generation. The power to the electrodes was then turned on, and the electrode voltage was checked in order to ensure that it was at the open-circuit voltage

in order to verify that there was no short-circuits in the reactor or in any of the electrical connections. Finally, the high-frequency generator was activated, igniting the arc.

After the arc was formed, the cathode assembly was raised immediately to prevent deterioration of the cathode tip and nozzle because of sputtering of molten steel from the anode surface. All instruments were then reconnected and turned on. Then the arc length, the argon flow rate and the current were readjusted to the desired values.

The arc was run at the preset arc length and current for between 10 and 15 minutes until the arc voltages and all cooling water temperatures reached stable values. The arc conditions could then be reset and new readings taken.

When feeding powdered solids, the reactor was shut down and cleaned before proceeding to a new solids feed rate, in order to determine what proportion of the feed was melted under the conditions tested.

To shut-down the reactor, the main power was first switched off. All cooling water lines were left running for a number of minutes following the power shut-down in order to permit the reactor and especially the solidified steel charge at the anode to cool.

2. Measurements of Overall Energy Distribution

The fractions of the input arc power transferred to the cathode and cathode nozzle, falling-film sleeve, reactor shell and roof, and finally to the anode were determined by calorimetric measurements. Before the arc was struck, the cooling water to the cathode and cathode nozzle, falling-film sleeve, reactor shell and roof, and anode was allowed to run until steady temperatures were reached. Approximately fifteen minutes were required to reach this stage. The water flow rates to the cathode and cathode nozzle (one water circuit) were 1.0 L/min, to the reactor shell and roof (one water circuit) 2.4 L/min. The water flow rate to the falling-film sleeve was varied between 5 and 8 L/min, and to the anode was varied between 2 and 8 L/min, depending on the operating conditions. The arc was then established and a number of different experiments were conducted.

In the first experiments, using the 1.0 cm cathode nozzle, the arc current was varied systematically at a given arc length, while the coolant outlet temperatures were measured. In a majority of experimental runs, arc currents of 100 to 400 amperes and arc lengths of 1, 2, 4, 8, 11 and 16 centimetres were used. These experiments were repeated using steel anode disks of two different thicknesses, 1.3 cm and 3.0 cm respectively, thus resulting in two different distances between the anode surface and the base of the falling-film sleeve.

A selected number of measurements were repeated using the smaller cathode (0.75 cm). Finally, for a fixed arc length and current, the plasma gas flow rate was varied in order to determine its effect on plasma characteristics and heat transfer to the various parts of the reactors. The arc current tended to drift slightly during a given run, so that frequent readjustment of the current was required. The arc was run at a given condition for at least ten minutes to obtain a steady temperature of the coolant, with the anode coolant temperature being the slowest to respond. The temperature rises between the inlet and outlet where <10°C for the cathode and cathode tip, <15°C for the reactor shell and roof and <25°C for the anode and falling-film sleeve. The experimental data were collected continuously without extinguishing the arc because of the time that would otherwise be consumed in opening the reactor and changing the anode disk.

In a second series of experiments, the arc was fixed at 16 cm and argon as carrier gas was injected tangentially into the reactor along the inner surface of the falling-film sleeve. Its effect on the arc characteristics and heat transfer to the various components of the reactor was measured. In the final sets of runs, steel powder was introduced along with the carrier gas and the experimental measurements repeated.

3. Powder Feeder Calibration

In order to calibrate the powder feeders, the flexible tubing connecting the feeders to the reactor was disconnected and the feed was allowed to discharge into a beaker, which was covered with a cloth held in place with a rubber band. The gas flow rate through the feeder was set to the desired rate. The feeder motor was started, and its speed setting was noted. The particulate feed was collected in the beaker for a measured period of time then weighed, yielding the feed rate for the particular motor speed used.

RESULTS AND DISCUSSION

The results of the experimental work in an open arc system are presented and discussed in this section. Phenomenological observations of the arc and of the electrodes are presented first. The arc voltage dependencies and overall energy distribution within the reactor are next shown as a function of a number of parameters, including arc length, arc current, axial and tangential gas flow rates and particulate feed rate and size. The melting efficiency, or the efficiency with which the arc energy is transferred to the particulate feed is also shown.

The reactor, as it has been described, had some equipment limitations which imposed some restrictions on the operation of the plasma reactor and prevented a more extensive and detailed study, in the limited time available. Suggestions for some equipment modifications will be given in a later section.

1. Phenomenological Observations

Figure 7 shows photographs of the plasma arc column at various operating conditions. The maximum arc length shown is 4 cm as the sleeve prevented viewing the fraction of the arc above 4 cm in length. The luminous region represents the current-conducting arc region in an approximate way. As the current increases for a given arc length, the diameter and luminosity of the plasma column both increase, as does the diameter of the molten pool.

Stable arc operation, as indicated by the lack of current and voltage fluctuations, were obtained under specific operating conditions. The argon arc was stable for currents as low as 100 amperes to 11 cm and as low as 150 amperes to 16 cm. At arc lengths of 16 cm, (maximum arc length possible in the reactor), the arc was operated at currents up to 300 amperes. Rectifier limitations prevented the current from being increased substantially beyond this point. At current above 250 A, the

FIGURE 7

PHOTOGRAPHS OF THE TRANSFERRED-ARC PLASMA

Legend

No. 1 : 2 cm, 100 A, 14 L/min Argon
No. 2 : 2 cm, 220 A, 14 L/min Argon
No. 3 : 2 cm, 300 A, 14 L/min Argon
No. 4 : 4 cm, 200 A, 14 L/min Argon
No. 5 : 4 cm, 200 A, 20 L/min Argon
No. 6 : 4 cm, 200 A, 30 L/min Argon

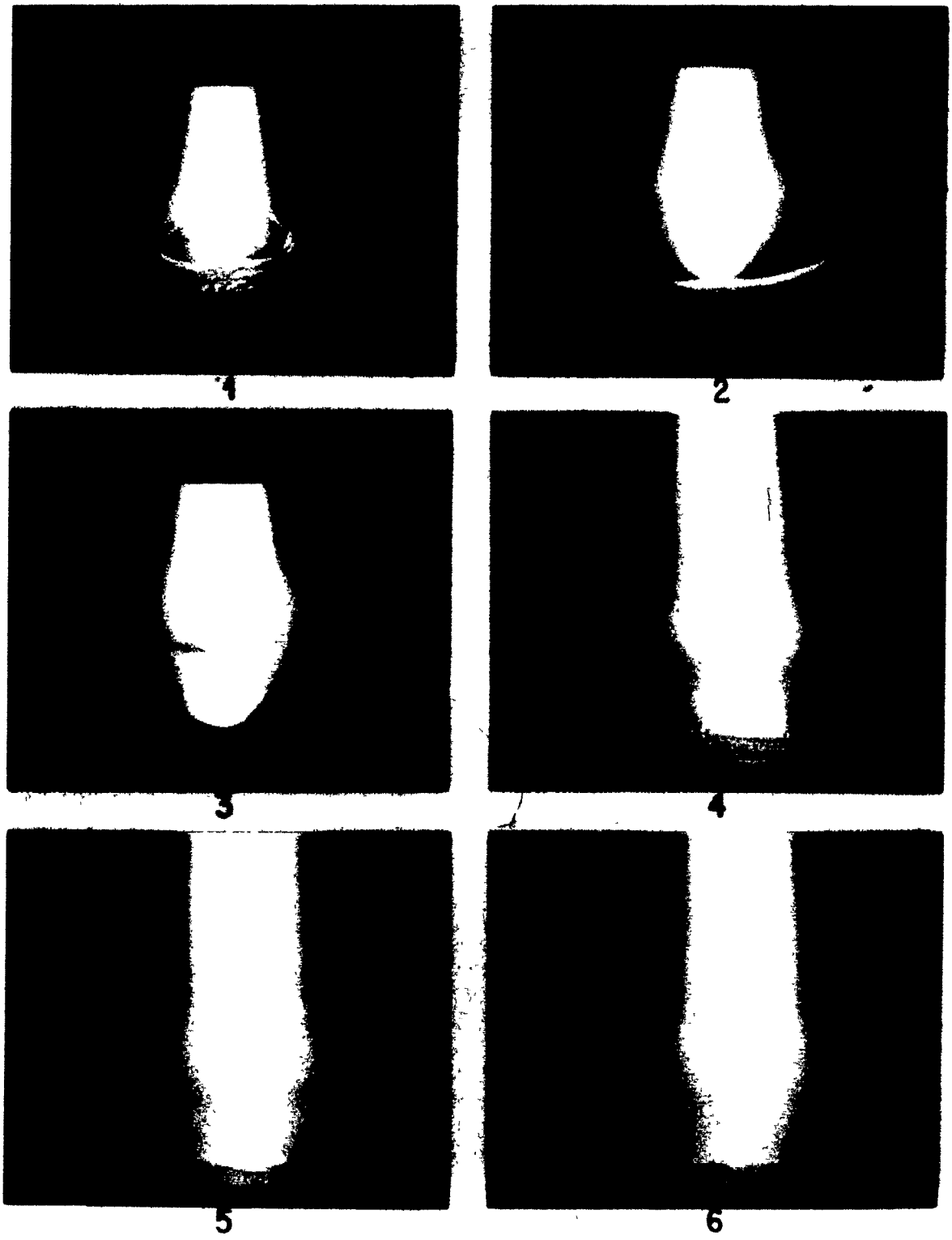
1
2
3
4
5
6

arc tended to bend to one side. This could have caused severe damage to the sleeve. Tangential gas injection tended to stabilize the arc, but could not fully straighten the arc. As the current was increased, the plasmagen gas enthalpy, hence its temperature was increased, resulting in a higher velocity. Also the Maecker effect becomes more important, resulting in a greater amount of gas being entrained into the arc at the cathode tip. Any alignment errors of the cathode tip, at the center of the nozzle would result in a deviation of the flow to one side. This effect would be exaggerated with increased arc current because of the higher gas temperatures and because of the extra gas aspirated by the Maecker effect, thus causing the arc deviation to one side to increase with arc current.

The problem of arc deviation was also more serious when a smaller cathode nozzle was used, as any error in cathode alignment would be proportionally greater.

Finally, operation with a cold reactor tended to be less stable than operation after an initial warm-up period. As the arc was lengthened and was exposed to the cold inner-surface of the sleeve, the arc tended to become less stable. After a couple of minutes, the arc stability increased and the arc voltage would drop by 2 to 8 volts, depending on arc length and current.

The use of nitrogen as the plasmagen gas resulted in an arc column of much smaller diameter, and in much higher arc voltages. Operation at arc lengths of less than 6 cm resulted in severe damage to the cathode tip and nozzle as a result of the sputtering of molten iron from the anode surface. At longer arc lengths, the arc stability was similar to that of argon arcs.

The anode consisted of an iron disk placed upon a water-cooled copper anode. A pool of molten iron would form in the center of the disk. The size of pool was directly proportional to the arc current.

At arc initiation, the arc root on the surface of the iron disk was not stable, moving randomly, until a molten pool had formed. At this point the arc root would become fixed to the surface of the molten pool. Before the pool was formed, the arc current would take a number of different paths through the iron disk before entering the copper anode. Once the pool was formed, establishing direct contact through the disk with the upper anode, the current proceeded through the molten pool, directly to the surface of the copper anode.

With tangential gas injection, it was possible to sustain the transferred arc with no axial gas injection. Arc stability appeared to be superior compared to operation with axial gas only, and arc voltage was comparable.

When feeding particulates into the reactor, it was impossible to view the arc. For the first 30 seconds to one minute of feeding, the arc tended to be unstable, but the stability of the arc increased with feeding time and was relatively stable after one minute of feeding. The particles injected tangentially along the inner surface of the sleeve were melted by the arc and deposited on the sleeve surface to form a falling film. It was possible to freeze the falling film in place (since the sleeve was cooled) by shutting off the arc power and the powder feed at the same time. It was thus possible to observe that the falling film coated the sleeve in a relatively uniform manner below the level of the feed port and that its thickness was between 1 and 4 mm.

2. Total Arc Voltage - No Particulate Feed

By using the experimental procedure described previously, the effects of the arc current (I), the arc length (ℓ), the axial gas flow rate (F_{ag}), the tangential gas flow rate (F_{tg}) and the nozzle diameter (d_{nz}) on the total arc voltage were studied. All the measurements are tabulated in Appendix A. The arc voltage is plotted as a function of the arc length up to 300 amperes in Figure 8. The arc voltage is replotted as a function of arc current up to 16 cm of arc length in Figure 9. The effects of argon axial flow rate are shown in Figure 10, and those of argon tangential flow rate are shown in Figure 11. Not enough data were obtained to

FIGURE 8

ARC VOLTAGE VARIATION WITH ARC LENGTH

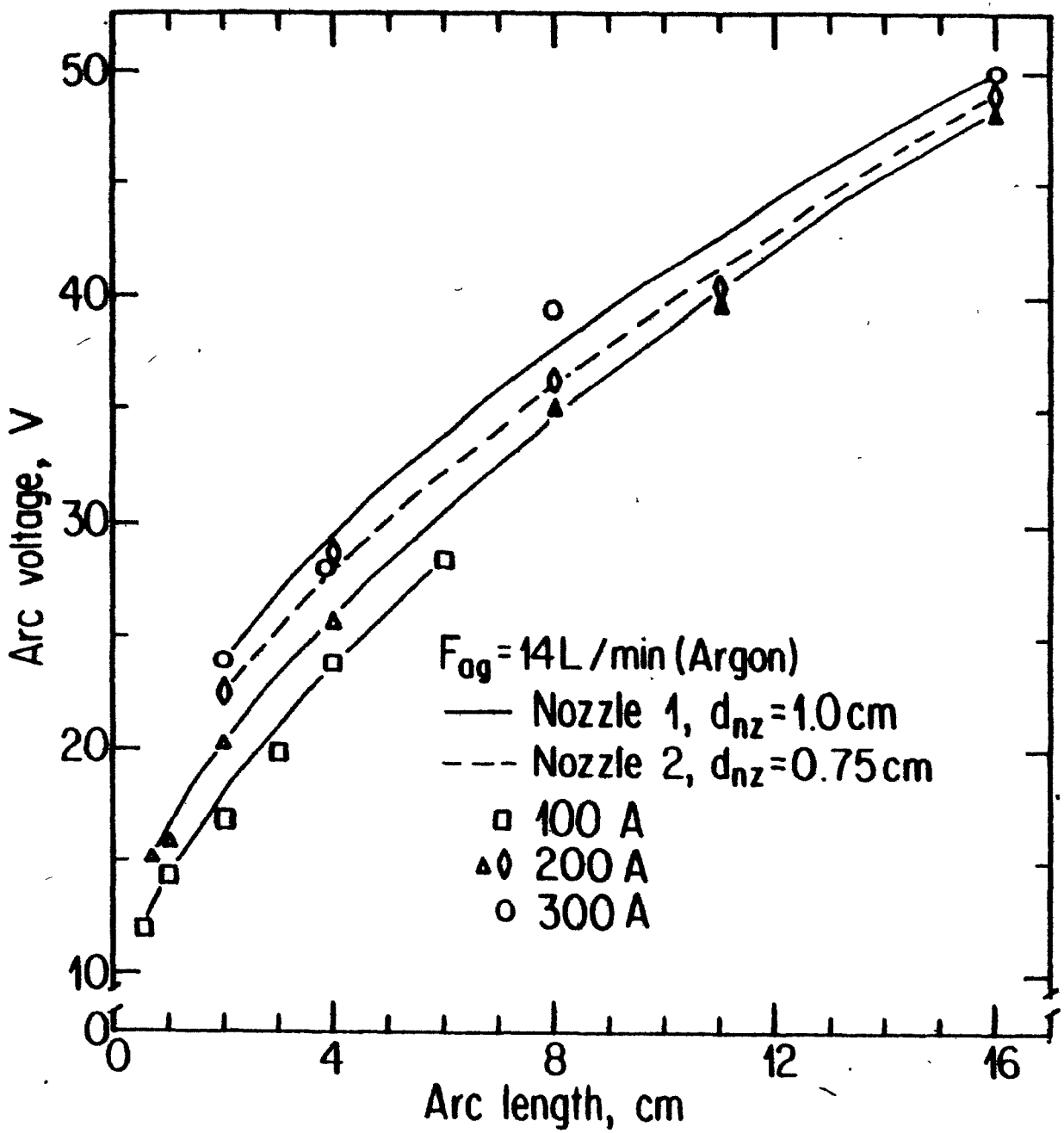
Arc voltage, V
50
40
30
20
10
0
0
4
8
12
16
Arc length, cm
F_{ag} = 14 L/min (Argon)
Nozzle 1, d_{nz} = 1.0 cm
Nozzle 2, d_{nz} = 0.75 cm
100 A
200 A
300 A

FIGURE 9

ARC VOLTAGE VARIATION WITH ARC CURRENT

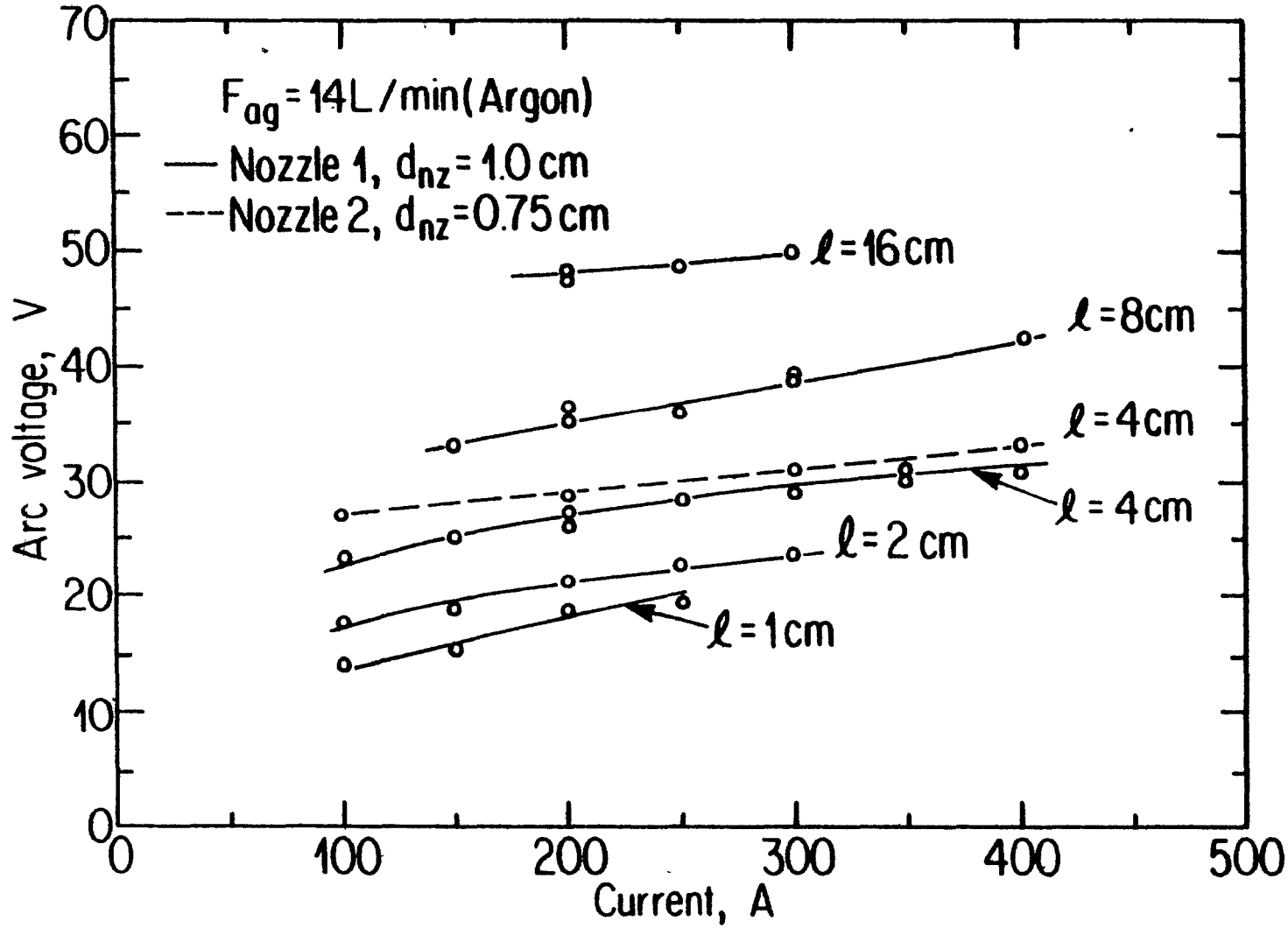
F_{ag} = 14 L/min (Argon)
— Nozzle 1, d_{nz} = 1.0 cm
---Nozzle 2, d_{nz} = 0.75 cm
ℓ = 16 cm
ℓ = 8 cm
ℓ = 4 cm
ℓ = 4 cm
ℓ = 2 cm
ℓ = 1 cm
Arc voltage, V
Current, A
0
10
20
30
40
50
60
70
0
100
200
300
400
500

FIGURE 10

ARC VOLTAGE VARIATION WITH

ARGON AXIAL FLOW RATE

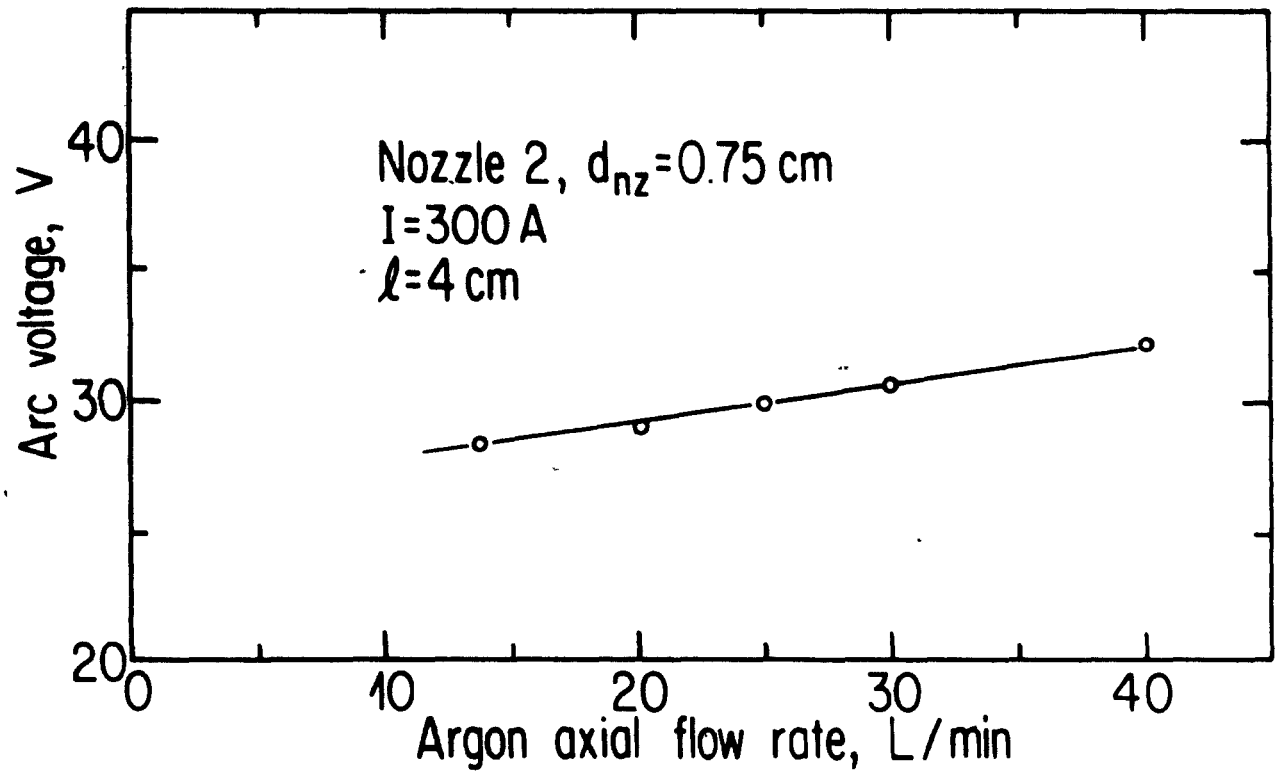
Nozzle 2, d_{nz}=0.75 cm
I=300 A
ℓ=4 cm
Arc voltage, V
40
30
20
0
10
20
30
40
Argon axial flow rate, L/min

FIGURE 11

ARC VOLTAGE VARIATION WITH

ARGON TANGENTIAL GAS FLOW RATE

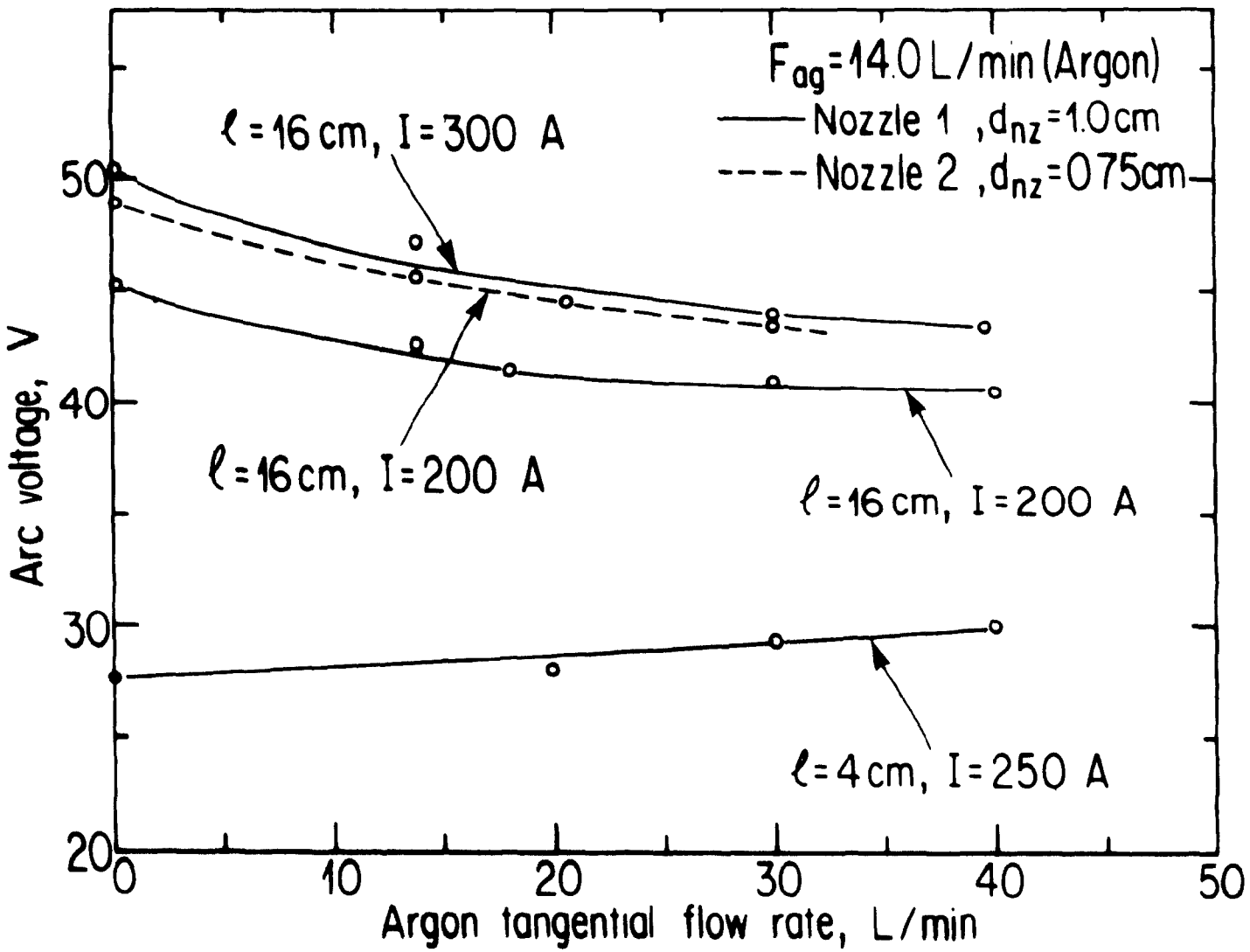
F_{ag}=14.0 L/min (Argon)
Nozzle 1 , d_{nz}=1.0cm
Nozzle 2 , d_{nz}=0.75cm
ℓ = 16 cm, I = 300 A
ℓ = 16 cm, I = 200 A
ℓ = 16 cm, I = 200 A
ℓ = 4 cm, I = 250 A
Arc voltage, V
Argon tangential flow rate, L/min
50
40
30
20
0
10
20
30
40
50

reproduce the same plots for nitrogen gas. Tsantrizos and Gauvin (1982) have shown that nitrogen is affected in the same way as argon by the above parameters except that the arc voltage is approximately double in all cases. This was confirmed in the present study. The measurements for nitrogen are tabulated in Appendix B.

As is evident from Figures 8 and 9, the arc voltage increases significantly with an increase in arc length. This was expected as the gas resistance is almost directly proportional to the arc length. This was demonstrated by Choi and Gauvin (1982). The effect of the arc current on the arc voltage is relatively minor, as indicated in Figure 9 The main reason for the latter effect is the fact that the electrical conductivity of argon at temperatures above 10 000 K is almost constant. Choi and Gauvin (1982) demonstrated that the temperature of an argon plasma above 250 amperes is consistently above 10 000 K. The arc voltages measured were comparable to those, reported by these authors, using a solid water-cooled copper anode, indicating that little or no iron vapour was penetrating the arc column.

The effect on the axial gas flow rate is to increase the arc voltage (Figure 8). Mehmetoglu and Gauvin (1983) showed that the gas velocity past the cathode tip was responsible for the voltage change and not the flow rate as such. Choi and Gauvin (1982)

showed that the effect of the axial gas flow rate on the arc voltage increased with decreasing nozzle diameter. The much higher inlet axial gas velocities obtained with a smaller nozzle cause the arc to constrict, with a resulting decrease in the conducting cross-section.

The effect of increasing the tangential gas flow rate is to stabilize the arc and thus decrease its voltage by 5 to 7 volts. The (Figure 9) vortex created by the tangential gas establishes a pressure gradient which is everywhere centrally-directed and forces the column to remain on the cylinder axis. The tangentially-injected gas also serves to create a region surrounding the arc containing relatively cool gas which further prevents the arc from moving off its axis and thus further helps to stabilize the arc.

Injection of nitrogen as tangential gas around an argon arc results in an arc voltage increase of approximately 50 volts. A portion of the less conducting nitrogen tangential gas is probably aspirated into the arc column as a result of the Maecker effect.

The effect of nozzle diameter is shown in Figures 8, 9 and 10. The arc voltage is significantly increased when a smaller nozzle is used. The arc voltage increases because the higher axial gas velocity reduces the conducting cross-section as has been reported in an earlier section.

The arc voltage for zero arc length, which is equivalent to the sum of the anode and cathode falls, is obtained by extrapolating the total arc voltage to zero arc length (Figure 8). The zero arc voltage for argon is almost independent of arc current and is about 8 to 11 volts, which agrees well with previous results (Choi and Gauvin, 1982; Goldman, 1961). The total arc voltage for zero arc length could not be estimated for a nitrogen plasma because of the lack of data at short arc lengths. Tsantrizos and Gauvin (1982) measured a total electrode fall voltage for a nitrogen arc of 15 to 20 volts.

The sleeve surrounding the arc over a portion of its full length does not have an effect on the arc voltages. Tests conducted in which the proportion of the total arc length surrounded by the sleeve was varied (by varying the distance separating the base of the sleeve and the anode disk) had similar total arc voltages, at the same arc lengths and currents.

3. Total Arc Voltage With Particulate Feed

The tangential introduction of a particulate feed along the inner surface of the sleeve resulted in an increase in arc voltage. The results in an argon atmosphere at 200 amperes and 300 amperes are plotted on Figure 12. The results for all tests are listed in Table I. Tests were performed for feed rates ranging from 0.75 kg/h to 35.6 kg/h. The arc voltage increased very rapidly with particulate feed

FIGURE 12

ARC VOLTAGE VARIATION WITH

PARTICULATE FEED RATE

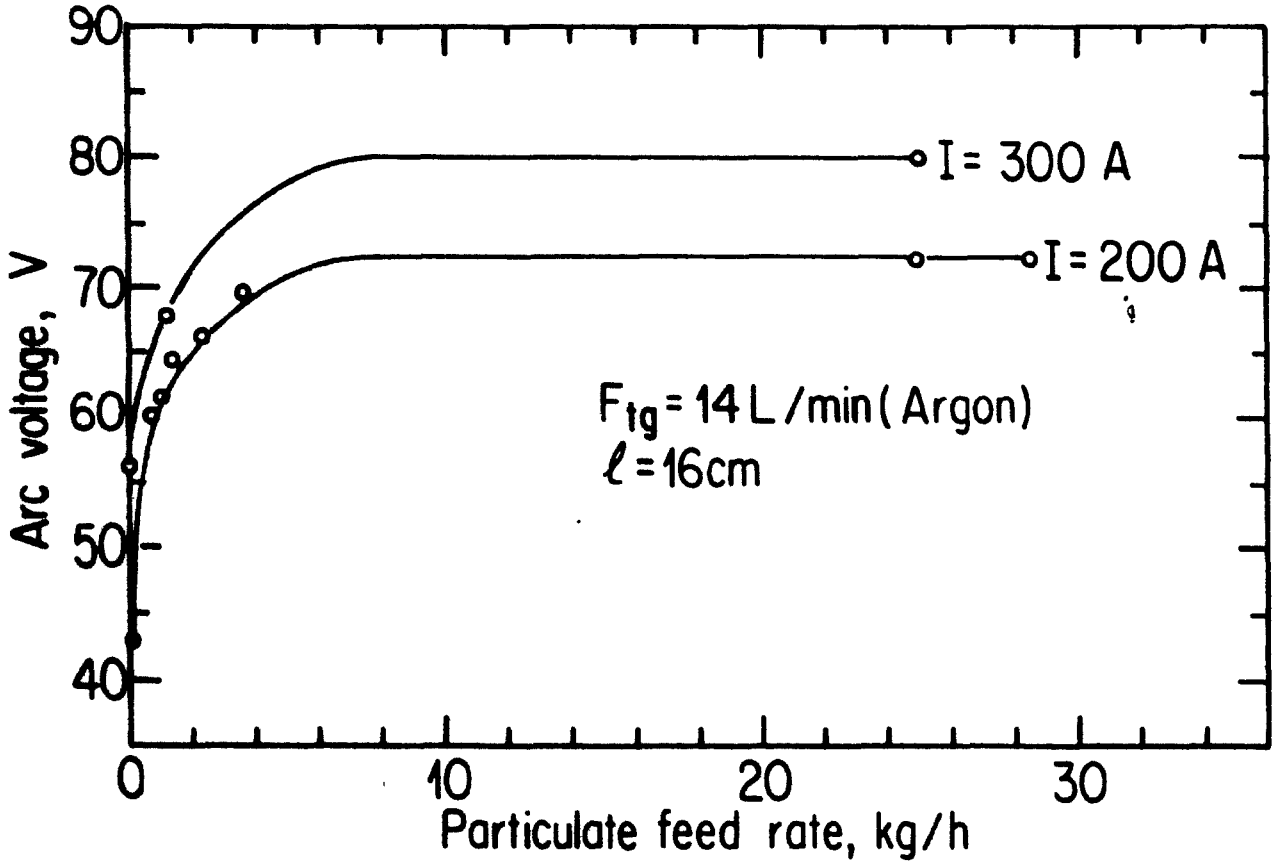
90
80
70
60
50
40
Arc voltage, V
I = 300 A
I = 200 A
F_{tg} = 14 L/min (Argon)
ℓ = 16cm
0
10
20
30
Particulate feed rate, kg/h

TABLE I

PARTICULATE MELTING RESULTS (ℓ = 16 cm)

TEST	F_{tg} L/min	V volts	I amps	P_t(V·I) kW	P_R kW	%	F_p kg/h	F_{pt} kg	d_p μm	MELTED %	EXHAUST %	P_t/F_p kWh/kg	P_t MELTED kWh/kg
12	30	62.2	200	12.4	12.1	97.0	0.75	-	75-88	100	-	16.5	16.5
12	30	65.8	200	13.6	-	-	1.4	-	75-88	100	-	9.6	9.6
13	20.5	59.9	200	12.0	12.4	103.3	0.66	-	75-88	100	-	18.8	18.8
13	20.5	63.5	200	12.7	12.5	98.4	1.3	-	75-88	100	-	9.8	9.8
13	20.5	65.9	200	13.2	12.6	95.3	2.3	-	75-88	100	-	5.7	5.7
13	20.5	69.5	200	13.9	12.0	86.1	3.7	-	75-88	100	-	3.8	3.8
14	20.5	65.9	300	19.8	18.7	94.7	3.7	-	75-88	100	-	5.1	5.1
15	20.5	67.8	300	20.3	19.0	93.4	1.3	-	75-88	100	-	15.6	15.6
18	12	72	200	14.4	7.8	54.2	24.9	0.81	75-88	41	-	0.58	1.4
22	12	72	200	14.4	10.5	72.7	24.9	1.97	75-88	55	0.1	0.58	1.1
22SS*	12	72	200	14.4	10.5	72.7	24.9	1.97	75-88	64	0.1	0.58	0.91
30	12	72	200	14.4	11.4	79.4	28.4	1.55	149-177	50	0.03	0.51	1.01
27	20.5	70	200	14.0	9.5	67.9	35.6	1.73	63-88	32	-	0.39	1.2
21	12	80	300	24.0	18.6	77.5	24.9	1.63	75-88	80	-	0.96	1.2
23**	12	152	200	30.4	23.7	78.0	22.6	0.75	75-88	80	-	1.35	1.7
25**	12	150	300	45.0	-	-	76.2	0.19	63-88	-	0.04	0.59	-

* Value corrected to reflect steady state operation.

**N_2 atmosphere, all other tests in Ar atmosphere.

rate, at low feed rates. No additional increase in voltage was observed at higher feed rates (above 6 to 10 kg/h). The maximum voltage increase for an argon arc at 200 amperes was 30 volts. At 300 amperes it was 25 volts. For a nitrogen arc at 200 amperes the increase was 20 volts.

The particulate size did not have an effect on the arc voltage, while increasing tangential flow rate did lower the voltage slightly (see Table I).

The voltage increase with particulate injection is probably a result of a small amount of the feed entering the arc column. The feed is most likely aspirated into the low-pressure region of the arc existing near the cathode tip (Maecker effect). The voltage increased as a result of the quenching effect occurring when the particles entered the arc column. It is interesting to note that only a small proportion is allowed to enter, beyond which no voltage increase resulting from additional particles is observed. The fact that a portion of the tangential gas stream enters the arc column has been demonstrated in a previous section.

4. Overall Energy Distribution - No Particulate Feed

The fractions of the total arc power transferred to the various sections of the reactor were measured. All of the measurements are tabulated in Appendix A for an argon atmosphere and

Appendix B for a nitrogen atmosphere. Figures 13 and 14 show the fractions of the total arc power transferred to the anode (P_a), the reactor wall and roof (P_w), the reactor sleeve (P_s), the cathode tip (P_c) and the sum of the cathode tip and nozzle (P_{cn}). The results shown in Figures 13 and 14 were taken for the same operating conditions, with the exception that the distance separating the base of the sleeve and the anode surface (iron disk), (ℓ_{sa}) was 3.5 cm in Figure 13 and 5.3 cm in Figure 14. In both cases, the fraction of the arc's energy transferred to the anode, cathode and cathode nozzle tended to decrease with increasing arc length. For short arc length Choi and Gauvin (1982) using a solid copper anode reported slightly higher values for the heat transferred to the anode. Less energy was absorbed by the liquid iron anode used, because a higher fraction of the arc radiation reaching the anode surface was reflected and because a small amount of the energy may have been removed by the evaporation of the iron and therefore, not absorbed by the anode.

The fraction of energy transferred to the anode decreased with increasing arc length except when the cathode tip was near the base of the sleeve (arc lengths of 3.5 cm for Figure 14 and 5.3 cm for Figure 13). In this region the function of the total arc energy transferred to the anode ceased to decrease and actually increased significantly, owing to a smaller energy dissipation through radiation resulting from a shorter plasma column.

FIGURE 13

PERCENT POWER DISTRIBUTION AS A

FUNCTION OF ARC LENGTH

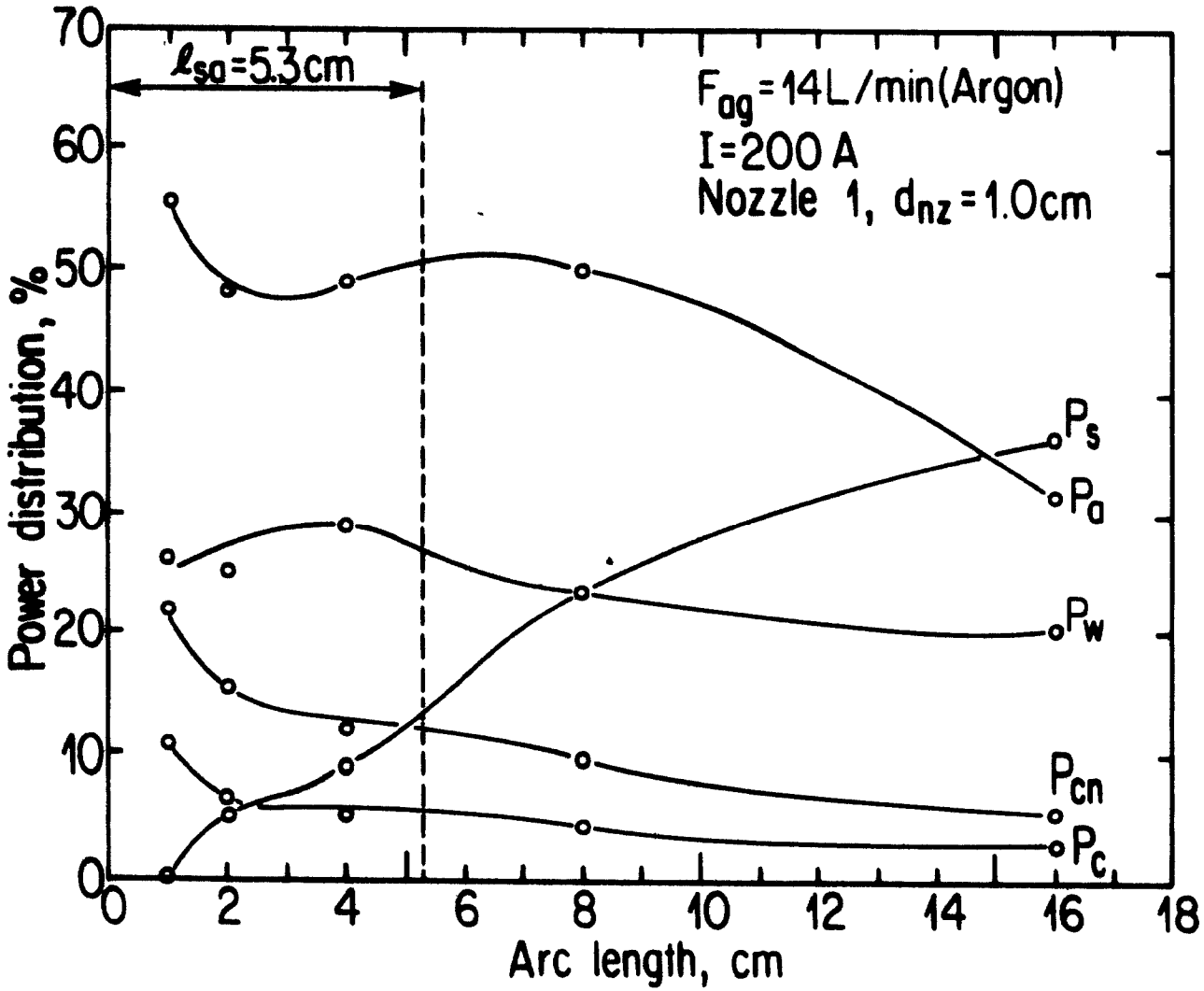
ℓ_{sa}=5.3cm
F_{ag}=14L/min(Argon)
I=200 A
Nozzle 1, d_{nz}=1.0cm
P_s
P_a
P_w
P_{cn}
P_c
Power distribution, %
Arc length, cm
0
10
20
30
40
50
60
70
0
2
4
6
8
10
12
14
16
18

FIGURE 14

PERCENT POWER DISTRIBUTION AS A

FUNCTION OF ARC LENGTH

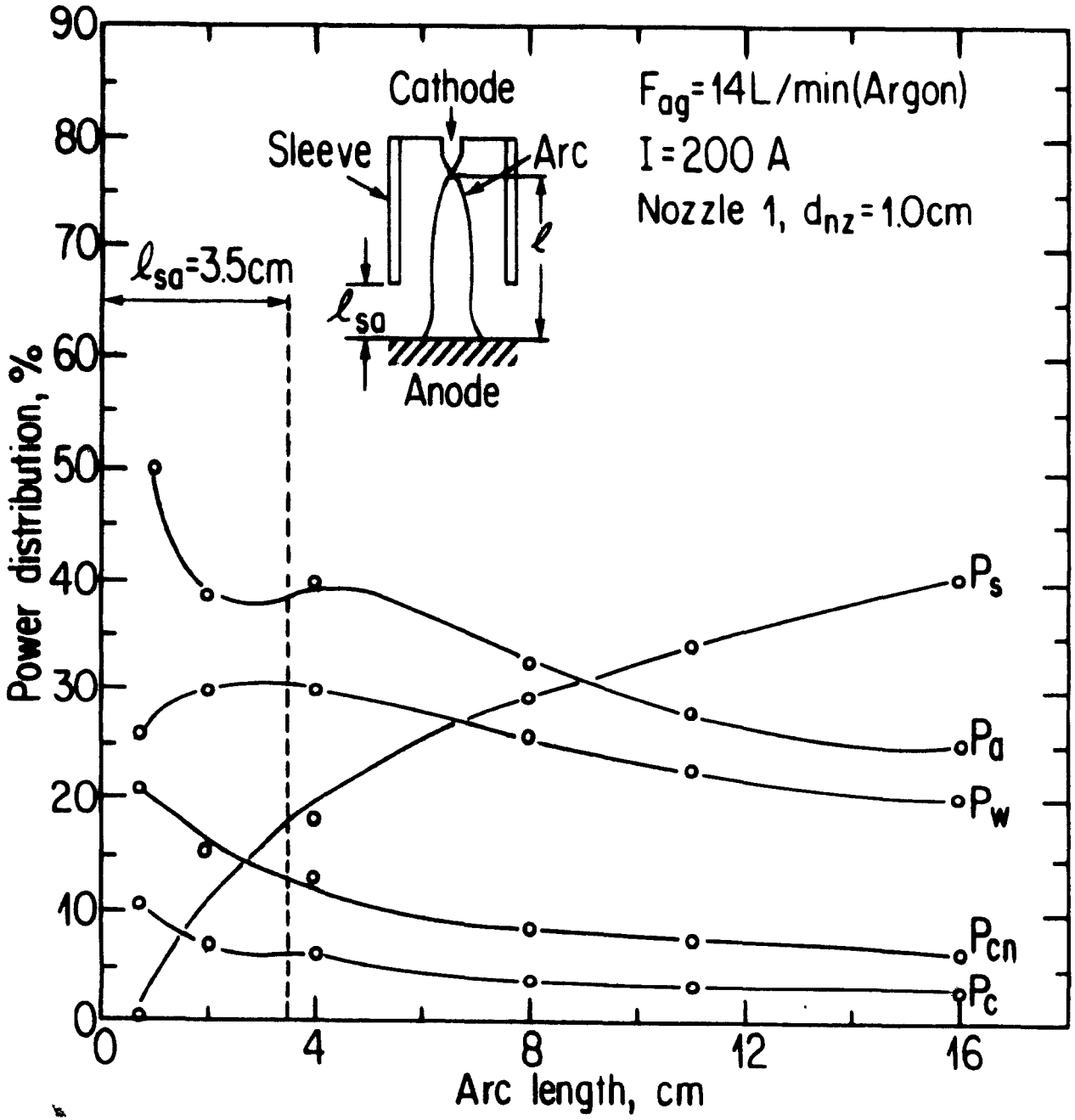
Cathode
Sleeve
Arc
Anode
ℓ_{sa}=3.5cm
ℓ_{sa}
ℓ
F_{ag}=14L/min(Argon)
I=200 A
Nozzle 1, d_{nz}=1.0cm
Power distribution, %
Arc length, cm
P_s
P_a
P_w
P_{cn}
P_c
0
10
20
30
40
50
60
70
80
90
0
4
8
12
16

The overall trend of decreasing energy transfer to the anode with increasing arc length results from a greater portion of the arc energy being radiated by the increasingly longer arc (hence higher arc voltage) to the walls and sleeve of the reactor.

The fraction of the arc's energy transferred to the anode was consistently higher when the distance separating the base of the sleeve and the anode surface (ℓ_{sa}) was greater (See Figures 11 and 12.) The sleeve being cooled probably acted as a heat sink Thus the closer it is situated to the anode surface the more radiant energy from the anode surface is absorbed. Also for equivalent arc lengths the sleeve whose length extended nearest to the anode surface would have surrounded the arc over a greater fraction of its length, thus absorbing more radiant and convective energy otherwise destined for the anode.

The fraction of the arc energy absorbed by the reactor walls and roof (P_w) increased with increasing arc lengths, as the luminous arc column was lengthened, until a portion of the arc began to be shielded by the sleeve. As the arc's length was increased further, a greater portion of the arc was confined within the sleeve and the proportion of the energy transferred to the wall and roof diminished.

The proportion of the arc's energy transferred to the cathode tip and cathode nozzle diminished with increasing arc length and represented only 6% of the total arc energy for arc lengths of 16 cm.

Figure 15 is a plot of the power distribution in kW for varying arc lengths. At constant arc currents, the power transferred to the anode (P_a) and the power transferred to the reactor wall and roof (P_w) did not change when the arc length was increased beyond 6 or 8 cm. In comparison, the slope of (P_s) is almost constant, increasing over the entire range of arc lengths, and the slope of (P_{cn}) remaining constant at zero over all arc lengths. At a fixed arc length, the fraction of the arc's energy transferred to the anode is essentially constant (Figure 16). As the total arc power is increased with increasing arc current for a fixed arc length, the actual power transferred to the anode also increases (Figure 17). This also is valid for other sections of the reactor.

The variation in the power distribution for a nitrogen plasma (Appendix B) with arc length and arc current is similar to that for an argon arc. The fraction of the nitrogen arc's power transferred to the anode (P_a) was consistently higher (5% to 15%) than for an argon arc, while the fraction transferred to the sleeve (P_s) and the cathode and nozzle (P_{cn}) was consistently lower by 10% to 20% for the sleeve and 2% to 5% for the cathode and nozzle. The fractions transferred to the reactor wall and roof were comparable.

Because of the nitrogen arc's higher voltage at the same conditions as that of an argon arc, the total power transferred to all portions of the reactor is much higher for a nitrogen arc

FIGURE 15

ACTUAL POWER DISTRIBUTION

WITH VARYING ARC LENGTH

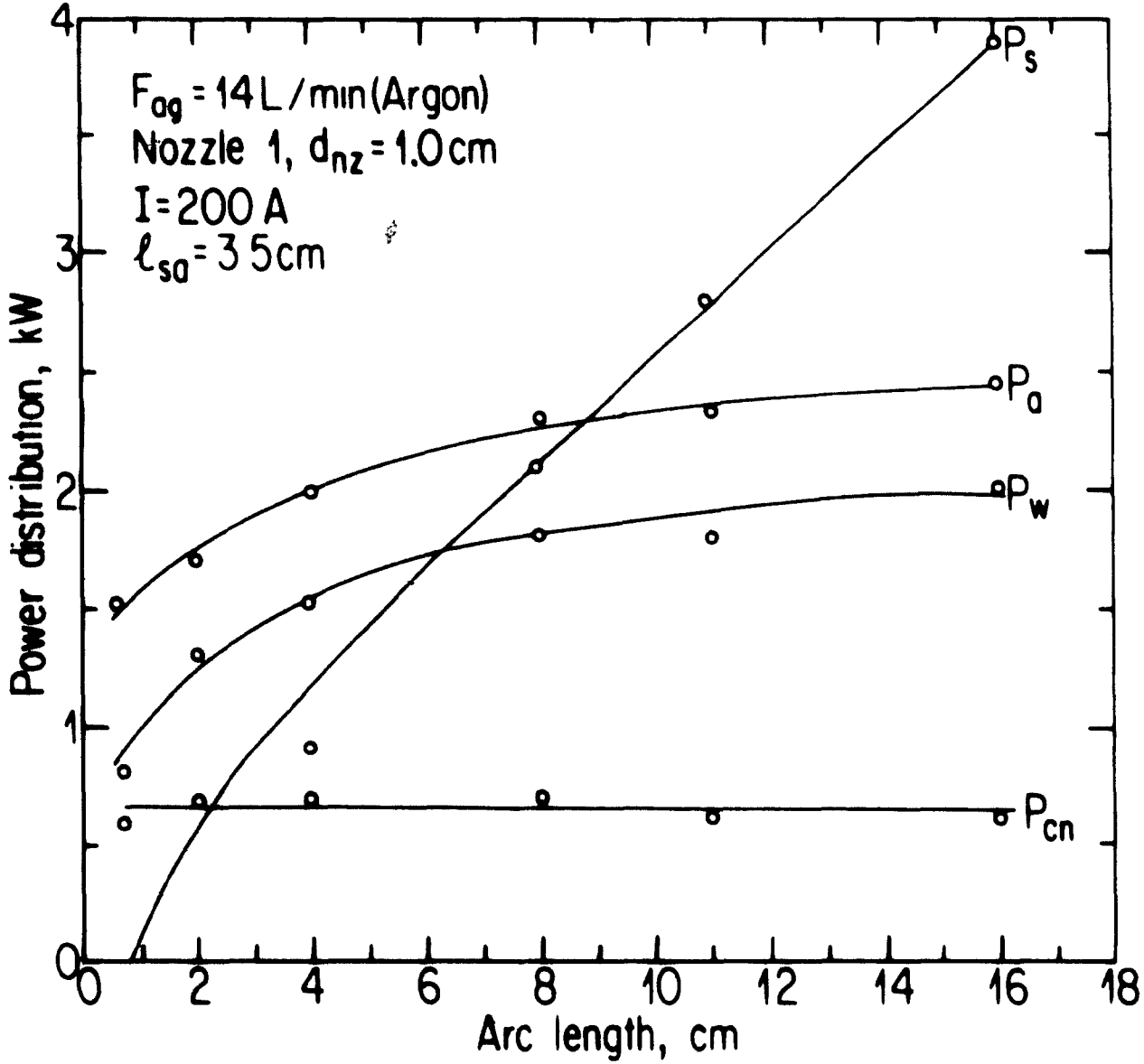
F_{ag} = 14 L/min (Argon)
Nozzle 1, d_{nz} = 1.0 cm
I = 200 A
ℓ_{sa} = 3.5 cm
P_s
P_a
P_w
P_{cn}
Power distribution, kW
Arc length, cm
0
1
2
3
4
0
2
4
6
8
10
12
14
16
18

FIGURE 16

FRACTION OF POWER TRANSFERRED TO THE ANODE

WITH VARYING ARC CURRENT

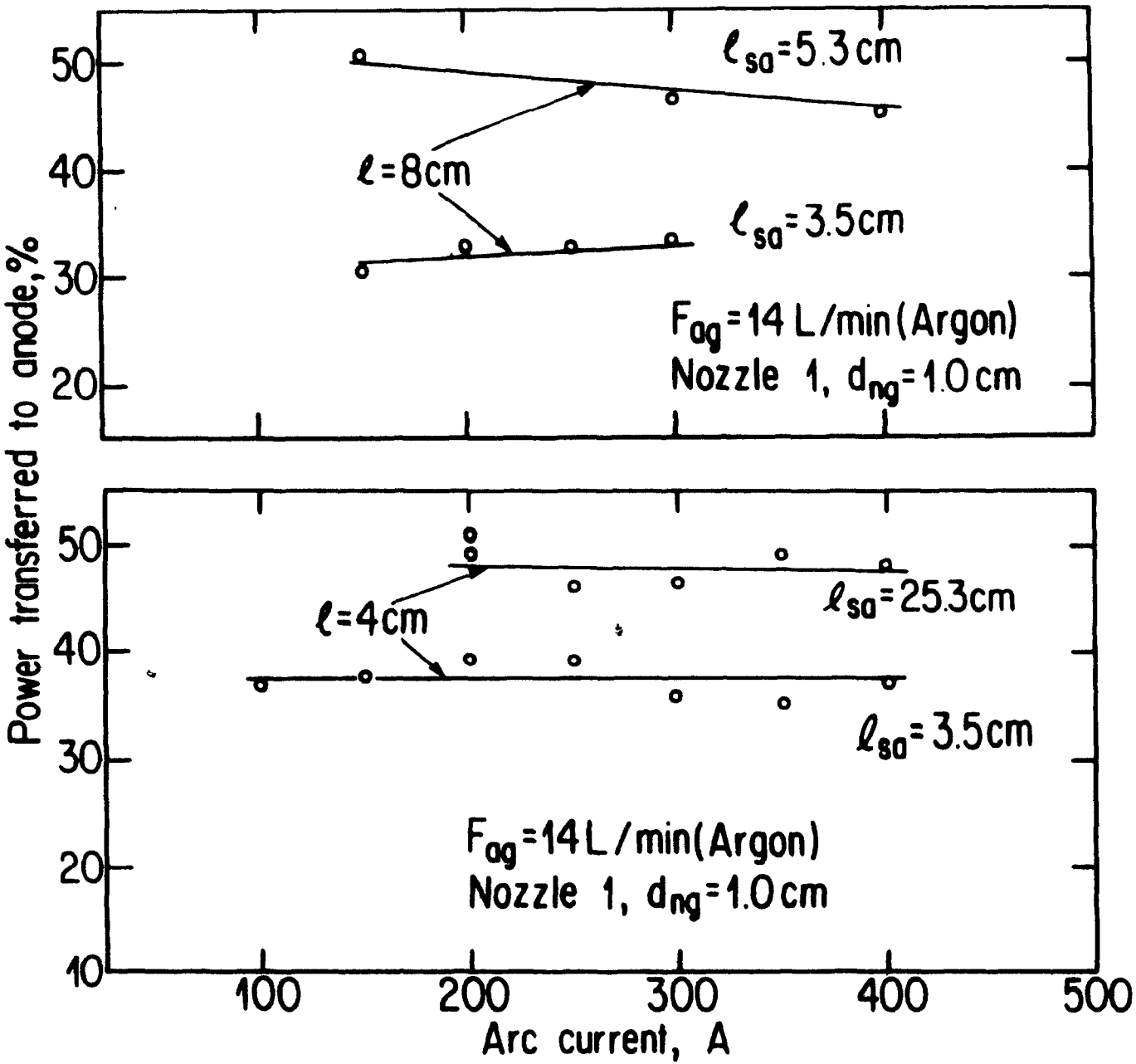
ℓ_{sa}=5.3cm
ℓ=8cm
ℓ_{sa}=3.5cm
F_{ag}=14 L/min(Argon)
Nozzle 1, d_{ng}=1.0cm
ℓ=4cm
ℓ_{sa}=25.3cm
ℓ_{sa}=3.5cm
F_{ag}=14 L/min(Argon)
Nozzle 1, d_{ng}=1.0cm
Power transferred to anode,%
Arc current, A
50
40
30
20
10
100
200
300
400
500

FIGURE 17

ACTUAL POWER TRANSFERRED TO THE ANODE

WITH VARYING ARC CURRENT

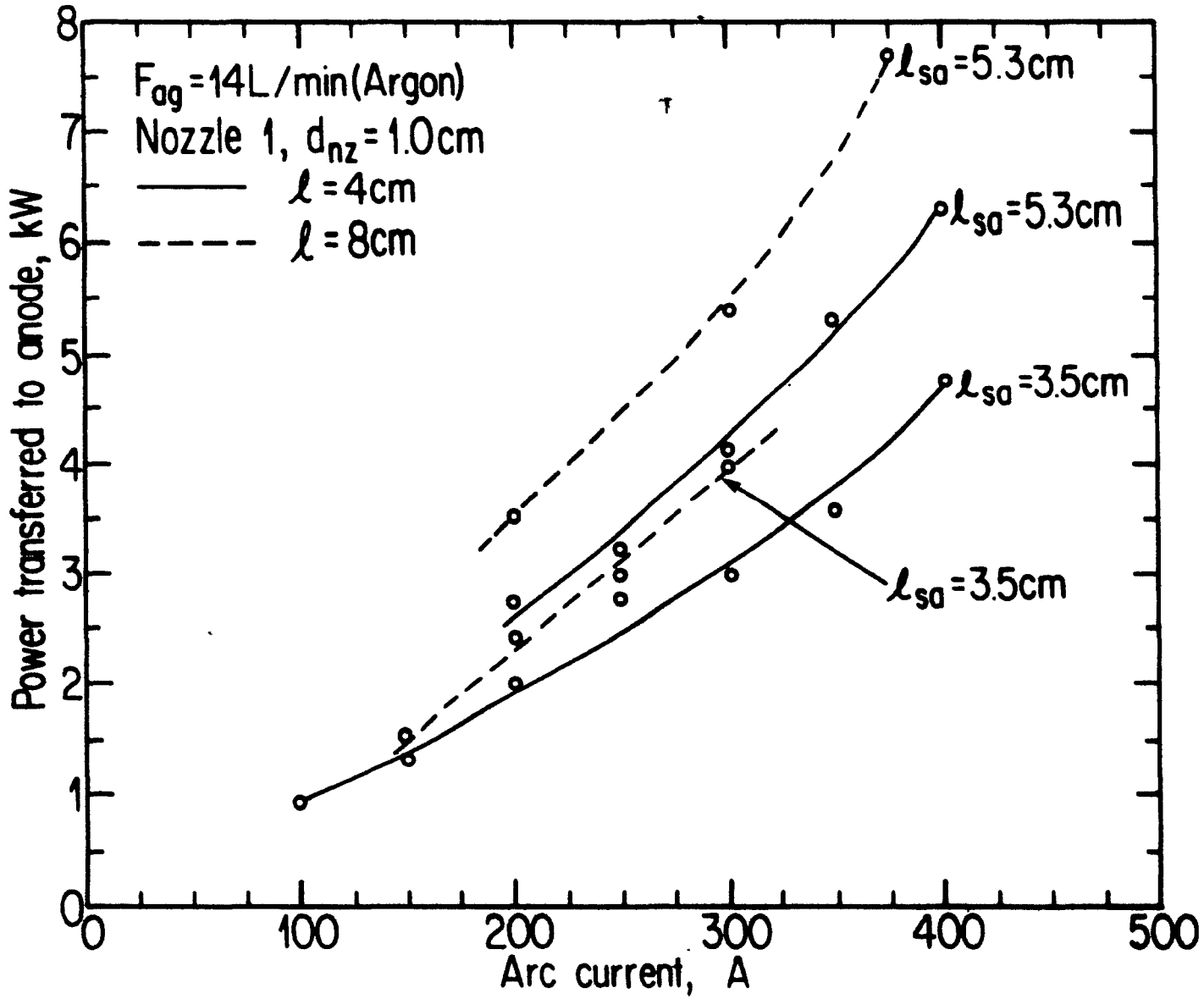
F_{ag}=14L/min(Argon)
Nozzle 1, d_{nz}=1.0cm
ℓ=4cm
ℓ=8cm
ℓ_{sa}=5.3cm
ℓ_{sa}=5.3cm
ℓ_{sa}=3.5cm
ℓ_{sa}=3.5cm
Power transferred to anode, kW
Arc current, A
0
1
2
3
4
5
6
7
8
0
100
200
300
400
500

Thus a reactor operating with a nitrogen plasmagen gas would be more powerful than a comparable reactor operating with argon.

The fraction of the total arc's power transferred to the exhaust gas stream was in all instances less than 1% when no particulate feeding was taking place, and thus was not considered in the preceding analysis.

5. Overall Energy Distribution with Particulate Feed

One of the most important results, as has already been mentioned, of introducing a particulate feed tangentially into the reactor sleeve is the significant increase in arc voltage and thus in the total arc power. This increase in arc voltage occurs even at very low feed rates. As the arc power increases as a result of the voltage increase, the major portion of this additional power is radiated over the full length of the arc and thus principally to the sleeve, which surrounds the arc over the major portion of its length. This is shown in Figures 18 and 19. In these figures, (P_f) represents the power absorbed by the feed. At low feed rates, the feed material is not present in sufficient quantity to absorb the extra arc power, and thus most of the extra power is transferred to the sleeve (P_s) with a small portion being transferred to the anode (P_a) and reactor wall and roof (P_w). At higher feed rates, the particulate feed forms a molten falling film on the inner surface of the sleeve and absorbs a fraction

FIGURE 18

PERCENT POWER DISTRIBUTION

WITH FEED RATE

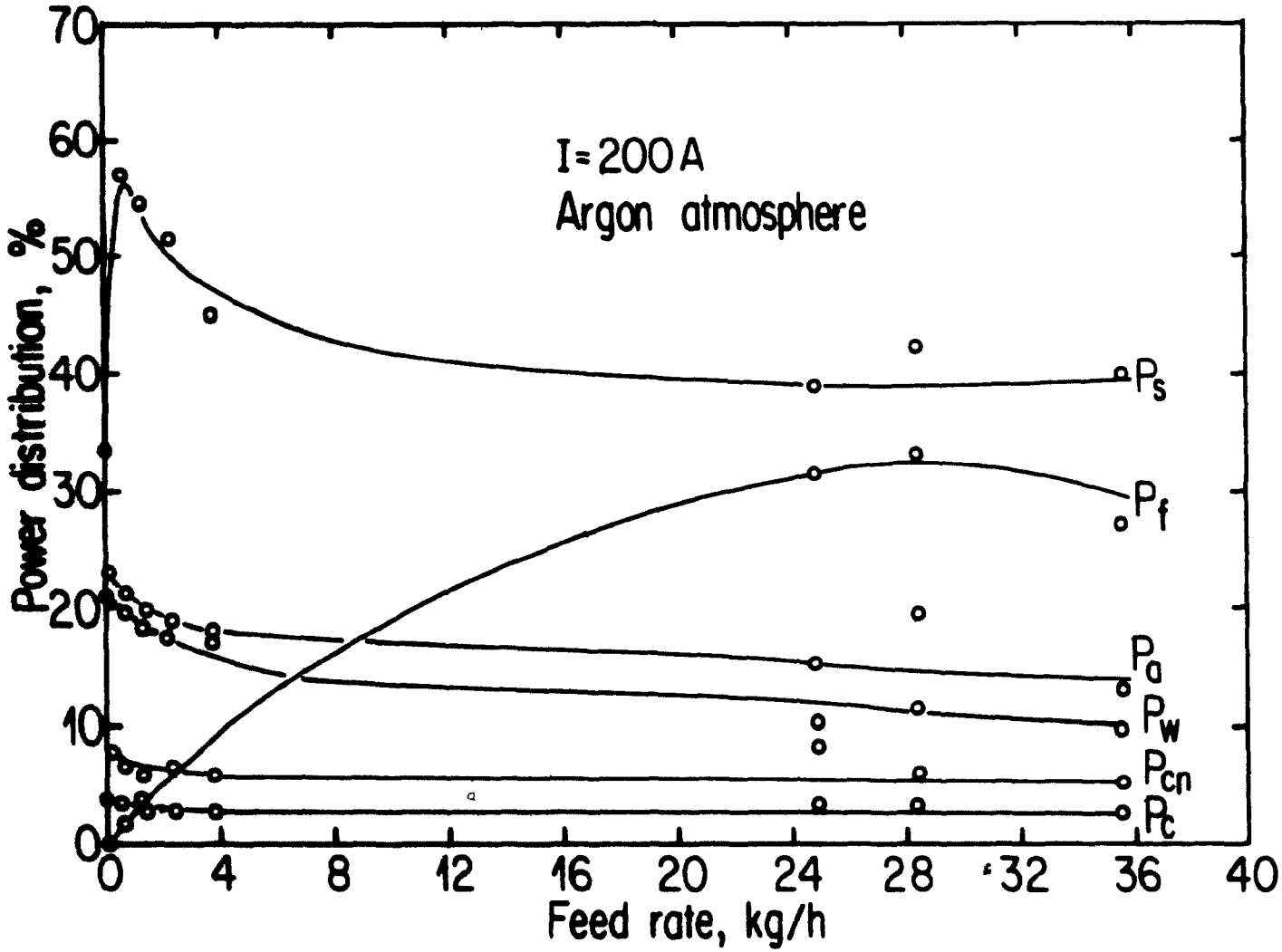
I=200A
Argon atmosphere
Power distribution, %
Feed rate, kg/h
Ps
Pf
Pa
Pw
Pcn
Pc
0
10
20
30
40
50
60
70
0
4
8
12
16
20
24
28
32
36
40

FIGURE 19

ACTUAL POWER DISTRIBUTION

WITH FEED RATE

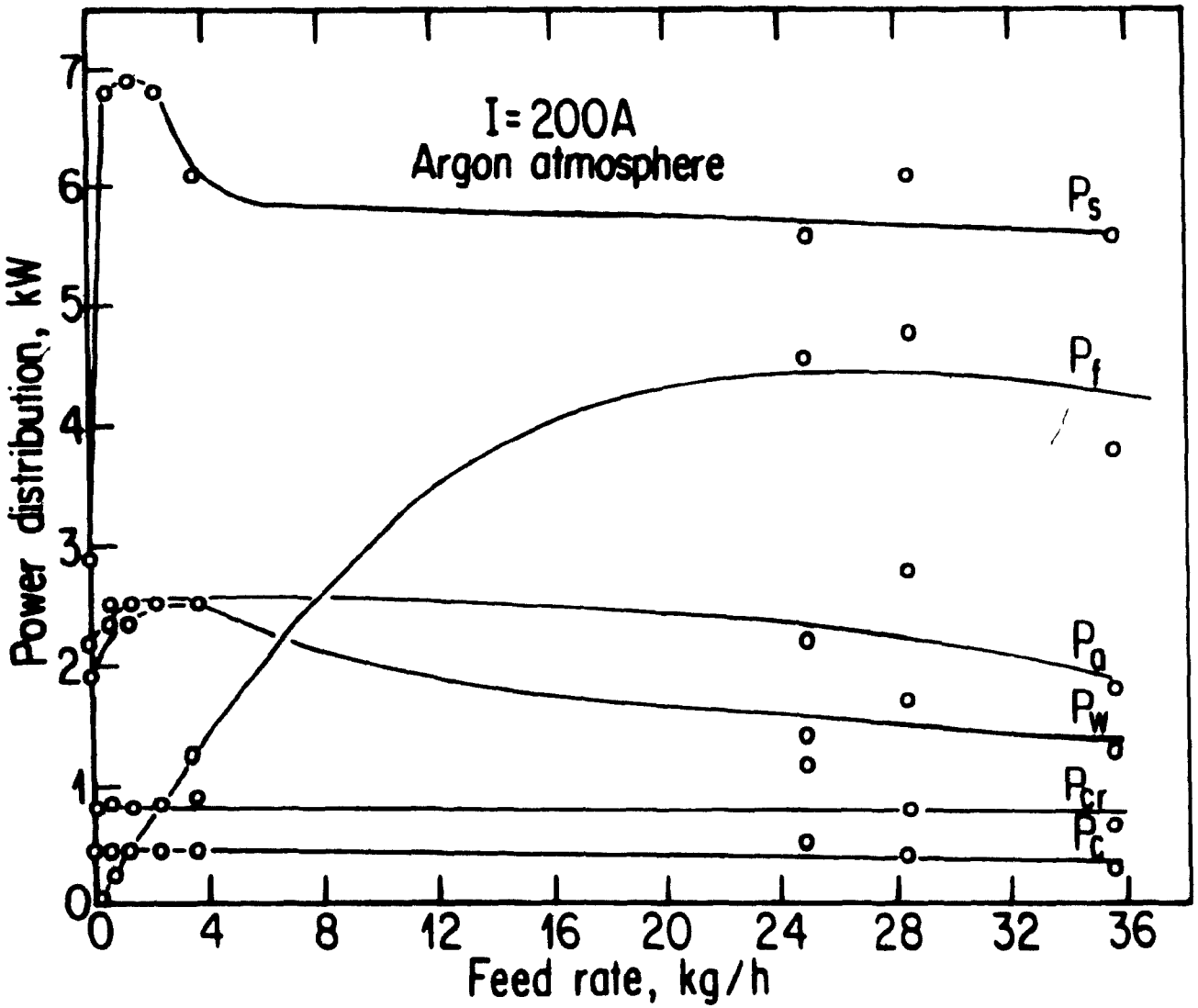
I=200A
Argon atmosphere
Power distribution, kW
Feed rate, kg/h
P_s
P_f
P_a
P_w
P_{cr}
P_c
0
1
2
3
4
5
6
7
0
4
8
12
16
20
24
28
32
36

of the arc's power Therefore at higher feed rates the power transferred to the sleeve diminishes The falling film protects and insulates the sleeve from the arc

As all the reactor surfaces are cooled, a large portion of the arc's energy is withdrawn from the reactor system As the power transferred to the sleeve and to the anode in an uncooled reactor is potentially usable, and only the energy transferred to the reactor wall, roof, cathode assembly and exhaust gas is lost, it should be possible to transfer to the feed and the charge at high feed rates 80 to 85% of the arc's power, with 10% being lost to the reactor wall and roof, and 5% being lost to the cathode assembly and approximately 3% to the exhaust gas stream (not shown in Figures 16 and 17)

The introduction of particulate feed into the reactor considerably reduced the fraction of the arc power lost to the wall and roof (P_w) and to the cathode and nozzle (P_{cn})

The proportion of the arc's power lost to the walls and roof could be reduced by insulating those surfaces indicating that in a properly designed and insulated reactor over 90% of the arc's power could be utilized for melting and/or chemical reactions within the reactor.

Figure 18 indicates that further increases in feed rate would not reduce the power lost through cooling of the sleeve and

anode. Thus energy losses to these surfaces would have to be reduced by reduced cooling and by insulating the surfaces, in order to achieve higher wall temperatures

Figures 16 and 17 also show the power absorbed by the feed entering the reactor. This curve was calculated by measuring the amount of feed melted in each test and calculating the theoretical power needed to heat and melt this amount The portion of the feed that was unmelted, but did absorb some of the arc's power as sensible heat was not included in the calculation as the final temperatures of the unmelted particles could not be measured. Thus, the curve for (P_f) on Figures 18 and 19 is conservative in its estimate of the power transferred to the feed

The sum of the values represented by each curve in Figure 18 exceeds 100% at high feed rates as a portion of the power transferred to the particulate feed is then transferred to the sleeve and anode The feed after melting in the falling film is cooled and solidifies along the inner surface of the sleeve and especially on the anode surface. This is shown in Table II where the value of P_{th} x % melted, (the power to melt the feed x fraction melted) is often greater than the value of $P_t - P_R$ (P_t is the arc power, P_R is the power withdrawn from the reactor cooling water.) A complete listing of the results of the tests involving the feeding of particulates into the reactor is given in Appendix C

TABLE II

PARTICULATE MELTING ENERGY REQUIREMENTS

TEST NO	F_p kg/h	P_t kW	P_R kW	$P_t - P_R$ kW	P_{th}[2] kW	% MELTED	P_f[4] kW	P_f[5] %
18	24 9	14 4	7 8	6 6	8 3	41	3 4	23 6
22	24.9	14 4	10 5	3 9	8 3	55	4 6	31 9
22SS[3]	24.9	14 4	10.5	3.9	8 3	64	5 3	36 8
27	35.6	14 0	9.5	4.5	11 9	32	3 8	27 1
30	28.4	14 4	11 4	3.0	9 5	50	4 8	33 3
21	24 9	24.0	18.6	5.4	8.3	80	6.6	27 5
23[1]	22.6	32.0	23.7	8.3	7 9	80	6 3	19 7

NOTE

1 N_2 atmosphere, all other tests in Ar atmosphere.

2 P_{th} = 0.34 kWh/kg x F_p (kg/h) (feed rate) = kWh/kg.

3. Values corrected to reflect steady-state operation.

4. $P_f = P_{th}$ x % Melted = energy absorbed by feed

5. % of overall reactor power absorbed by powder (calculated).

Table II also lists the fraction of the particulate feed melted in each of the high feed rate tests ($F_p > 20$ kg/h). The fraction melted ranged from 41% to 80%. In the low feed rate test ($F_p < 4$ kg/h), the fraction melted was in all cases 100%.

Test 22 (argon, 200 amperes) was performed under the same conditions and with the same feed rate as test 18, with the exception that the duration of test 22 was double that of test 18. This was done in order to estimate the steady-state operating conditions. As is shown in Table I and II, the steady-state melting efficiency was 10% higher than that for the entire run, and the fraction of the arc's power used to melt the feed was 5% greater. Thus the reported values of melting efficiency and power transferred to the feed in the other test, where no steady-state correction was applied, are conservative. Tests reporting 80% melting efficiency probably had steady-state melting efficiency of greater than 90%.

The lowest energy consumption per kg of feed melted was 0.91 kWh/kg. The theoretical energy requirement is 0.34 kWh/kg which includes the sum of the sensible heat required to raise the temperature of the solid iron feed to its melting point, and the heat of fusion necessary to melt the iron. The performance of the reactor must take into consideration that the reactor was heavily cooled and that over 70% of the arc's power was lost to the cooled

surface. In an insulated reactor, where the losses to the wall would be greatly reduced, the melting performance would be considerably improved, probably by a factor of 2 or 3 times. Thus at the same reactor power levels, considerably higher feed rates could be utilized.

The total time of particulate injection was limited because of limited hearth capacity and because of problems with leaks in the sleeve. (Leaks tended to occur at the welded joints exposed to the arc's radiation.) Also because the anode was cooled, melted feed tended to solidify directly below the base of the sleeve, and not flow and form a pool over the entire diameter of the hearth, thus reducing the effective capacity of the latter and limiting the feed time per test.

It might be argued that the feed is melted by the arc radiation and that the power transferred to the anode is not utilized. In fact, the power transferred to the anode can be utilized in a number of ways. It can be utilized to melt a charge placed in the reactor hearth prior to arc initiation, or during reactor operation. It can also be used to supply the energy necessary for reaction taking place in the melt. The reactants either in the form of a solid or a gas could be introduced into the melt during reactor operations. And finally, the power transferred to the anode could be used as a supplement to the sleeve. At very high feed rates the power transferred to the anode could be used to melt the portion of the feed not melted by the arc's radiation before reaching the hearth.

The amount of dust in the exhaust gas was measured by placing filters over the reactor's outlets. The results are listed in Table I. The proportion of the feed lost to the exhaust gas stream was very small in all cases where it was measured and ranged from 0.03% to 0.1% of the feed. The particles collected in the exhaust stream were very fine. A portion of the feed was probably vaporized upon entering the arc and recondensed in the cool outlet gas stream, forming a dark fume.

CONCLUSIONS AND RECOMMENDATIONS

This thesis deals with a novel plasma reactor design (the Noranda - Hydro-Québec plasma reactor) which was successfully designed, constructed and operated. The performance of the reactor was studied over a wide range of operating conditions. The operating parameters studied included the arc length and current, the axial and tangential gas flow rates, the type of plasmagen gas used and the particulate feed rate and size.

Measurements indicated that the majority of the arc's power is transferred to the particulate feed, the sleeve and the anode. In an uncooled reactor, all of this power constitutes the useful part of the energy supplied to the furnace. In order to minimize heat losses to the wall and roof of the reactor, the sleeve must always surround the plasma arc over the maximum portion

possible of its length. A properly designed and insulated Noranda - Hydro-Québec type of reactor should be able to utilize over 90% of the power supplied to the reactor. A reactor of such efficiency would open the door to the development of many new plasma metallurgical or chemical processes. It is important to note that this level of efficiency applies to the process as a whole. Most manufacturers of plasma torch report fairly high efficiencies, but the latter is from the d.c. line to the plasma gas, and does not include the transfer of energy from the gas to the process. Thus their overall efficiency is considerably less than that reported here.

In addition to its high power efficiency, this reactor is capable of accepting a wide range of particulate feed sizes and at the same time produces very little fume, thus minimizing the problem of cleaning the exhaust gases. In addition, future designs might be able to operate with lower plasmagen gas rates, by eliminating the axial gas stream, thus reducing energy lost to the exhaust stream and operating costs.

The modifications that should be implemented in order to improve the reactor are as follows:

i. The sleeve design has to be modified in order to eliminate the problem of water leaks. All welds must be located in such a manner as not to be exposed to direct radiation emanating from the arc. Most of the water leaks in the sleeve occurred along the welds.

ii. The sleeve should be movable so as to at all times surround the maximum fraction of the arc.

iii. The cooling of the anode, sleeve, reactor walls and roof should be reduced to a minimum in order to maximize the melting efficiency of the reactor.

Future studies of the reactor should include:

i. Study of the effect of varying the diameter of the sleeve.

ii. Study the heat transfer rates and mechanism between the arc, the falling film and the sleeve.

iii. Study of the melting efficiency in an uncooled reactor, in order to determine the optimum power consumption rates per kg of feed and melting efficiency.

A summary of the more important observations and conclusions which were derived from the experimental part of this work is as follows:

i. In the reactor design studied 80% to 85% of the transferred-arc's power was transferred to the anode, sleeve and feed and is thus potentially usable.

ii. With 70% of the arc's energy lost to the cooled surfaces, the energy consumption was 0.91 kWh/kg compared to a theoretical requirement of 0.34 kWh/kg.

iii. The voltage of an argon arc increases by 25 to 30 volts with the addition of a particulate feed. The voltage of a nitrogen arc increases by 20 volts.

iv. Tangential gas injection into the sleeve stabilizes the arc and lowers the arc voltage by 5 to 7 volts.

v. The exhaust gas stream contains negligibly little dust (fume) and always less than 3% of the total power input.

vi. Utilizing nitrogen instead of argon as the plasmagen gas results in a 100% increase in the arc's voltage, hence power, thereby doubling the power and operating rate of the reactor.

REFERENCES

REFERENCES

Asada, C. and Adachi, T., "On Plasma Induction Melting," 3rd Int. Symp. on Electroslag and Other Special Melting Technologies, Ed. Bhat, G.K., and Simkovich, A., p. 165 (June 1971)

Bhat, G.K., "Plasma Technology and Its Industrial Applications," A survey report prepared for EPRI, Pittsburgh, Pa. (December 1981)

Chase, J.D. and Skriven, J.F., "Process for the Beneficiation of Titaniferous Ores Utilizing a Hot Wall Continuous Plasma Reactor," U.S. Patent 3856918 (1974)

Choi, H.K., "Operating Characteristics and Energy Distribution in Transferred-Arc Plasma Systems," Ph.D. Thesis, McGill University (August 1980)

Choi, H.K., and Gauvin, W.H., "Operating Characteristics and Energy Distribution in Transferred-Arc Systems," Plasma Chemistry and Plasma Processing, 2 (4) p. 361-386 (December 1982)

Curr, T.R. et al., "The Design and Operation of Transferred-Arc Plasma Systems for Pyrometallurgical Applications," Proc. of the 6th Int. Symp. on Plasma Chemistry, Montreal p. 175-180 (July 1983)

Ettingler, L.A., "Applications of High-Temperature Plasmas," Mitre Corp. for Electricité de France contract No. 14-070 (1979)

Foster-Wheeler/Tetronics : News Feature, "Plasma Process is Ready for Metal Recovery," Chem Eng. 86 (4) (1979)

Gauvin, W.H., Kubanek, G.R., and Irons, G.A., "The Plasma Production of Ferromolybdenum - Process Development and Economics," Journal of Metals, 33 (1) p. 42-46 (January 1981)

Gauvin, W.H. and Kubanek, G.R., "A Novel Transferred-Arc Plasma Reactor for Chemical and Metallurgical Applications," U.S.A. 382 415 (May 26, 1982), plus 15 other countries

Gauvin, W.H. and Choi, H.K., "Plasmas in Extractive Metallurgy," Proc. of Symp. on Plasma Processing and Synthesis of Materials, Sponsored by the Materials Research Society, Boston (November 1983)

Goldman, K., Proc. 5th Int. Conf. on Phenomena in Ionized Gases, Munich p. 863 (1961)

Hamblyn, S.M.L., "Plasma Technology and Its Applications to Extractive Metallurgy," Mineral Sci. Engng. 9 (3) (July 1977)

Lachner, W. et al., "Results with Plasma Torch Furnaces for Melting High Quality Steels from High Alloy Scrap," Proc. 4th Int. Conf. on Vacuum Metall. (1973)

MacRae, D.R., "Plasma Processing in Extractive Metallurgy: The Falling-Film Plasma Reactor," Plasma Chemical Processing, AIChE Symp. Series 186, (75) (1979)

Mehmetoglu, M.T., "Characteristics of a Transferred-Arc Plasma," Ph.D. Thesis, McGill University (1980)

Mehmetoglu, M.T. and Gauvin, W.H., "Characteristics of Transferred-Arc Plasma," AIChE Journal 29 (2) p. 207-215 (March 1983)

Sheer, C. et al., "Arc-Vaporization of Refractory Powders," Proc. of the Fine Particles Symp. Electrochem Soc. Boston (October 1973)

Takei, H. and Ishigami, Y., J. Vac. Sci., Tech. 8 (6) (1971)

Tsantrizos, P., "Operating Characteristics and Energy Distribution in a Nitrogen Arc Plasma," M. Eng. Thesis, McGill University (1981)

Tsantrizos, P. and Gauvin, W.H., "Operating Characteristics and Energy Distribution in a Nitrogen Arc Plasma," C.J.Ch.Eng., 60 (6) p. 822-830 (1982)

Tylko, J.K., "High Temperature Treatment of Materials," Can. Pat. 957733 granted to Tectronics Ltd. (1974)

A P P E N D I X A

EXPERIMENTAL RESULTS ARGON - NO FEED

TABLE A-1

OVERALL REACTOR ENERGY DISTRIBUTION IN A PURE ARGON ATMOSPHERE[1]

ℓ cm	I A	V V	P_t kW	P_c kW	%	P_n kW	%	P_s kW	%	P_w kW	%	P_d kW	%	P_R kW	%	ℓ_{sa} cm
0.5	100	12.2	1.2	0.1	(8.6)	0.2	(12.9)	0.0	(0.0)	0.3	(24.0)	0.6	(24.0)	1.2	(97 0)	3 5
0.7	200	15.1	3.0	0.3	(10.4)	0.3	(10.4)	0.0	(0.0)	0.8	(25.9)	1.5	(49.9)	2.9	(96 5)	3 5
1	100	14.4	1.4	0.1	(9.7)	0.1	(9.7)	0.0	(0.0)	0.4	(27.1)	0.6	(43.6)	1.3	(90.1)	3 5
1	150	15.2	2.3	0.2	(9.2)	0.2	(9.2)	0.0	(0.0)	0.6	(25.7)	0.9	(38.5)	1.9	(82.6)	3.5
1	200	16.0	3.2	0.4	(10.9)	0.4	(10.9)	0.0	(0.0)	0.8	(26.1)	1.8	(55.1)	3.3	(103.0)	5.1
1	250	19.2	4.8	0.4	(8.3)	0.5	(9.7)	0.0	(0.0)	1.2	(24.4)	2.3	(47.2)	4.3	(89.6)	3 5
2	100	17.1	1.7	0.2	(13.8)	0.2	(9.2)	0.0	(0.0)	0.4	(24.5)	1.0	(55.7)	1.8	(103.1)	3 6
2	150	18.7	2.8	0.2	(7.5)	0.2	(7.5)	0.4	(13.9)	0.7	(27.8)	1.0	(35.8)	2.6	(92 5)	3.5
2	200	21.7	4.3	0.3	(7.2)	0.4	(8.0)	0.7	(15.9)	1.3	(29.6)	1.7	(38.8)	4.3	(99 5)	3 5
2	200	20.0	4.0	0.3	(7.0)	0.4	(8.7)	0.2	(5.6)	1.0	(25.1)	1.9	(48.1)	3.8	(94.7)	5 1
2	250	22.8	5.7	0.4	(6.7)	0.5	(8.1)	0 4	(6.9)	1.6	(27.4)	2.4	(42.8)	5 3	(92.2)	3 5
2	300	23.8	7.1	0.4	(4.9)	0.6	(7.8)	0 9	(12.9)	2.3	(31.7)	2 8	(39 4)	6 9	(96.7)	3 5
2	300	24.0	7.2	0.4	(5.3)	0.7	(9.7)	0.7	(9.7)	2.0	(27.8)	3.0	(41.2)	6.7	(93 7)	3 5
2	300	22.8	6.8	0.4	(5.6)	0.6	(8.7)	0 5	(6.7)	1.7	(24.5)	3 4	(49 0)	6 5	(94 5)	5 1
3	100	20.0	2.0	0.3	(14.4)	0.2	(8.0)	0.0	(0.0)	0.6	(29.3)	0.9	(43.1)	1.9	(94 6)	3.6
3	150	21.5	3.2	0.2	(6.5)	0.2	(6.5)	0.4	(12.1)	1 0	(30 3)	1.3	(38 9)	3.0	(94 3)	3 5
4	100	23.9	2.4	0.2	(6.7)	0.1	(4.4)	0 2	(8.2)	0.7	(28.6)	0 9	(36 8)	2 0	(84 5)	3 5
4	150	24.7	3.7	0.2	(5.7)	0.3	(7.1)	0.4	(10.5)	1.2	(31.6)	1.4	(37 3)	3 4	(92.1)	3 5
4	200	25.4	5.1	0.3	(6.2)	0.4	(6.9)	0.9	(18.1)	1 5	(30.0)	2.0	(39.5)	5 1	(100 6)	3 5
4	200	27.0	5.4	0.3	(5.8)	0.4	(6.5)	0 5	(9.0)	1.7	(29.4)	2 7	(49.0)	5 4	(99 8)	5 3
4	250	28.3	7.1	0.4	(5.6)	0.5	(6.6)	1.2	(16.6)	2.0	(27.6)	2.8	(39.4)	6 8	(95 8)	3 5
4	250	28.1	7.0	0.4	(5.0)	0.5	(7 0)	0.5	(7.0)	1.8	(25.1)	3.2	(45 3)	6 4	(90 3)	5 3
4	300	28.6	8.6	0.4	(4.1)	0.5	(5.7)	1.8	(21 5)	2.5	(29.5)	3 0	(35.3)	8.2	(95 9)	3 5
4	300	29.8	8.9	0.4	(4.3)	0.6	(7.0)	1.2	(13 7)	2.3	(26.2)	4.1	(45 9)	8 7	(97 1)	5 3

continued /A.2

...continued

TABLE A-1

OVERALL REACTOR ENERGY DISTRIBUTION IN A PURE ARGON ATMOSPHERE[1]

ℓ cm	I A	V V	P_t kW	P_c kW	%	P_n kW	%	P_s kW	%	P_w kW	%	P_a kW	%	P_R kW	%	ℓ_{sa} cm
4	350	29.8	10.4	0.4	(4.0)	0.6	(6.0)	2.3	(22.1)	3 0	(28.4)	3.6	(34 2)	9.9	(94.7)	3 5
4	350	30.6	10.7	0.4	(3.6)	0.6	(6.0)	0.7	(6.8)	2.8	(25.8)	5 3	(49.2)	9 8	(91 3)	5 3
4	400	31.9	12.8	0.4	(3.3)	0.6	(4 9)	2.3	(18.0)	3 8	(30.1)	4 8	(37 3)	11.9	(93 5)	3 5
4	400	32.6	13.0	0.5	(3.5)	0.8	(6.4)	1.2	(9.4)	3 6	(27 6)	6 3	(48.3)	12 4	(95 1)	5 3
6	100	28.5	2.9	0.2	(5.5)	0.1	(3.7)	0 4	(3 7)	0 8	(27 4)	1 0	(35.2)	2 4	(85 5)	3 5
8	150	33.3	5.0	0.2	(4.2)	0.3	(5.3)	1.4	(27.4)	1 4	(27.4)	1 5	(30 2)	4 7	(94 3)	3 5
8	200	35.7	7.1	0.3	(3.9)	0.4	(4.9)	2.1	(29.0)	1 8	(25.8)	2.3	(32 6)	6 9	(96 2)	3 5
8	200	34.5	6.9	0.3	(4.6)	0.4	(5 1)	1 6	(23.4)	1.6	(23.1)	3.5	(50 6)	7 4	(106 8)	5 3
8	250	35.9	9.0	0.4	(4.4)	0.5	(5.2)	2.3	(26 1)	2 2	(23.9)	3 0	(33 0)	8 3	(92 7)	3 5
8	300	39.8	11.9	0.4	(3.0)	0.4	(3.5)	3.7	(31.2)	2.8	(23.6)	4 0	(33 8)	11.2	(94 1)	3 5
8	300	38.8	11.6	0.4	(3.6)	0.6	(4.8)	2 5	(21.8)	2 4	(20.9)	5 4	(46 5)	11 3	(97 4)	5 3
8	400	42.6	17.0	0.4	(2.5)	0.8	(4 5)	3 7	(21.5)	3 2	(18.7)	7 7	(45 2)	15 7	(92 3)	5 3
11	150	37.3	5.6	0.2	(3.7)	0 3	(4.7)	1 8	(31 4)	1 4	(24.4)	1.5	(26 9)	5 1	(91 2)	3 5
11	200	40.3	8.1	0.3	(3.5)	0 3	(3 9)	2 8	(34.3)	1.8	(22 9)	2 3	(27 9)	7 4	(92 4)	3 5
11	250	39.4	9.9	0.4	(4.0)	0.4	(4 0)	2 7	(27 8)	2 2	(21 8)	3 1	(31 9)	8 8	(89 5)	3 5
16	200	48.1	9.6	0.3	(3.3)	0.3	(3.3)	3.9	(40 6)	2 0	(20.3)	2 4	(24 8)	8 9	(92 2)	3 5
16	200	47.2	9.4	0.3	(3.0)	0.3	(3 3)	3.5	(36.6)	1 9	(20 4)	3.0	(31 9)	9 0	(95 2)	5 3
16	250	48.4	12.1	0.4	(3.3)	0.4	(3.3)	4 7	(38 7)	2 3	(18.6)	3 3	(27 4)	11 0	(91 2)	3 5
16	300	49.4	14.8	0.4	(2.4)	0.4	(2 8)	7.4	(49.7)	2.6	(17.7)	3.2	(21 9)	14 0	(94 4)	3 5
16[2]	300	54.0	16.2	0.4	(2.4)	0.5	(3 0)	6.5	(39 8)	1.8	(20.4)	3.0	(34 8)	15 7	(96 9)	5 3

NOTES:

1. Nozzle 1, d_{nz} = 1.0 cm, F_{ag} = 14 L/min.
2. V not considered accurate.

TABLE A-2

OVERALL REACTOR ENERGY DISTRIBUTION IN A PURE ARGON ATMOSPHERE[1]

ℓ cm	I A	V V	P_t kW	P_c kW	%	P_n kW	%	P_s kW	%	P_w kW	%	P_a kW	%	P_R kW	%	ℓ_{ba} cm
2	200	22.1	4.4	0.4	(7.9)	0.3	(6 3)	0 2	(5.4)	1 4	(31.4)	1.9	(43 4)	4 2	(94 2)	4 2
4	100	27.3	2.7	0.4	(10.2)	0.1	(5.1)	0 2	(8.7)	0.9	(31.9)	1 3	(47 0)	2 8	(102 9)	4 2
4	200	28.5	5.7	0.4	(6.1)	0.4	(6.1)	0 5	(8 3)	1 8	(32.1)	2 3	(39 4)	5 3	(92 1)	4 2
4	300	30.6	9.2	0.4	(4.6)	0.6	(6 5)	1 2	(12 9)	3.0	(32.3)	3 5	(38 4)	8 7	(94 7)	4 2
4	400	33.6	13.4	0.5	(3.6)	0 9	(6 8)	1 9	(14 1)	4.2	(31.1)	4 9	(36 4)	12 4	(92 0)	4 2
8	200	36.1	7.2	0.4	(4 8)	0 4	(5 3)	1 9	(26 3)	1.8	(25.4)	2 3	(31 1)	6 7	(92 9)	4 2
11	200	40.2	8.0	0.4	(4 3)	0.4	(5.2)	2 4	(29 5)	1 9	(23 9)	2 3	(27 9)	7 3	(90 8)	4 2
16	200	48.9	9.8	0.4	(3.6)	0.4	(4 3)	3 8	(38 8)	2 0	(20.5)	2 3	(23 0)	8 8	(90 1)	4 2

NOTE:

[1] Nozzle 2, d_{nz} = 0.75 cm, F_{ag} = 14 L/min

TABLE A-3

ARC VOLTAGE AND REACTOR ENERGY DISTRIBUTION

WITH VARYING AXIAL GAS FLOW RATE[1]

ℓ	I	V	P_t	P_c	%	P_n	%	P_s	%	P_w	%	P_a	%	P_R	%	F_{ag}
cm	A	V	kW	kW		kW		kW		kW		kW		kW		L/min
4	300	28.6	8.6	0.4	(4.1)	0.5	(5 7)	1.8	(21 5)	2 5	(29 5)	3 0	(35 3)	8 2	(95 9)	14
4	300	29.2	8.8	0.4	(4.0)	0.4	(4.8)	1.8	(21.0)	2.8	(31 8)	3 5	(39 5)	8 9	(101 1)	20
4	300	29.9	9.0	0.4	(3.9)	0.4	(4.7)	1.8	(20.5)	2 8	(31 1)	3.2	(36 2)	8 6	(96 3)	25
4	300	30.7	9.2	0.4	(3.8)	0.4	(4.5)	1.8	(20 0)	2 8	(30.3)	3 2	(35.2)	8 6	(93 8)	30
4	300	32.2	9.6	0.4	(3.6)	0.4	(4.3)	1.8	(19 0)	3.0	(30 6)	3 2	(33.6)	8.8	(91 3)	40

NOTE:

1. Pure argon atmosphere, nozzle 2, d_{nz} = 0.75 cm.

TABLE A-4

ARC VOLTAGE AND REACTOR ENERGY DISTRIBUTION

WITH VARYING TANGENTIAL GAS FLOW RATE[1]

ℓ cm	I A	V V	P_t kW	P_c kW	z	P_n kW	z	P_s kW	z	P_w kW	z	P_a kW	z	P_R kW	z	F_{tg} L/min
16	200	45.3	9.1	0.3	(3 5)	0.3	(3.1)	3.9	(43.2)	1.8	(20.4)	2 2	(23 9)	8.5	(94 1)	0.0
16	200	42.3	8.5	0.4	(5 1)	0.3	(3.9)	3.6	(42.5)	1.8	(20.8)	2.5	(29.9)	8.6	(102 2)	14 0
16	200	41.5	8.3	0.4	(5.2)	0.3	(4.0)	3.1	(37.1)	1.6	(19.2)	2 4	(28 4)	7.8	(93.8)	18.0
16	200	41.1	8.2	0.4	(5.2)	0 3	(4.0)	3.1	(37.5)	1.6	(19.3)	2.0	(24.0)	7 4	(90 5)	30.0
16	200	40.4	8.1	0.4	(5.3)	0.3	(4.1)	3.1	(38.4)	1.6	(19.8)	2.0	(24.7)	7.4	(92.1)	38.0
16	300	51.4	15.4	0.4	(2.8)	0.4	(2.7)	6.9	(44.7)	2.8	(18.1)	3.5	(22 1)	13.9	(90.3)	0.0
16	300	47.0	14.1	0.4	(2.5)	0.4	(2 7)	6.5	(45.7)	2 7	(19.2)	3 6	(25 3)	13 4	(95.4)	14 0
16	300	44.6	13.4	0.4	(2.6)	0.4	(2.9)	6.0	(44.7)	2.6	(19.5)	3.2	(24 2)	12.9	(96 2)	20 5
16	300	43.8	13.1	0.4	(2.7)	0.4	(2.9)	5.5	(42.0)	2.6	(19.9)	3.0	(23.0)	11 9	(90.8)	30 0
16	300	43.0	12.9	0.4	(2.7)	0.4	(3.0)	5.5	(42.8)	5.5	(20.3)	3.0	(23 5)	11 9	(92 2)	39 0
4	250	27.6	6.9	0.5	(7.1)	0.5	(7.1)	1.0	(14.6)	2.0	(28.9)	2.4	(35 2)	6.4	(92 8)	0 0
4	250	28.4	7.1	0.4	(5.6)	0.6	(7.9)	1.0	(14.1)	2.2	(30.6)	2.4	(34 2)	6.6	(92 7)	20.0
4	250	29.6	7.4	0.4	(5.6)	0.6	(7.6)	1.0	(13.6)	2.3	(30.6)	2.4	(32.8)	6.7	(90 2)	30.0
4	250	29.9	7.5	0.4	(5.6)	0.6	(7.5)	1 3	(16 8)	2.4	(31.5)	2.4	(32.5)	7.0	(93 9)	40 0

NOTE:

1. Pure argon atmosphere, ℓ_{aa} = 3.5 cm, nozzle 1, d_{nz} = 1.0 cm, F_{ag} = 14 L/min

TABLE A-5

ARC VOLTAGE AND REACTOR ENERGY DISTRIBUTION

WITH VARYING TANGENTIAL GAS FLOW RATE[1]

ℓ cm	I A	V V	P_t kW	P_c kW	%	P_n kW	%	P_s kW	%	P_w kW	%	P_a kW	%	P_R kW	%	F_{tg} L/min
16	200	48.9	9.8	0.4	(3.6)	0.4	(4.3)	3.8	(38.8)	2.0	(20.5)	2.3	(23.0)	8.8	(90.1)	0.0
16	200	45.9	9.2	0.4	(3.8)	0.4	(3.8)	3.5	(38.3)	1.9	(20.9)	2.3	(24 5)	8.4	(91.2)	14.0
16	200	44.5	8.9	0.4	(3.9)	0.4	(3.9)	2.9	(32.9)	1.9	(21.6)	2.1	(23.4)	7.6	(85.7)	20.5
16	200	43.5	8.7	0.4	(4.0)	0.4	(4.0)	2.9	(33.7)	1.9	(22.0)	1.9	(22.1)	7.5	(85.8)	30.0
16	300	46.8	14.0	0.4	(3.1)	0.5	(3.4)	5.9	(42.2)	2.9	(20.6)	3.9	(27.4)	13.6	(96.7)	20 5

NOTE:

1. Pure argon atmosphere, ℓ_{sa} = 4.2 cm, nozzle 2, d_{nz} = 0.75 cm, F_{ag} = 14 L/min.

A P P E N D I X B

EXPERIMENTAL RESULTS NITROGEN - NO FEED

TABLE B-1

OVERALL REACTOR ENERGY DISTRIBUTION

IN A PURE NITROGEN ATMOSPHERE[1]

ℓ cm	I A	V V	P_t kW	P_c kW	%	P_n kW	%	P_s kW	%	P_w kW	%	P_a kW	%	P_R kW	%	F_{tg} L/min
6	100	74.3	7.4	0.3	(3.8)	0.2	(2.7)	0.9	(11.8)	2.3	(31.0)	4.0	(53.4)	7.6	(102.7)	0
6	150	70.0	10.5	0.3	(2.7)	0.3	(3.2)	1.1	(10.2)	2.6	(24.6)	6.3	(59.9)	10.6	(100.5)	0
6	200	82.0	13.2	0.3	(1.7)	0.5	(3.2)	2.2	(13.6)	4.4	(26.6)	9.1	(55.7)	16.5	(100.8)	0
8	100	87.9	8.8	0.3	(3.2)	0.2	(1.9)	1.3	(14.4)	2.9	(32.5)	4.6	(51.7)	9.1	(103.8)	0
8	150	88.0	13.2	0.3	(2.1)	0.3	(2.5)	1.7	(12.6)	4.3	(32.2)	6.7	(50.6)	13.2	(100.0)	0
8	200	98.0	19.6	0.4	(1.8)	0.5	(2.4)	3.1	(15.9)	5.7	(29.1)	9.1	(46.6)	18.8	(95.7)	0
11	150	112.0	16.8	0.3	(1.7)	0.3	(2.0)	4.8	(28.5)	5.4	(32.0)	6.3	(37.4)	17.1	(101.5)	0
16[2.]	200	90.0	18.0	-	-	-	-	-	-	-	-	-	-	-	-	12
16	200	132.0	26.4	0.4	(2.0)	0.3	(1.7)	5.0	(27.5)	4.4	(23.9)	6.6	(36.3)	16.7	(63.3)	12

NOTES:

1. Nozzle 1, d_{nz} = 1.0 cm, ℓ_{sa} = 4.5 cm, F_{ag} = 14 L/min.
2. Ar axial gas, N_2 tangential gas.

A P P E N D I X C

EXPERIMENTAL RESULTS PARTICULATE FEED

TABLE C-1

ARC VOLTAGE AND REACTOR ENERGY DISTRIBUTION

WITH PARTICULATE FEED

TEST #	ℓ cm	I A	V V	P_t kW	P_c kW	%	P_n kW	%	P_s kW	%	P_w kW	%	P_a kW	%	P_R kW	%	F_{tg} L/min	F_p kg/h
12	16	200	62.2	12.4	0.4	(2.9)	0.4	(2.8)	7.2	(58.1)	2.1	(17.2)	2.0	(16.0)	12.1	(97.0)	30.0	0.75
12	16	200	65.8	13.6	-	-	-	-	-	-	-	-	-	-	-	-	30.0	1.4
13	16	200	59.9	12.0	0.4	(3.2)	0.4	(3.5)	6.8	(56.7)	2.3	(19.3)	2.5	(20.8)	12.4	(103.3)	20.5	0.66
13	16	200	63.5	12.7	0.4	(2.9)	0.4	(3.3)	6.9	(54.3)	2.3	(18.2)	2.5	(19.6)	12.5	(98.4)	20.5	1.3
13	16	200	65.9	13.2	0.4	(2.8)	0.4	(3.2)	6.8	(51.5)	2.5	(18.9)	2.5	(18.9)	12.6	(95.3)	20.5	2.3
13	16	200	69.5	13.9	0.4	(2.6)	0.5	(3.5)	6.1	(44.1)	2.5	(17.9)	2.5	(18.0)	12.0	(86.1)	20.5	3.7
14	16	300	69.5	19.8	0.5	(2.5)	0.6	(3.2)	11.5	(58.2)	3.1	(15.4)	3.1	(15.4)	18.7	(94.7)	20.5	3.7
15	16	300	67.8	20.3	0.4	(2.2)	0.6	(3.1)	10.1	(49.5)	3.5	(17.4)	4.3	(21.3)	19.0	(93.4)	20.5	1.3
18	16	200	72.0	14.4	0.3	(2.2)	0.4	(2.4)	2.7	(18.9)	2.3	(15.7)	2.2	(15.0)	7.8	(54.2)	12.0	24.9
22	16	200	72.0	14.4	0.5	(3.4)	0.7	(5.3)	5.6	(38.7)	1.4	(10.0)	2.2	(15.3)	10.5	(72.7)	12.0	24.9
27	16	200	70.0	14.0	0.3	(2.3)	0.4	(3.1)	5.6	(40.0)	1.3	(9.6)	1.8	(12.9)	9.5	(67.9)	20.5	35.6
30	16	200	72.0	14.4	0.4	(3.0)	0.4	(2.6)	6.1	(42.4)	1.7	(11.6)	2.8	(19.7)	11.4	(79.4)	12.0	28.4
21	16	300	80.0	24.0	0.4	(1.5)	0.8	(3.5)	9.2	(35.4)	3.1	(12.7)	5.2	(21.5)	18.6	(77.5)	12.0	24.9
23	16[1.]	200	152.0	30.4	0.4	(1.3)	0.8	(2.6)	12.8	(42.1)	4.4	(14.5)	5.3	(17.4)	23.7	(78.0)	12.0	22.6
25	16[1.]	300	150.0	45.0	-	-	-	-	-	-	-	-	-	-	-	-	12.0	76.2

NOTE:
1. N_2 atmosphere, all other tests in Ar atmosphere.

NOMENCLATURE

NOMENCLATURE

A	-	constant (60 A/cm^2K^2), Equation 3
B	-	magnetic field
d_{nz}	-	nozzle diameter, cm
d_p	-	particulate diameter, μm
e	-	electronic charge
E	-	electric field
F	-	force
F_{ag}	-	axial gas flow rate, L/min
F_p	-	total amount of particulate fed to reactor, kg
F_{pt}	-	particulate feed rate, kg/h
F_{tg}	-	tangential gas flow rate, L/min
I	-	arc current, ampere
J	-	current density
J_s	-	saturation current density
k	-	thermal conductivity
K	-	Boltzmann's constant
ℓ	-	arc length, cm
ℓ_{sa}	-	distance from base of sleeve to the anode surface, cm

P - pressure

P_a - power transferred to anode

P_c - power transferred to cathode

P_{cn} - power transferred to cathode and cathode nozzle

P_f - power transferred to particulate feed

P_n - power transferred to cathode nozzle

P_R - power absorbed by all cooled surfaces in reactor

P_r - radiative power density

P_s - power transferred to sleeve

P_t - total arc power (V·I)

P_{th} - theoretical power required to melt particulate feed = 0.34 kWh / kg x F_p (kg/h)

P_w - power transferred to reactor wall and roof

Q - rate of heat transfer

Q_a - kinetic energy, which is caused by the acceleration of the electrons through the anode boundary layer

Q_c - heat conducted into the anode

Q_{cd} - heat conduction from the hot gas

Q_{chj} - heat from chemical reaction and joule heating

Q_{conv} - heat transferred by convection from plasma to anode

Q_{cs} - heat conducted or convected away to the surrounding gas

Q_{evap} - heat lost by the vaporization of the anode material

Q_{jw} - kinetic energy of the electrons comprising the arc current and penetrating the anode surface

Q_k - thermal energy which is transferred from the hot gas to the electrons in the arc column (Thompson effect)

Q_{ra} - heat transferred by radiation from the arc to the anode

Q_{re} - heat radiated by the anode surface to the reactor wall and roof

Q_{sp} - heat lost by sputtering

Q_ϕ - heat of condensation of the electrons equivalent to the work function of the anode material

r - radial distance

T - temperature

T_e - electron temperature

T_w - wall temperature

V_a - anode fall voltage

V_i - ionization potential

V_k - equivalent voltage drop at the anode

V_ϕ - work function

x - degree of ionization

Greek Letters

σ - electrical conductivity

Subscripts

a - acceleration of electrons or anode

c - conduction or cathode

cn - cathode and cathode nozzle

e - electron

f - feed

n - cathode nozzle

r - radiation

s - sleeve

t - total

w - wall